EXPERIMENTAL AND COMPUTATIONAL STUDY OF MULTI-LEVEL COOLING SYSTEMS AT ELEVATED COOLANT TEMPERATURES IN DATA CENTERS

By

MANASA SAHINI

Presented to the Faculty of the Graduate School of

The University of Texas at Arlington in Partial Fulfillment

of the Requirements

for the Degree of

DOCTOR OF PHILOSOPHY

THE UNIVERSITY OF TEXAS AT ARLINGTON

August 2017

Copyright © by Manasa Sahini 2017

All Rights Reserved

ACKNOWLEDGEMENTS

My sincere thanks and heartfelt gratitude to Dr. Dereje Agonafer for his guidance and support over the course of my doctoral degree. He has always encouraged me to lead industry-related IUCRC projects, gain internship experience and attend conferences that helped me widen my professional network.

I am thankful to Dr. Haji-Sheikh, Dr. Butler, Dr. Mulay and Dr. Amaya for serving on my dissertation committee. I would also like to thank Dr.Veerendra Mulay for providing resources in completing the projects.

I take the privilege to express my deepest gratitude to Dr. John Fernandes for his consistent mentorship and training that essentially inspired me throughout my doctoral program. He has been a great example for me to gain the sense of discipline and dedication towards my research.

I would like to thank Dr. Betsegaw Gebrehiwot for guiding me during my initial stages of my research. I am always grateful to Ms. Sally Thompson for helping me sort through administrative aspects of the program.

Last, but not the least, I would like to thank my dear dad (Prakash Rao Sahini) and mom (Ramalaxmi Murahari Rao) and little brother (Sree Harsha) for believing in me to achieve success in my endeavors. I would not be the woman I am today if it is not for their unconditional love and support.

July 15, 2017

ABSTRACT

EXPERIMENTAL AND COMPUTATIONAL STUDY OF MULTI-LEVEL COOLING SYSTEMS AT ELEVATED COOLANT TEMPERATURES IN DATA CENTERS

Manasa Sahini, PhD

The University of Texas at Arlington, 2016

Supervising Professor: Dereje Agonafer

Data centers house a variety of compute, storage, network IT hardware where equipment reliability is of utmost importance. Heat generated by the IT equipment can substantially reduce its service life if $T_{J,Max}$, maximum temperature that the microelectronic device tolerates to guarantee reliable operation, is exceeded. Hence, data center rooms are bound to maintain continuous conditioning of the cooling medium. This approach often results in over-provisioned cooling systems. In 2014, U.S. Data center electricity consumption is about 1.8% of the total electrical energy in the country. Hence, data center power and cooling have become significant issues facing the IT industry.

The first part of the study focuses on air cooling of electronic equipment at room level. Data centers are predominantly cooled by perimeter computer air handling units that supply cold air to the raised floor plenum and the cold air helps in removing the heat generated by IT equipment. This method tends to be inadequate especially when the average power density per rack rises above 4 kW. As a solution to mitigate this problem, different rack and row based cooling solutions have been proposed and used. The primary focus of these cooling methods is to bring cooling closer to the heat source which

is the IT rack thereby improving the heat dissipation process along with controlled air flow management in the data center room. Mostly known close-coupled cooling solutions include rear-door heat exchanger, in-row coolers, and over-head cooling. In this study, a new end-of-aisle close-coupled cooling solution for small data center cooling room has been proposed. As oppose to the existing designs, this design is distinctive in eliminating the risk of placing the liquid on top of IT racks along with achieving cooling energy efficiency. Three different configurations of the proposed designs are studied for its thermal performance using computational modeling.

The second part of the study focuses on liquid cooling at rack level. Liquid cooling addresses the critical issues related to typical air cooling in servers because of its better heat transfer characteristics. Water-cooling at the device level can be an efficient solution since water has higher thermal capacitance when compared to traditional heat carrying medium i.e., air. The emerging practice in the data center industry is to maximize the use of economizer usage by reducing/eliminating the usage of chiller while taking advantage of outside ambient conditions to cool the data centers. Liquid cooled racks are generally designed with different configuration of pumping systems. Empirical study is conducted on a state-of-art liquid cooled electronic rack for high coolant inlet, commonly known as warm-water cooling in order to evaluate the cooling performance of distributed vs. centralized coolant pumping systems. Experimental set up is instrumented such that detailed analysis is employed to study component temperatures as well as cooling performance of the rack at elevated inlet conditions.

The third part of the study focuses on the impact of high server inlet temperatures to static power at server level. In order to maximize the use of economizers, the IT hardware will be exposed to higher inlet temperatures which would lead to higher operating temperatures of the processors. The operating temperature of

the CPU has direct influence on the static power due to subthreshold leakage which is known to reduce the performance of the processor. The current work serves as a firsthand investigation to study trade-off between IT performance and energy efficiency for elevated inlet temperature in air vs. liquid cooled servers. Air cooled IT along with the liquid cooled counter-parts are instrumented and extensively tested to simulate the high ambient conditions at the test bed data center.

Table of Contents

ACKNOWLEDGEMENTS iii

ABSTRACT iv

List of Illustrations x

List of Tables xiv

Nomenclature xv

CHAPTER 1 INTRODUCTION 1

1.1 Data Center Power Usage and Industry need 1

1.2 Thermal Management and Energy Efficiency 4

CHAPTER 2 LITERATURE REVIEW 9

2.1 Close-Coupled Cooling Solutions for IT PODS 9

2.2 Effects of High Temperature Inlet Conditions 11

CHAPTER 3 ROOM LEVEL STUDY: CFD ANALYSIS ON NEW CLOSE-COUPLED COOLING SOLUTION 13

3.1 Modeling of Room level data center 14

3.1.1 Model Definition 14

3.2 Modeling of the Heat Exchanger Units 16

3.3 Case 1 Rack Fan Wall Selection 18

3.3.1 Case 1 Results 19

3.4 Case 2 24

3.4.1 Case 2 Results: 25

3.5 Case 3 27

3.6 CONCLUSION 29

3.7 Cooling Failure Scenarios 30

3.7.1 Fan Control considering the failure scenarios 45

CHAPTER 4 RACK LEVEL STUDY: COMPARISON OF DISTRIBUTED AND CENTRALIZED PUMPING SYSTEMS 47
4.1 Experimental Setup 48
4.1.1 Server Configuration 48
4.1.2 Rack Configuration 52
4.2. Cooling Process 54
4.3 Testing Procedure 56
4.3.1 Hardware For Power Measurements 58
4.3.2 Desired Coolant Inlet Temperature 58
4.3.3 Synthetic Load Generation and Data Collection 60
4.3.4 Experiment Process 62
4.4. Results & Discussions 62
4.4.1 Distributed pumping results 62
4.4.2 Centralized pumping results 68
4.5. Conclusions 74
4.6. Failure Conditions for Distributed Vs. Centralized Systems 75
4.6.1 Distributed Pumping Failure Scenario 76
4.6.2 Centralized Pumping Failure Scenario 78
CHAPTER 5 SERVER LEVEL STUDY: EFFECT OF HIGH TEMPERATURE INLET CONDITIONS ON THERMAL PERFORMANCE OF AIR VS. LIQUID COOLED SOLUTIONS 81
5.1 Experimental Set Up 82
5.2 Test Procedure 87
5.3 Results And Discussion 90
5.4 Conclusion 100

CHAPTER 6 Conclusion 102

REFERENCES 105

List of Illustrations

Figure 1-1: Projected Data Center Total Electricity Usage……………………………….…2

Figure 1-2: Estimated US Data Center Electricity Consumption by Market Segment [4]...3

Figure 1-3: Graph showing the relationship between carbon intensity with energy intensity and data center size [5]...3

Figure 1-4: Energy Consumption Impact of Mechanical Equipment and Systems [9] 5

Figure 1-5: ASHRAE TC 9.9 2011 Thermal Guidelines for Air Cooled IT[12] 6

Figure 3-1: Top View of the Close-coupled Cooling Solution 15

Figure 3-2: Isometric View of data center CFD model...16

Figure 3-3: System Resistance Curve of 1U server 17

Figure 3-4: Water-to-Air Finned Tube Heat Exchanger System Resistance 17

Figure 3-5: a) Server Stack with one row of three 120 mm fans b) System Resistance and Derived Fan curve the server stack and fan system..19

Figure 3-6: Temperature Streamlines of the Air Flow Movement 20

Figure 3-7: Rack Average Inlet/Outlet Temperature..21

Figure 3-8: Rack Average Inlet/Outlet Temperature..21

Figure 3-9: Individual Cabinet Flow Rates...22

Figure 3-10: Individual Heat Exchanger Flow Rates 22

Figure 3-11: Schematic Layout of Case 2 with Active heat Exchangers and Rack level fans..24

Figure 3-12: Air Flow Streamlines colored by temperature 25

Figure 3-13: Rack Inlet and Outlet Flow rates 25

Figure 3-14: Cooling Design Schematic for Case 3...27

Figure 3-15: Pressure Plot for Case 3-Top view of the room with cut section running through the center of the rack height 28

Figure 3-16: Pressure Plots from case 2- Top view of the room with cut section running through the center of the rack height 29

Figure 3-17: Isometric View of the room 32

Figure 3-18: Case 3A Heat Exchanger Flow rate and Temperature parameters 32

Figure 3-19: Heat Exchanger Air Flow and Temperature Parameters 33

Figure 3-20: Temperature Plot when HXs on one side were disabled 35

Figure 3-21: Heat Exchanger Air Flow and Temperature Parameters 36

Figure 3-22: Heat Exchanger flow and Temperature Parameters 37

Figure 3-23: Heat Exchanger Flow and Temperature Parameters 38

Figure 3-24: Pressure Plot for Case 3C (for same legend) 39

Figure 3-25: Pressure Plot for Case 2B (for same legend as figure 3-24) 40

Figure 3-26: Heat Exchanger Flow and Temperature Parameters 41

Figure 3-27: Rack Air Flow Rates Showing Lower Flow Rates for J3 and E3 42

Figure 3-28: Hot Air Exhaust from E3 rack entering neighboring racks 43

Figure 3-29: Pressure Plot in the room with cut plane across mid height of the racks (circled areas) 44

Figure 4-1: Intel based 2OU Air-Cooled Server 48

Figure 4-2: Cover with ducting for the server 49

Figure 4-3: Server showing fans and cold plates air circulation 1) fans with radiator 2) cold plate on CPU1 3) Cold plate on CPU0 4)Quick disconnects with arrows showing server inlet and outlet 50

Figure 4-4: Active V-groove cold plate with pump attached to it 51

Figure 4-5: 2U Centralized Pumping Module integrated with liquid to liquid heat exchanger (CHX40) 51

Figure 4-6: Mini-rack showing 1) power shelf 2) network switch 3) four 2OU slots 53

Figure 4-7: Liquid to liquid HX (circled area) 1)CHx coolant reservoir 2)Shut off vale 53

Figure 4-8: Side car liquid to air HX with arrow marks showing the direction of inlet and exhaust air 55

Figure 4-9: Inlet and Outlet Manifolds (highlighted areas) 56

Figure 4-10: a) CHX 40 (left) replaced on the top of the rack with centralized pumps driving the flow in the system b) previous design of centralized system (right) - the location of the pumps are highlighted 57

Figure 4-11: Prototype board used to measure the power of fan and pump 58

Figure 4-12: LabVIEW interface showing input and control parameters 59

Figure 4-13: Six servers tested in the rack a) distributed pumping case b) centralized case with CHx 40 replacing CHx 61

Figure 4-14: Change in fan speeds based on PCH temperatures for various inlet temperatures 64

Figure 4-15: Maximum CPU core temperatures at 100% power level for server 123 65

Figure 4-16: Maximum DIMM temperatures at CPU and memory test for server 123 66

Figure 4-17: CPU core temperature for different inlet temperatures for server 123 68

Figure 4-18: DIMM temperatures for different inlet temperatures for server 123 69

Figure 4-19: PCH temperatures for different coolant inlet temperatures for server 123 .. 69

Figure 4-20: PCH extruded heat sink and air flow direction inside the server (arros are colored to represent the cool and hotter air) 72

Figure 4-21: ANSYS Icepak model of the open compute server 73

Figure 4-22: Server 123 showing location of fan and pump that are not powered in distributed pumping case 76

Figure 4-23: Circled Pump is disabled for running the test 78

Figure 5-1 : Enterprise Class Liquid Cooled Server (the arrows show direction of liquid coolant in and out of the server) 83
Figure 5-2: Experimental schematic for liquid cooled server testing 84
Figure 5-3: 1U enterprise server with front to rear air cooling 85
Figure 5-4: Characterization of flow curves for the air-cooled IT server 86
Figure 5-5: Environmental Chamber Thermotron unit (left); Simple schematic of air-cooled IT server testing (right) 88
Figure 5-6: Variation of total server power with stress load condition 89
Figure 5-7: Graph for Power vs. RPM for 40 mm Fan 90
Figure 5-8: Increasing CPU temps with increased coolant temperature at 100% stress load 90
Figure 5-9: Change in fan speeds with increase in coolant inlet temperatures 91
Figure 5-10: IT power dissipation vs. Inlet Coolant Temperature at 100% utilization 92
Figure 5-11: CPU0 temperatures for varying pump supply voltage 93
Figure 5-12: Pumping power for different supply volatage conditions 94
Figure 5-13: IT power vs. pump supply voltage for different coolant inlet temperatures 95
Figure 5-14: CPU maximum core temperatures for different air inlet temperatures at 100% CPU load 96
Figure 5-15: Average Fan Speeds varying with respect to inlet air temperature 97
Figure 5-16: Maximum DIMM temperatures for varying air inlet conditions at CPU+MEM load 97
Figure 5-17: Total IT power consumption for different inlet air temperature for 100% CPU stress load and prime95 memory stressing test (CPU+MEM) 98
Figure 5-18: Air vs. Liquid Cooled CPU die temperatures for varying inlet temperatures at 100% stress load 100

List of Tables

Table 1-1 : ASHRAE IT Equipment Classification and Corresponding Environmental Control 6

Table 1-2: ASHRAE Liquid Cooled Thermal Guidelines [13] 7

Table 3-1: Different Failure Scenarios .... **Error! Bookmark not defined.**

Table 3-2: The cooling power consumption of the entire rack for different coolant temperatures 67

Table 3-3: The cooling power consumption of the entire rack for different coolant temperatures 70

Table 4-1: Comparison of average component temperatures and average fan speeds for distributed pumping (DP) and centralized pumping systems (CP) 71

Table 4-2: Temperature and power parameters for failed vs. regular operation of server 123 77

Table 4-3: Comparison of component temperatures and power for centeralized pumping regular vs. failure design 79

Table 5-1: Cooling power consumption vs. IT power consumption 99

Nomenclature

Q - Total heat dissipated (W)

m_w - Mass flow rate of water (kg/sec)

m_a - Mass flow rate of air (kg/sec)

C_{pw}- Specific heat of water (kJ/kgK)

C_{pa} - Specific heat of air (kJ/kgK)

ΔT_w- Temperature difference on water side (K)

ΔT_a- Temperature difference on air side (K)

dP - Static pressure drop across the server (Pa)

$\dot{v}$ - Volumetric flow rate (m3/sec)

$\dot{Q}$ - Volumetric flow rate (CFM)

ΔP - Fan static pressure drop (in w.c.)

μ_f - Fan efficiency (%)

CHAPTER 1

INTRODUCTION

Data centers house a variety of compute, storage, network IT hardware where equipment reliability is of utmost importance. The U.S Environmental Protection Agency (EPA) defines a data center as "primarily electronic equipment used for data processing, data storage, and communications. Collectively, this equipment processes, stores and transmits digital information and specialized power conversion and backup equipment to maintain reliable, high quality power, as well as environmental control equipment to maintain the proper temperature and humidity for the ICT equipment" [1]. The sole purpose of data centers is to process information. While, Information and communication equipment (ICT) is the primary part of data centers, power delivery, cooling infrastructure and back up equipment turns out to be secondary part of data centers. Data centers are seen to have significant role in driving the modern economy that includes Internet, medical services, energy, telecommunication, banking, mobile phones, various retail business stores, urban traffic, transport, security systems etc. Data center facility sizes range from few tens of servers referred as server rooms to few hundred thousands of servers referred as enterprise-class data centers. Some of the world largest internet companies like Google, Facebook, Yahoo, Amazon, eBay, Microsoft, Twitter etc. constitute large scale enterprise-class data centers. Typically, an enterprise-class data center consists of more than 100,000 servers with a facility size more than 5000 sq.ft. Each data center can consume anywhere between 1 and 500MW of electrical energy.

1.1 Data Center Power Usage and Industry need

Data centers continue to be significant consumers of world electricity consumption. According to the United States Data center Energy Usage Report, U.S.

data centers consumed an estimated 70 billion kilowatt-hours of electricity in 2014 which represents 1.8% of total U.S energy consumption [2]. By 2020, these data centers are projected to consume around 140 billion kilowatt-hours causing millions of metric tons of carbon pollution. Also, it has been estimated that data center dedicated space will globally increase to 2 billion square feet by 2018 [3] Human induced climate change and rising carbon footprint is the major challenge facing the world. Increased demand for the cloud computing services, big data, infrastructure deployments that need continuous connectivity translates to ongoing expansion for the data center industry which directly impacts the energy consumption of the industry and also the carbon footprint contributed by the sector. The cabinet heat loads are expected to achieve increasing trends through years. As the IT equipment packaging tends to be denser due to increasing capabilities.

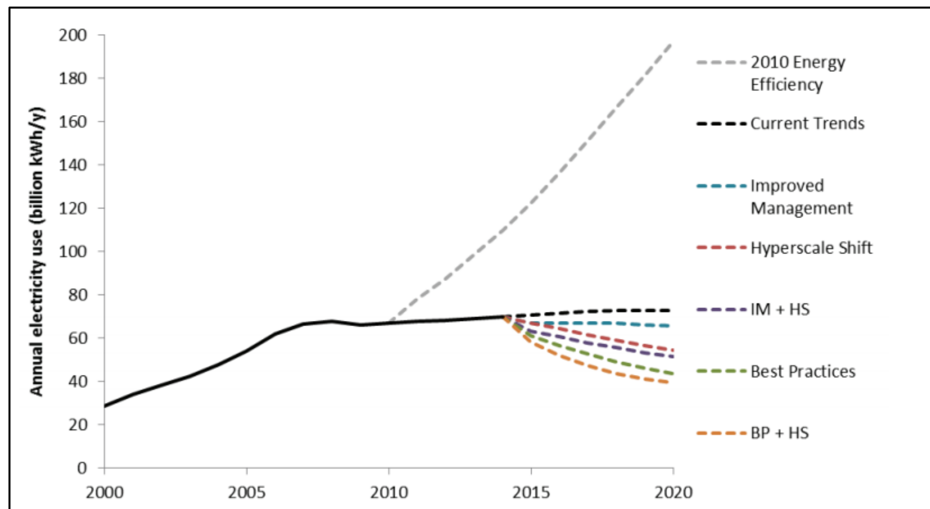

Figure 1-1: Projected Data Center Total Electricity Usage

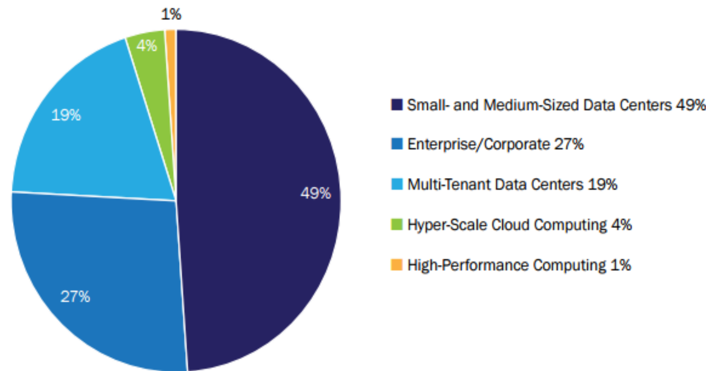

Figure 1-2: Estimated US Data Center Electricity Consumption by Market Segment [4]

It is interesting to note that high-performance computing market only contributes to 1% of the industry while small and medium sized data centers contribute to 49% of the market as shown in Figure 2. This is important because recent studies have shown that these small and medium scale data center industries have shown less progress in terms of energy efficient usage practices compared to the hyper-scale or high performance computing industry. This tendency gives an implicit understanding of the extensive power usage in the entire data center market.

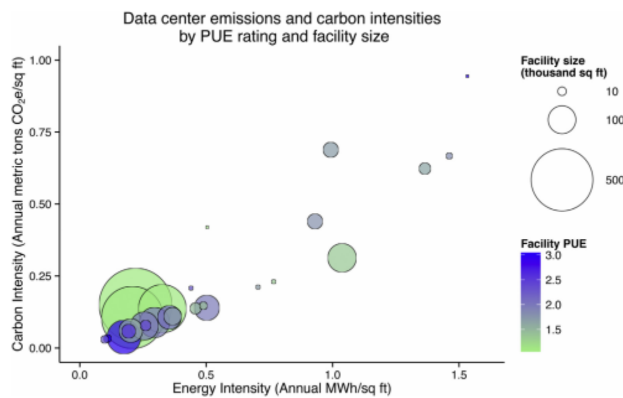

Figure 1-3: Graph showing the relationship between carbon intensity with energy intensity and data center size [5]

Studies indicate that the energy estimates for coming years show growing trend for Hyperscale data centers while staying the same rest of the data center types [6]. Considering the significance of the current power usage in data center industry, it is critical to recognize that the energy demands are continuing to rise which means the consequence for sustainable as well energy smart IT and infrastructure design is pressing.

1.2 Thermal Management and Energy Efficiency

The main purpose of housing the electronic equipment is to maintain the safe environmental conditions to ensure the IT equipment runs continuously and reliably. Various cooling techniques are employed in data centers such that the IT equipment does not overheat causing failure of the electronics which in turn is a loss of computational time along with equipment cost. The common approach used is to deploy an overly conservative thermal management which leads to squandered cooling resources.

As mentioned in the previous section the growth in new data center has abated recently and for next few years. However, a significant number of existing data centers i.e. small / medium and multi-tenant data centers which constitute of around 95% of electricity share in data center market are in compelling need for energy efficiency [4]. A typical data center consumes 45-55% of energy for IT equipment and around 30-40% of cooling energy is consumed by cooling. In terms of energy costs, cooling and electricity infrastructure contribute to 70-80% of the capital costs [1]. In order to track the data center energy efficiency, the Green Grid Association has introduced metrics such as Power Usage Effectiveness (*PUE*) [7]. PUE provides the sum of IT and Cooling energy as a fraction of IT power consumption from data centers. In addition to PUE, Green Grid has later introduced metric known as Data Center Energy Productivity (DCeP) [8]. This

metric serves to quantify the useful work the data center produces based on the energy it consumed.

$$PUE = \frac{Total\ Facility\ Energy}{IT\ Equipment\ Energy}$$

$$DCeP = \frac{Useful\ work\ produced}{Data\ center\ energy\ consumed\ to\ produce\ this\ work}$$

Average Power allocation

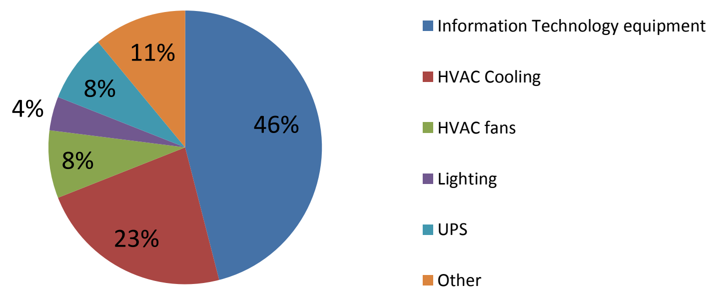

Figure 1-4: Energy Consumption Impact of Mechanical Equipment and Systems [9]

A recent study conducted in 2013 conducted by Campos Research and Analysis, the average PUE in the North American data center industry ranges between 1.8 and 2.9 while only 20% of the companies had reported PUE less than 2.0 [10]. When PUE is considered as a measure to energy efficiency in data centers and the metric can be improved by reducing the overhead on support infrastructure especially on cooling energy consumption.

American Society of Heating, Refrigeration and Air-Conditioning Engineers (ASHRAE) TC 9.9 chapter conducts extensive work in analyzing and defining the model codes, standards and guidelines for data center and mission critical facilities [11].

Table 1-1 : ASHRAE IT Equipment Classification and Corresponding Environmental Control

2011 classes	2008 classes	Applications	IT Equipment	Environmental Control
A1	1	Datacenter	Enterprise servers, storage products	Tightly controlled
A2	2		Volume servers, storage products, personal computers, workstations	Some control
A3	NA		Volume servers, storage products, personal computers, workstations	Some control
A4	NA		Volume servers, storage products, personal computers, workstations	Some control
B	3	Office, home, transportable environment, etc.	Personal computers, workstations, laptops, and printers	Minimal control
C	4	Point-of-sale, industrial, factory, etc.	Point-of-sale equipment, ruggedized controllers, or computers and PDAs	No control

Based on different classes of IT equipment the environments are classified into recommended and allowable ranges. The recommended envelope represents the limitations of operating the IT equipment with utmost reliability and sensible energy efficiency. As the data center operating envelope is expanded from A1, A2 towards A3, A4 higher energy efficiency is achieved however considerable trade-off exists in terms of reliability of the equipment.

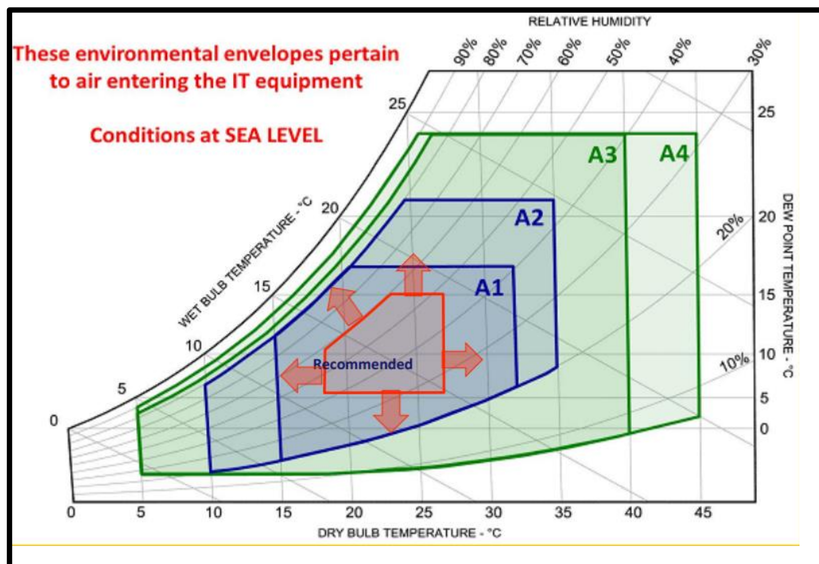

Figure 1-5: ASHRAE TC 9.9 2011 Thermal Guidelines for Air Cooled IT [12]

Table 1-2: ASHRAE Liquid Cooled Thermal Guidelines [13]

Classes	Typical Infrastructure Design		Facility Supply Water Temp (C)	IT Equipment Availability
	Main Cooling Equipment	Supplemental Cooling Equipment		
W1	Chiller/Cooling Tower	Water-side Economizer Chiller	2 – 17	Now available
W2			2 – 27	
W3	Cooling Tower	Chiller	2 – 32	Not generally available, dependent on future demand
W4	Water-side Economizer (with drycooler or cooling tower)	Nothing	2 – 45	
W5	Building Heating System	Cooling Tower	> 45	Specialized systems

Since the use of liquid cooling at module and rack level has been wide-spreading, ASHRAE TC 9.9 has introduced liquid cooling classes as well with varying coolant temperature ranges as shown in Table 1-2. Based on the type of infrastructure cooling design that is to be used the facility supply side water temperature ranges are defined as shown in Table 1-2.

Several efforts are being made by IT industry for years in order to achieve the improved energy efficiency. Thermal management in data center is of multi-scale nature [14]. The thermal architecture needs to be coupled at different sizes or scales such that the overall energy management can be effectively designed and monitored. The multiple cooling scales can be divided as chip level, server level, chassis level, cabinet level, room level and plenum level [14]. In the context of current study, the cooling scales that are studied are module level i.e. the chip level cooling using heat sinks or cold plates,

server/chassis level i.e. thermal transport across the IT server using fans or heat exchangers, room-level i.e. cooling configuration with CRAH/CRAC or AHU units.

CHAPTER 2

LITERATURE REVIEW

This section will contain a review of close-coupled cooling solutions for IT PODS, effects of high temperature inlet conditions on air as well as liquid cooling for high power IT.

2.1 Close-Coupled Cooling Solutions for IT PODS

Data centers are managed mostly managed by overly conservative thermal management approaches [14]. The typical thermal solution for data centers is perimeter computer air handlers (CRAH). The traditional cooling method includes supplying air through raised floor plenum that is blown by the CRAH blowers and the chassis fans typically located at the rear end of the IT pull the air across the server collecting the heat and the exhaust air from fans is again collected by the CRAH return. This architecture provides adequate cooling for rack densities below 5kW. However, as the rack densities raise beyond 5kW the removal using CRAH based cooling becomes challenging [15]. To address this issue, data centers have adopted the concept of close-coupled cooling i.e. bringing the cooling source closer to the IT equipment [16]. Some of the close-coupled cooling solutions are overhead cooling, rear-door heat exchanger cooling, in-row cooling, bottom located cooling etc. The key objectives of close-coupled cooling is to enable a controlled cooling of the IT equipment, flexible as well as modular design architecture, containment of hot air exhaust from the cold air [17].

Overhead cooling is a row-based cooling design where the cooling coils are placed on top of the IT rack which removes the heat by circulating the air across the row. Steady and Transient Behavior of overhead cooling systems has been conducted to compare the cooling effectiveness and energy efficiency of overhead downward flow and overhead upward flow [18]. InRow Cooling is another row-based cooling design where

the cooling coils coupled with blowers are placed at specified locations in between the cabinets and in-line with the rows. In Row Coolers are also used to complement the CRAH based cooling which is referred as hybrid cooling; detailed CFD analysis is conducted to show how In Row cooling coupled with CRAH unit can provide uniform cooling energy distribution [19]. Rear door heat exchanger is a water cooled rack based cooling solution where cooling coils are mounted on the rear side of the cabinet [20]. Transient models for cross flow heat exchangers have been developed in order to understand the dynamic response of the heat exchanger during varying operating conditions [21]. Bottom-located cooling unit is compared with perimeter based cooling system in terms of air flow energy using CFD [22] . Computational study analysis has been conducted in developing innovative server rack design with bottom located cooling unit [23]. Close-coupled cooling solutions are considered to be best fit for data centers high density racks where retrofit upgrades are needed [24]. In terms of reliability, the different types of in-row, above-row and rear door HXs are capable of providing continuous redundant cooling more effectively compared to CRAC based cooling [25]. Various basic heat removal methods have been compared to cool IT and it has been found that rack and row based cooling solutions are more efficient compared to CRAH based cooling; however, these close-coupled solutions highly rely on server or rack fans to operate [26]. While comparing the annual electric cost for different close-coupled solutions, it has been found out that row-based cooling coupled with hot air containment showed lowest costs while room-based traditional crac-based design showed highest costs and also the average rack power also played an important role where an increased rack density of around 12kW that is cooled using rack based cooling solution showed lowest dip in the annual electricity costs [27]. Various factors such as agility, system

availability, serviceability, total cost of ownership, system availability and so on should be considered while selecting appropriate close-coupled cooling solution [27].

2.2 Effects of High Temperature Inlet Conditions

ASHRAE TC 9.9 has defined the thermal guidelines of specified dry bulb and humidity ranges for different IT equipment classes [12]. Increasing the data center operating temperatures has been an emerging practice to partially or eliminates chiller usage. Experimental study has been conducted for a 1 MW data center and the results suggested just one degree rise in the temperature set point could save 2-5% of the overall energy consumption in data centers; the study also provides a multi-faceted understanding of temperature management in data centers in terms of performance and reliability [28]. Customized control mechanism known as on-demand cooling has been introduced to implement high operational temperatures in data centers with thermal safety because without the customized IT design the high inlet conditions could bring benefit and challenge at the same time [29]. Computational modeling has been used to demonstrate that increasing the ambient conditions up to 35°C along with other factors like hot aisle/cold aisle containment, eliminating cable obstructions, by-pass and re-circulation reduction for a CRAH based cooling system has improved data center level power savings with the use of economizers [30]. Before adopting the high ambient and free cooling technology, key factors like server stability along with optimal temperature and corrosion resistant hardware design should be studied because increasing temperatures to ASHRAE class A3, A4 classes will need orchestrated collaboration between the IT and cooling infrastructures [31]. In regards to the correlation between high ambient inlet with reliability of the IT hardware, the effect of data center inlet temperature

on the chip leakage power has been modeled and found out that the COP of the data center cooling infrastructure has a negative impact from the leakage current which is the direct function of the chip operating temperature; this study challenges the perception to hot air cooling and demonstrates the significance of determining the optimum operating strategy for the data center while trading off the infrastructure energy savings [32]. Based on the limitations of operating temperatures using air cooling, energy-efficient liquid cooling has been examined for its high temperature effects on temperature-dependent leakage and it has been found that the total data center power consumption as a function of coolant temperature, the computational state of chip, weather factors that employ free cooling has not shown improved energy efficiency even during maximized free cooling due to additional leakage power incurred by the associated higher coolant temperatures [33]. As data center liquid cooling envelops are expanded towards W3, W4 classes' significant energy savings that are as low as 3.5% of the typical air cooled chiller based data center [34]. Warm water cooling in data centers has been adopted where the return water is as high as 95°F and the hot return water is used as a primary heating source for building [35]. Experimental and analytical studies have been conducted to show that warm water cooling of data centers coupled with energy re-use help remove the usage of chillers showing significant improvements in PUE and ERE metrics [36]. Comprehensive liquid cooling design guidelines have been analyzed for building supplied warm water cooled IT at 15 national laboratory sites while estimating the total cost of ownership that showed reduced capital as well as ongoing energy consumption costs [37]. Based on the related research, the high ambient inlet conditions have been considered to test the IT hardware for its reliability and energy efficiency impacts.

CHAPTER 3

ROOM LEVEL STUDY: CFD ANALYSIS ON NEW CLOSE-COUPLED COOLING SOLUTION

(Reprinted with permission © 2017 ASME) [38]

The objective of this work is to introduce and evaluate a new end-of-aisle cooling design which consists of three cooling configurations. The key objectives of close-coupled cooling are to enable a controlled cooling of the IT equipment, flexible as well as modular design, and containment of hot air exhaust from the cold air. The thermal performance of the proposed solution is evaluated using CFD modeling. A computational model of a small size data center room has been developed. Larger axial fans are selected and placed at rack-level which constitute the rack-fan wall design. The model consists of 10 electronic racks each dissipating a heat load of 8kw. The room is modeled to be hot aisle containment i.e. the hot air exhaust exiting for each row is contained and directed within a specific volume. Each rack has passive IT with no server fans and the servers are cooled by means of rack fan wall. The cold aisle is separated with hot aisle by means of banks of heat exchangers placed on the either sides of the aisle containment. Based on the placement of rack fans, the design is divided to three sub designs- case1: passive heat exchangers with rack fan walls; case2: active heat exchangers (HXs coupled with fans) with rack fan walls;case 3: active heat exchangers (hxs coupled with fans) with no rack fans. The cooling performance is calculated based on the thermal and flow parameters obtained for all three configurations. The computational data obtained has shown that the case 1 is used only for lower system resistance IT. However, case 2 and Case 3 can handle denser IT systems. Case 3 is the

design that can consume lower fan energy as well as handle denser IT systems. The paper also discusses the cooling behavior of each type of design.

3.1 Modeling of Room level data center

3.1.1 Model Definition

A computational model of a small size data center room will be developed based on the typical data center room designs. The servers are modeled to be passive components with no in-built fans. Larger axial fans are selected and placed at rack-level which constitute the rack-fan wall design. Active as well as passive heat exchangers are selected based on the commercial designs available. The cooling performance is calculated based on the thermal and flow parameters obtained for all three configurations. There is no raised floor plenum.

The primary focus of the close-coupled cooling methods is to bring cooling closer to the heat source which is the IT rack thereby improving the heat dissipation process along with controlled air flow management in the data center room. The objective of the current study is to analyze the thermal performance of a new kind of close-coupled cooling solution for small data center cooling room using computational software.

A small sized data center room has been modeled using commercial CFD software called 6SigmaRoom [39]. The model consists of 10 electronic racks each dissipating a heat load of 8kW. There are two rows with five racks placed on each row. The room is modeled to be hot aisle containment i.e. the hot air exhaust exiting for each row is contained and directed within a specific volume. . Each rack has passive IT with no server fans and the servers are cooled by means of rack fan wall. The cold aisle is separated with hot aisle by means of banks of heat exchangers placed on the either sides of the aisle containment as shown in figure 1. There is no raised floor plenum. The

air flow movement includes the cold air being pulled in by the rack fans across the servers and the exhaust air then takes a turn passing through the heat exchanger units placed on either side of the room containment.

$$Q = m_w C_{pw} \Delta T_w = m_a C_{pa} \Delta T_a \qquad (1)$$

Passive heat exchangers with rack fan wall shows that the data center room consists of 10 42U rack (1 rack U =1.72 inch). The dimensions of the rack are 2004x597x1008 mm³. The rack slots are filled with 1U servers. The servers are modeled in passive type by defining the system resistance in terms of viscous and inertial resistance coefficients as shown in equation 2. The server dimensions are assumed to be 711.4x444.5x43.9 mm³. Each server dissipates 190.5 W of heat.

$$dP = Viscous\ res\ Coef * \dot{v} + Inertial\ res\ Coef * \dot{v}^2 \qquad (2)$$

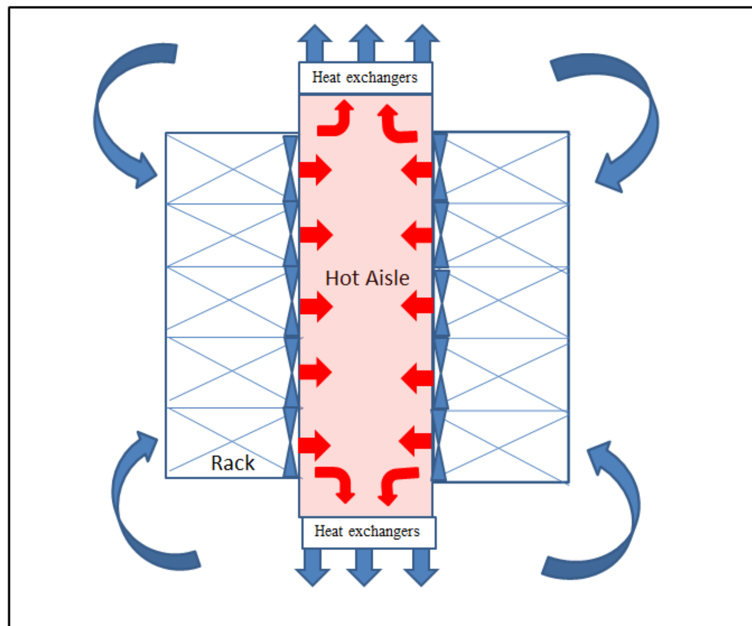

Figure 3-1: Top View of the Close-coupled Cooling Solution

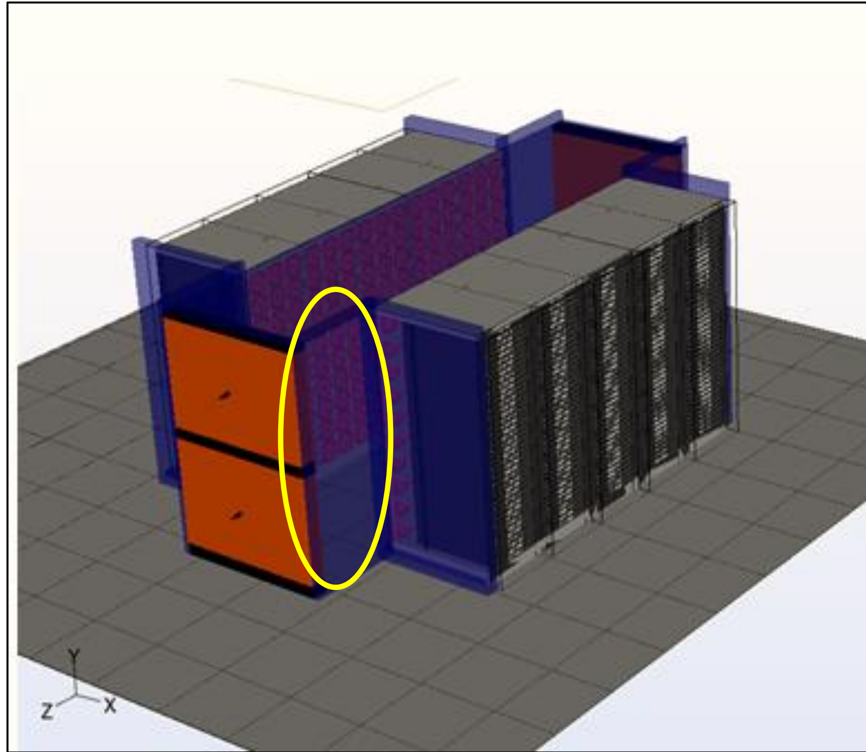

Figure 3-2: Isometric View of data center CFD model

The hot aisle and cold aisle widths are considered as 1500 mm. The range hot aisle width in industry practice varies between 3' and 6' [40] The hot aisle entrance width (circled space in figure 2) of 838 mm is designed to accommodate the space used to access into the hot aisle typically used for servicing or maintaining of the IT/ cooling equipment.

3.2 Modeling of the Heat Exchanger Units

The heat exchangers are the primary cooling sources that cool the return air exhaust and the cool air supply coming out will be pushed back into the cabinet racks. The heat exchanger design is considered to be a water to air finned tube model.

Commercially available heat exchanger designs are selected in order to consider the cost, practicality and feasibility of the cooling design. The heat exchanger system resistance, for each configuration, is obtained using the coil selection software [41]. The system resistance curve of server measured for case 1 is shown in figure 4. The coil selection software has been leveraged to estimate the performance of the selected heat exchanger design for the given air side and water side boundary conditions. The heat exchanger effectiveness has been calculated using the effectiveness-NTU method. The air side and water side volumetric flow rates are specified based on equation 1 where the water and air side temperature difference is assumed based on typical industry practice.

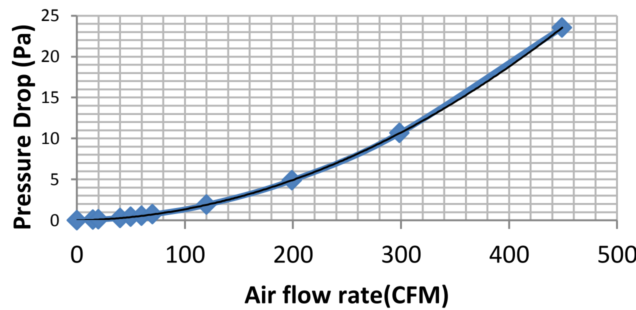

Figure 3-3: System Resistance Curve of 1U server

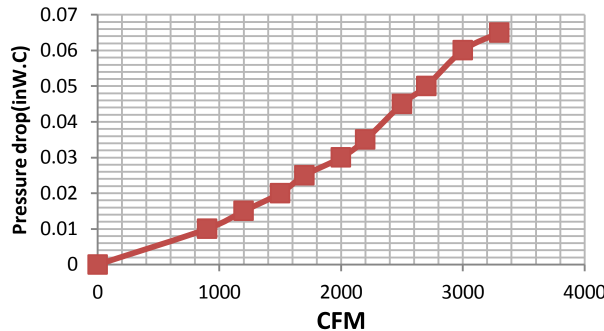

Figure 3-4: Water-to-Air Finned Tube Heat Exchanger System Resistance

The heat exchanger dimensions are 33x47x5 in^3 based on the available commercial designs. The geometry of the heat exchanger design is also influenced by the size of the hot aisle (width and height). There are total four heat exchanger banks each assumed to handle a sensible heat load of 20kW. The entering water and leaving water temperatures are assumed to be 17°C and 22°C respectively according to typical industry practices used to make sure the water temperature is about dew point temperature of ambient air. The effectiveness values calculated based on these boundary conditions is 0.65. The water flow rate based on energy equation to dissipate 20 kW is 15.2 GPM. The entering air temperature is 38 °C. These are the values that are defined for modeling the performance of the heat exchanger unit.

3.3 Case 1 Rack Fan Wall Selection

The total air flow requirement based on the air side energy balance equation (1) for 8kW total load and a ΔT of 10°C is 1375 CFM per rack. Each server needs 32.7 CFM of air flow rate. A total of 42 pieces in terms of 14 rows of 3 120 mm parallel fans have been grouped.

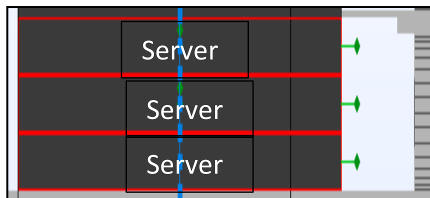

(a)

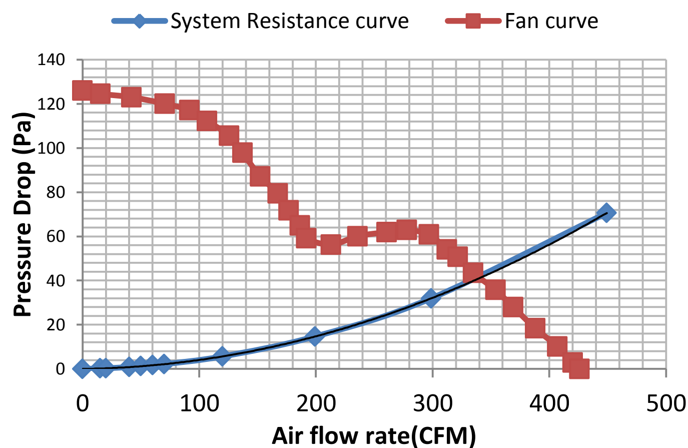

Figure 3-5: a) Server Stack with one row of three 120 mm fans b) System Resistance and Derived Fan curve the server stack and fan system

Based on the geometry of the rack space and the server system resistance, the servers and fan system are arranged as shown in Figure 5 (a). The Fan curve for three parallel fan curves is calculated based on fan curve information of single 120 mm fan curve [42] as shown in Figure 5 (b). Even though the derived fan curve and system resistance curve shows the fans are operating in the low resistance points, the following system has been considered to account for additional resistance that will be offered by the heat exchanger banks and the air flow movement.

3.3.1 Case 1 Results

The model is studied for steady state conditions. Standard K-ε turbulence model has been chosen. The total grid generated is 23 million cells. The conformal meshing technique known as grid control method is used in the software to mesh certain geometry such as IT servers and cabinets which develops finer mesh. This helps in achieving higher accuracy during the iterative solver procedure opted by the CFD.

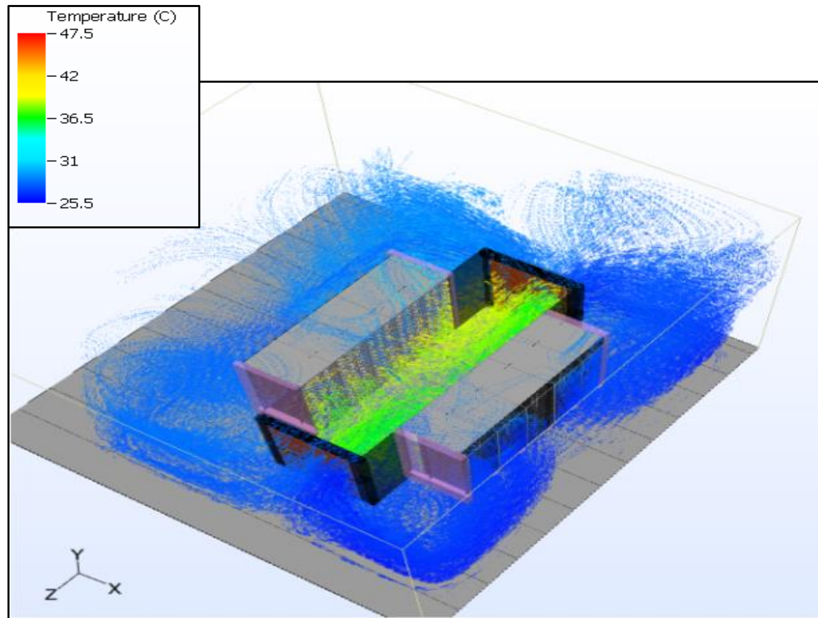

Figure 3-6: Temperature Streamlines of the Air Flow Movement

The temperature streamlines shown in figure 6 demonstrate the air flow movement in the room. The average temperature different across each cabinet is around 10 (±1) °C as shown in figure 7.

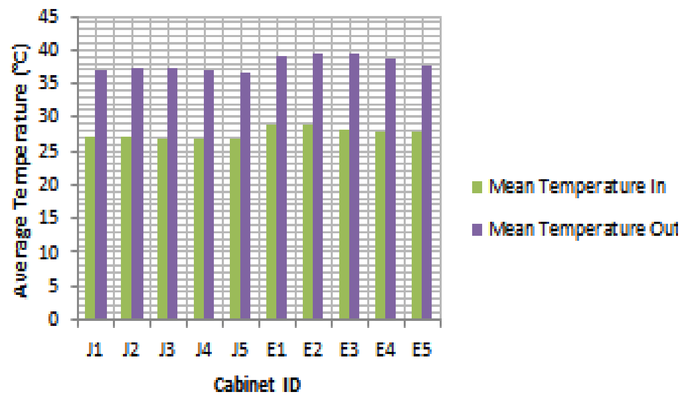

Figure 3-7: Rack Average Inlet/Outlet Temperature

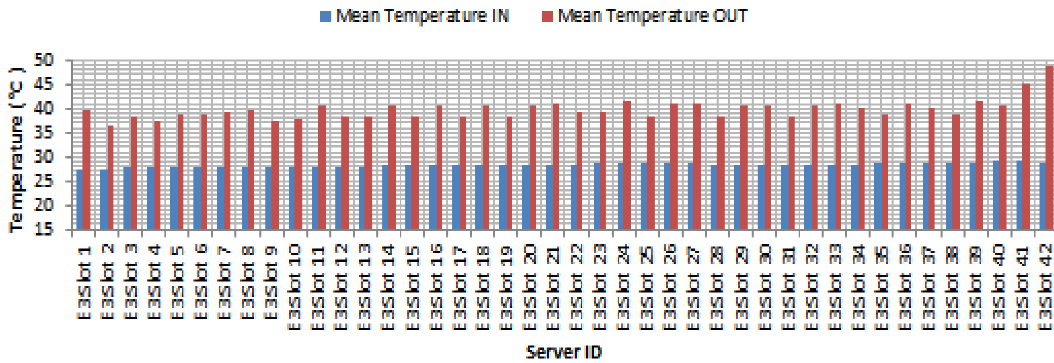

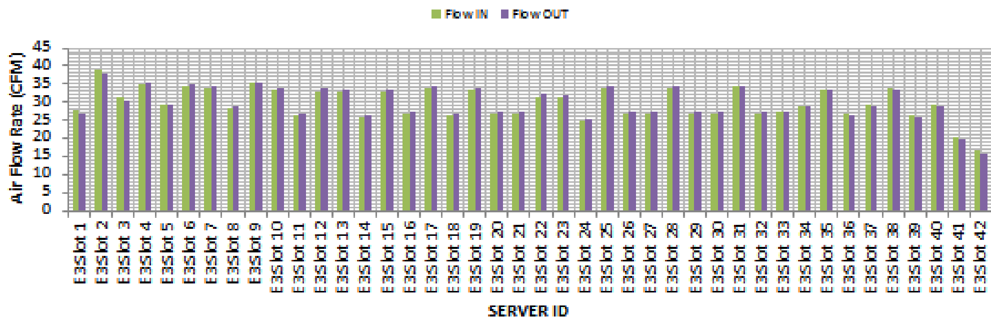

Figure 3-8: Rack Average Inlet/Outlet Temperature

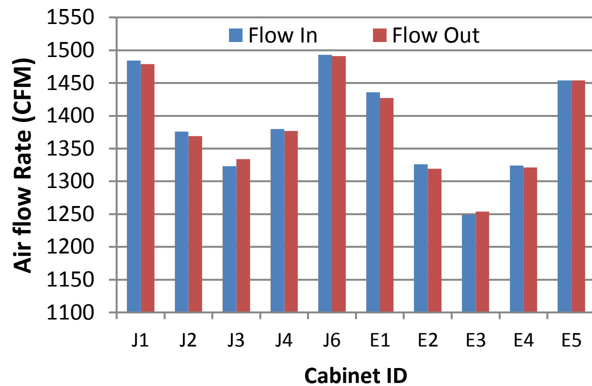

Figure 3-9: Individual Cabinet Flow Rates

The rows are labeled as Row J and Row E with 5 cabinets in each row. J1, J5, E1 and E5 represent the outermost cabinets on each row. From figure 9, it can be seen that the middle cabinets do not receive sufficient air flow. The reason can be attributed to the air flow path in the specific design and this data helps understand the limiting factor for the number of cabinets in each row. Currently, the model works well with 5 cabinets in each row, because the middle cabinet receives around 150 CFM lesser air flow rate than the peripheral cabinets. The middle cabinets did not exhibit relatively higher temperatures due to lesser flow rates.

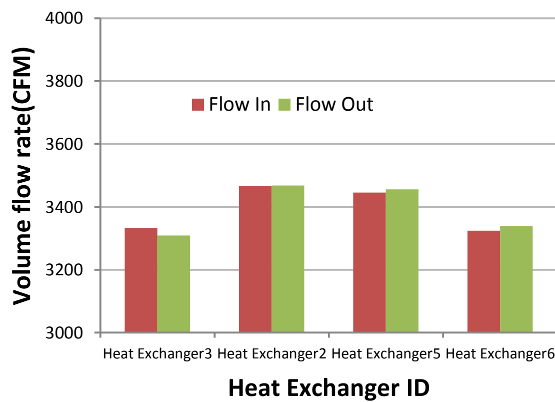

Figure 3-10: Individual Heat Exchanger Flow Rates

The air flow rates through individual heat exchangers are reported in figure 10. The heat exchanger 3 and heat exchanger 6 are located at the bottom section on either side of the aisle. It can be seen that these heat exchangers receive lower air flow rates. Because of the tendency of the hot air to rise within the aisle, the units located at the top section receive higher flow rates. This factor can influence in sizing the heat exchangers to different capacities. The difference between the top and bottom heat exchanger flow rate is 135 CFM. The hot air entering the top section heat exchangers is around 1°C higher compared to the bottom section heat exchangers. The flow going in and out of cabinets and heat exchanger is the same which ensures that there is no recirculation within the system.

Because the middle cabinet showed lower inlet temperatures, the cabinet E3 is considered to examine the temperatures and flow rates of individual servers as shown in figure 8. The flow rate varies across the height of the server. However, there is no recirculation. The individual server flow rate did not follow a specific pattern in the flow distribution. However, it is noticed that the top few servers (E39-E42) receive lower flow rates and hence exhibit higher exhaust temperatures. The total fan power in the room is calculated to be 1038 W for 24% fan efficiency based on equation 3.

$$Fan\ Power = \Delta P * \dot{Q} * \frac{0.1175}{\mu_f} \quad (3)$$

It is identified that there are three main variables that mainly influence the cooling design. It is the system resistance of the IT, pressure drop that is overcome by the fans (i.e. the only air movers in the room), temperature difference across the rack.

3.4 Case 2

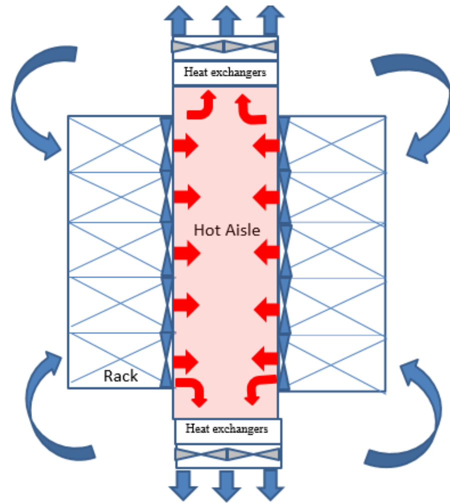

Figure 3-11: Schematic Layout of Case 2 with Active heat Exchangers and Rack level fans

This case is the same as Case 1 with group of fans arranged in series with the heat exchangers as shown in figure 11. Placing fans in series with heat exchangers enables the design to handle high resistance IT placed inside the room. The fans across the heat exchanger (second-stage fans with 200mm diameter) are selected such that they are geometrically arranged along the same size as HX surface area and in parallel to each other. The server resistance considered for the IT is based on resistance for HPSE1102 [43].

Multi-stage fans in series should handle the same amount of volumetric capacity as the first stage fans (rack level fans) [44]. Hence, the second stage fans (Φ200 mm) are selected from the commercially available axial fan catalogue based on the total CFM requirement from each heat exchanger-fan system. Figure 12 shows the air flow movement in the room.

3.4.1 Case 2 Results:

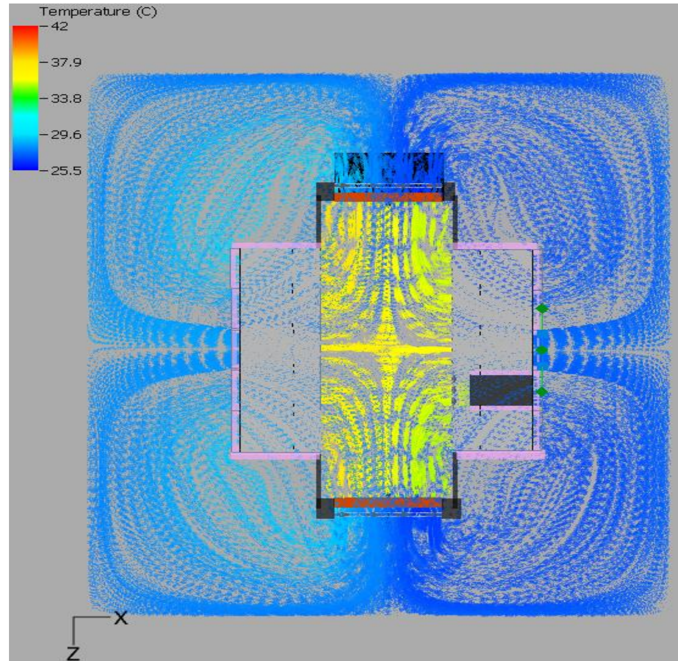

Figure 3-12: Air Flow Streamlines colored by temperature

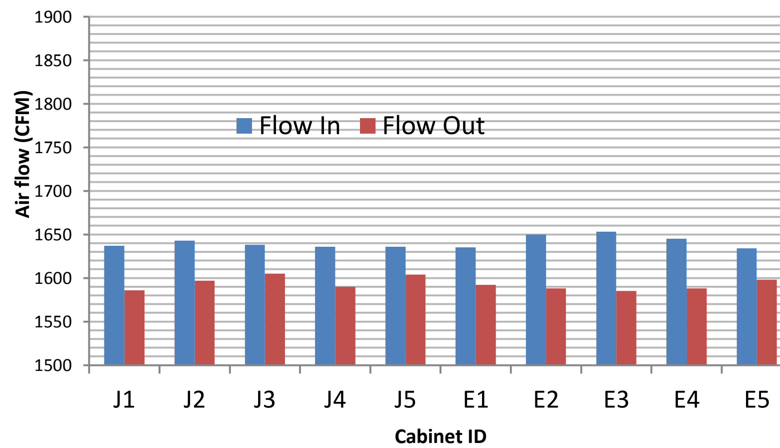

Figure 3-13: Rack Inlet and Outlet Flow rates

The total rack fan power in the room is calculated as 896.9 W. The total heat exchanger series fan power is 1227.83 W. Rack fans operate at lower pressure drop for wider hot aisle widths. The hot aisle size determines the pressure drop overcome by rack fans. Compared to case 1, the rack fans operate at lower static pressure. However, overall fan power is higher. The main advantage of case 2 over case 1 is that it can handle high resistance IT. The average temperature difference observed across the rack is 8.8°C. The average rack flow rate is 1640.7 CFM. Since the cooling design can more handle volumetric capacity the rack heat load is also scalable for increased loads.

The fan operating speeds between first stage and second stage fans is important. The fan control algorithm of the rack level fans typically controls the fan speeds based on the maximum operating temperature of a group of servers (in our case 3 servers shown in figure 5). The coordination for fan speeds between multiple stages should be such that the when rack level fans are running idle the second stages should also run at lower speeds.

3.5 Case 3

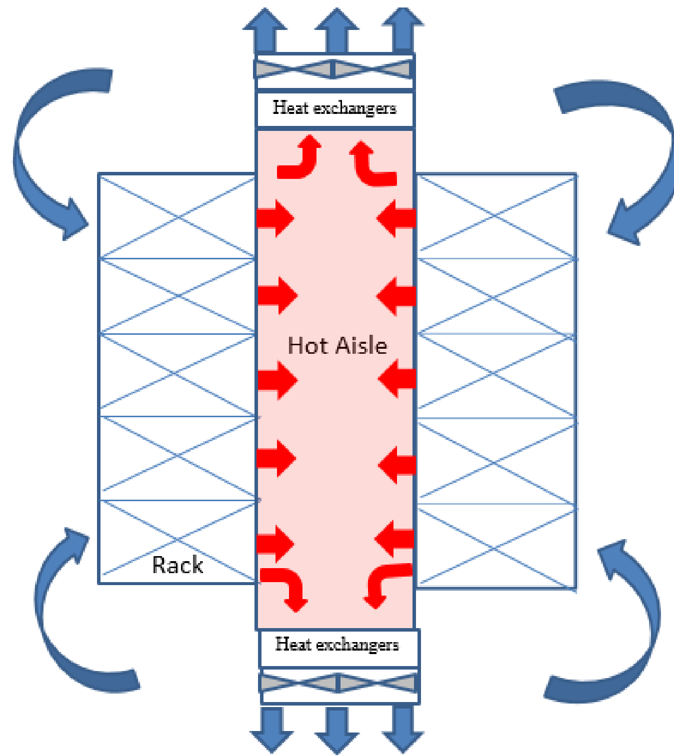

Figure 3-14: Cooling Design Schematic for Case 3

In this case, there are no rack level fans; the fans (Φ200 mm) are located only in series with the heat exchanger as shown in figure 14. This cooling design also handles higher IT system resistances in the room. The heat exchanger fans would operate at higher static pressure compared to the previous case because they are the only air movers in the room. The average temperature difference observed across the rack is 9.3°C. The average rack flow rate is 1572.9 CFM.

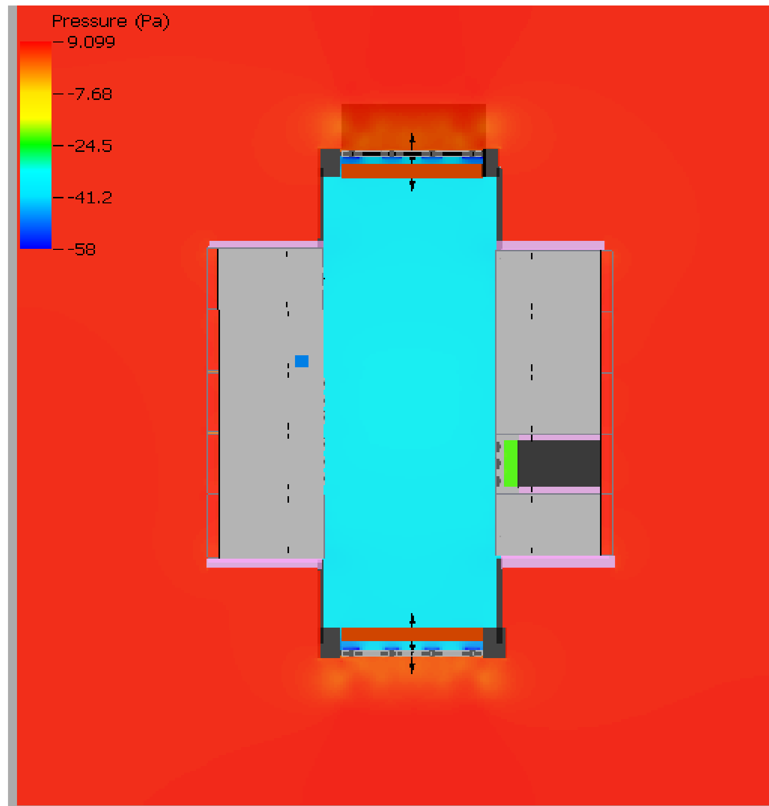

Figure 3-15: Pressure Plot for Case 3-Top view of the room with cut section running through the center of the rack height

If the fan movers are only located across heat exchanger (as in case 3) the room is more pressurized compared to case 2 as seen from figures 15 and 16. These kind of over pressurized systems might lead to an increased risk of leakage between hot aisle and cold aisle. The total heat exchanger fan power consumption in the room is 1010.55 W. The overall fan power consumption is reduced compared to case 2 and comparable to case 1.

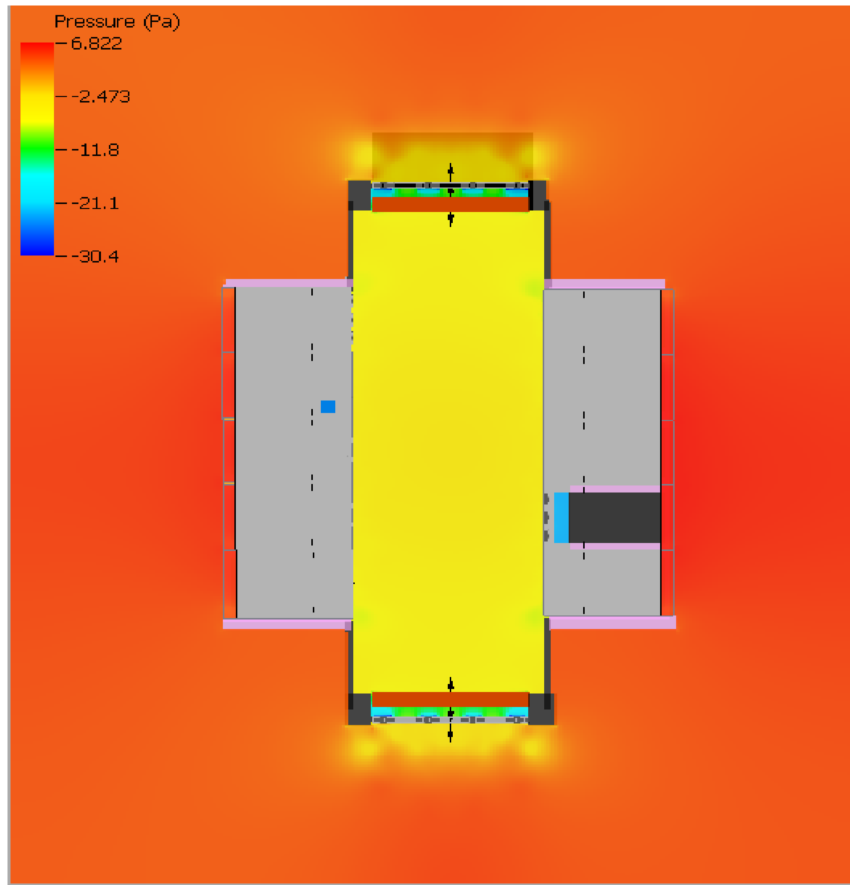

Figure 3-16: Pressure Plots from case 2- Top view of the room with cut section running through the center of the rack height

3.6 CONCLUSION

The study evaluates a new type of end-of-aisle cooling system for a small data center room using CFD. The methodology for modeling passive IT, selection of rack fan wall and heat exchanger designs including the design boundary conditions based on industry practice has been presented. The system showed acceptable temperature and air flow profile based on the given boundary conditions. The volume resistances considered for case1 design are for low resistance IT systems. However, it has been

seen that such a system if had air movers arranged in series with the IT rack fans or in series with heat exchangers can handle higher system resistance. Larger fan systems that can overcome higher resistance systems should be used to for denser IT components. The heat exchanger units are placed such that it would eliminate the risk of having cooling coils at the top of the electronic racks. The top section of servers showed higher exhaust temperatures but overheating of the IT is not observed. The fan power consumption for all three cases have been quantified. Case 2 has been an over pressurized system compared to other two cases. This can be addressed by increasing the hot aisle volume. It has also been noticed that the distance between heat exchangers and the axial fans in series for case 2 and case 3 is of importance. If the fan systems are closer to heat exchangers, then they would pull the air fasters across heat exchangers coils reducing the thermal performance of the heat exchanger. Further analysis is needed to determine the best case cooling design. The analysis would include response of the system during failure conditions, system air flow behavior when it is not isolated i.e. if neighboring IT rows are present, using blowers instead of axial fans design. Overall, the current study proposes a new cooling design that addresses the challenges for placing cooling coils at the top of the IT or at the bottom of the IT. The CFD analysis comparing the thermal performance of all three cases gave multiple design considerations to be made by opting to certain case of design.

3.7 Cooling Failure Scenarios

For all three different cases, different failure cases have been simulated by turning off heat exchangers and rack fans and heat exchanger fans in various scenarios as shown in the table 3-1 below. In typical data center set up, the IT equipment is connected to Uninterrupted Power Supplies (UPS) that turn up during a loss of utility

power to the facility. However, the CRAC/CRAH systems, chilled water pumps, chillers are often not connected to the UPS [45] . The objective is to quantify the increase in inlet temperatures and reduction in the supply rack air flow in the room due to any imposed failure conditions. The scenarios will be discussed individually as well as in comparison against default designs or other failure scenarios for all three cases. The following cases considered to be in steady state conditions.

Case	**Status of Rack Fans**	**Status of Heat Exchanger fans**	**Status of Heat Exchangers**
Case 3A	OFF	HX1-OFF	HX1-OFF
Case 3B	OFF	HX1-OFF;HX2:OFF	HX1-OFF;HX2-OFF
Case 3C	OFF	HX1-OFF;HX2:OFF	ALL-ON
Case 3D	OFF	All-ON	HX1-OFF;HX3-OFF
Case 2A	ON	HX1-OFF;HX2:OFF	HX1-OFF;HX2-OFF
Case 2B	ON	All-ON	HX1-OFF;HX3-OFF
Case 1A	ON	-	HX1-OFF;HX3-OFF
Case 1B	2 middle Rack fans OFF	-	ALL-ON

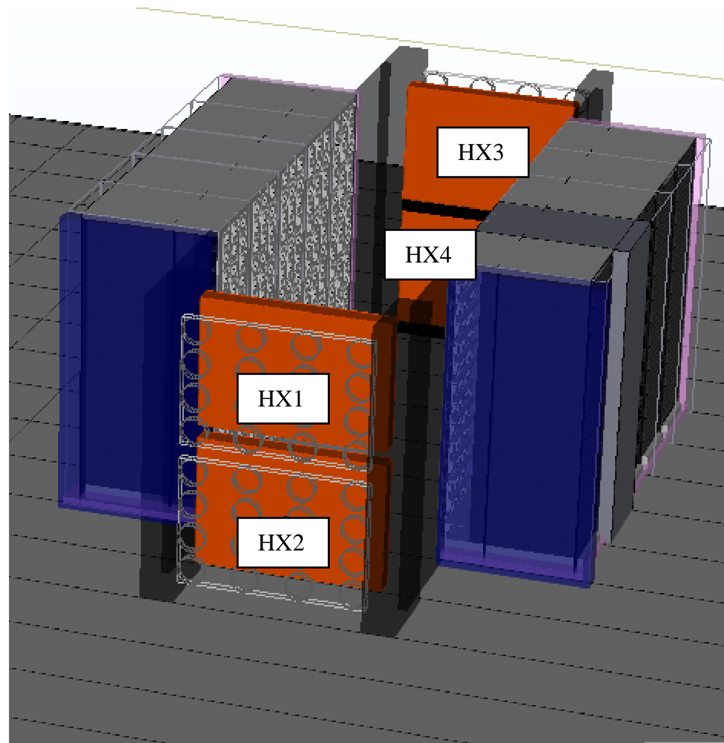

Figure 3-17: Isometric View of the room

Case 3A: This case has all rack fans turned off, with one top heat exchanger turned off and the corresponding heat exchanger fans have been turned off as well.

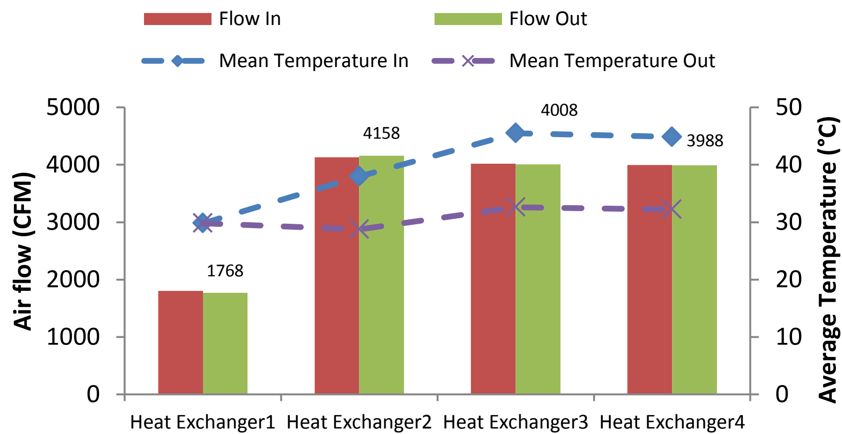

Figure 3-18: Case 3A Heat Exchanger Flow rate and Temperature parameters

As anticipated, the supply air and return air temperatures of the failed heat exchanger is the same. The air flow rate going into the failed heat exchanger is merely due to the pressure difference between the hot aisle and the cold air but no induced air flow. The average reduction in the air flow rate is 2286.7 CFM for failed HX1. HX2 has shown reduced temperature difference between supply and return air i.e. 9.2 °C compared to the temperature difference across HX3 and HX4 being i.e. 12.6 °C. The supply air temperature across HX3 and HX4 has been increased by 4.9 °C. The reason for this is being the corresponding heat exchanger fans draw the same amount of air flow not uniformly from all the rack but disproportionately. If we consider the air side energy balance equation, these heat exchanger fans (of HX3 and HX4) by drawing the same amount of air flow and increased heat load i.e. imposed due to the failed heat exchanger (HX1), the corresponding average air side temperature difference has been increased, along with rise in both supply and return air temperatures.

Case 3B: This case has both top heat exchangers (HX1 and HX3) disabled and the corresponding fan systems have been disabled as well.

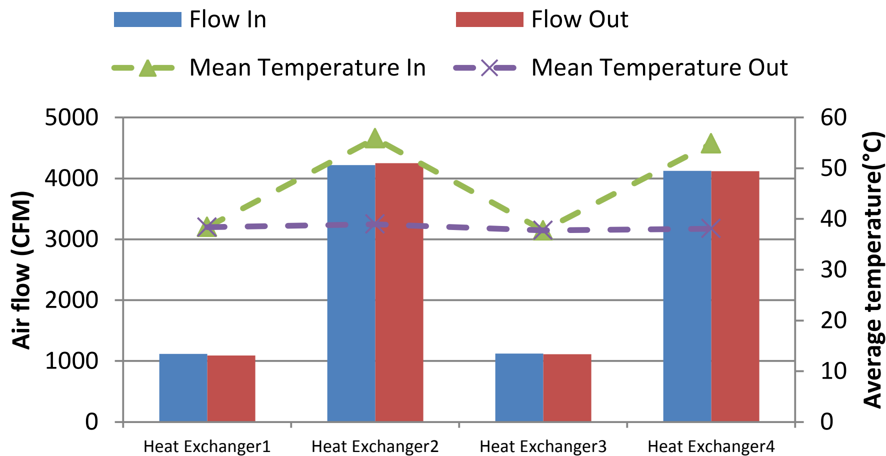

Figure 3-19: Heat Exchanger Air Flow and Temperature Parameters

The heat exchangers that have been disabled are drawing about 3101.5 CFM lower than the other two heat exchangers. The mean inlet temperatures of HX3 and HX4 have been higher by 17.3 °C. As explained in previous section (for case 3A), the reason for this is that the HX2 and HX4 that draw the same amount of air flow; with increased heat load on them, the air side temperature difference increased along with the return and supply air temperatures. This rise in inlet temperatures can be mitigated by employing fan control over individual heat exchanger fan systems. The heat exchanger fan PWMs (second-stage fan systems) must be modulated accordingly based on the return air temperatures. This type of fan control will help the fans draw in more air flow thereby reducing the overall supply air temperatures in the room in case of failure.

In terms of the rack air flow rates and the supply temperatures, there is uniformity. The average rack air flow rate is 624.06 CFM. The average temperature difference across the racks has increased to 22.9 °C by ~2.5 times compared to the default case (Case 3). The corresponding server air flow rates have decreased. However, there is no major non-uniformity even within the rack in terms of air flow rates.

Additional case has been run as a part of case 3B, where heat exchangers on one side of the aisle have been disabled i.e. HX1 and HX2, it has been noticed that the top heat exchanger (HX1) has higher return air temperature compared to HX2 by 6 °C. One the active side (HX3 and HX4), the top heat exchanger, HX3, has highest return air temperature which is 28% more than the HX4 return air temperature as shown in figure 3-21. The reason for this can be attributed to the fact that hotter air rises and quickly being drawn by the active fans of top located HX3. The temperature distribution across

the racks fluctuated by about +/- 1.5 °C for the inlet and outlet temperatures. The average rack flow rate in the room is 627.5 CFM.

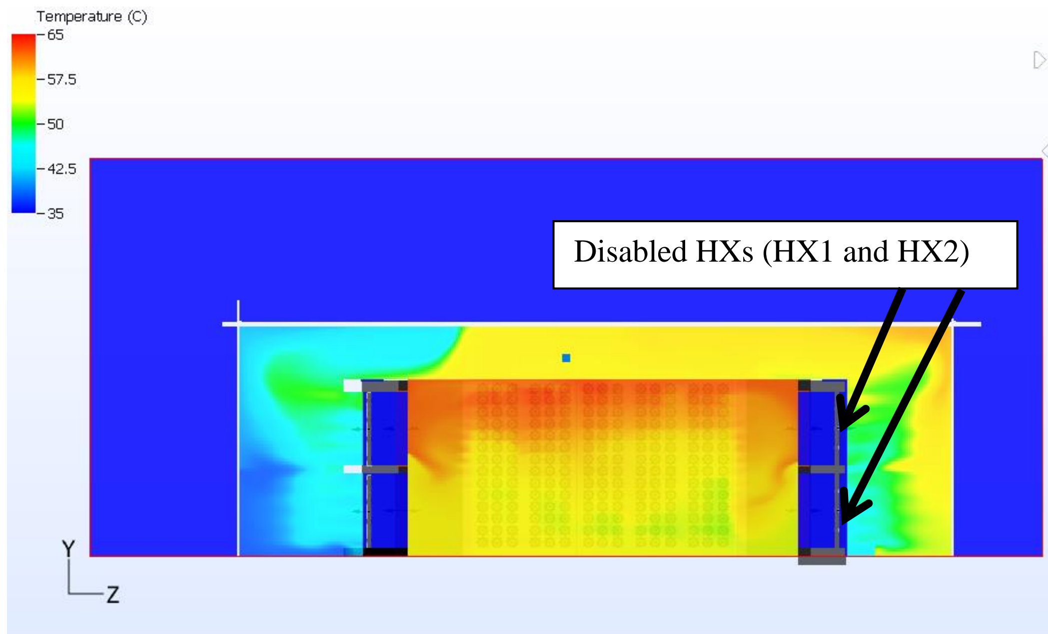

Figure 3-20: Temperature Plot when HXs on one side were disabled

Case 3C: This case represents the case where two heat exchangers on one side (HX1 and HX2) are disabled but all the heat exchanger fan systems are turned on. This scenario can be represented as work case failure scenario, since the fans are all turned on. The expectation is that hot exhaust is quickly recirculated across the room as the corresponding heat exchanger has failed. HX1 and HX2 showed inlet and exhaust temperatures (being the same) to be 58.8 °C and 53.9 °C which is about ~2.3 times more than the default case as shown in figure 3-22. The return air temperatures of HX3 and

HX4 are 36.8 °C and 39.9 °C respectively. The heat exchangers located at the top once again received higher return air temperatures. There is an average air side temperature difference of 18 °C across HX3 and HX4. Since all heat exchanger fans are working, the average HX fan air flow is 3840.8 CFM.

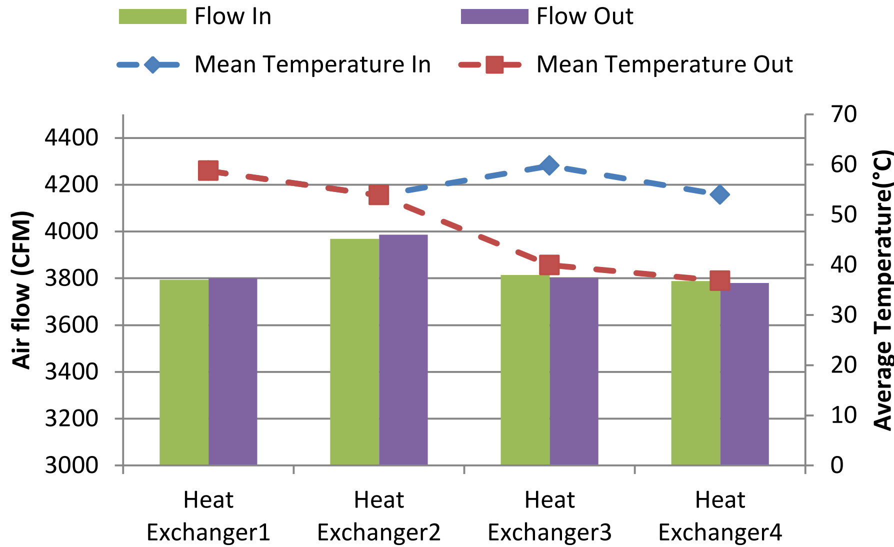

Figure 3-21: Heat Exchanger Air Flow and Temperature Parameters

The cabinet had a mean inlet temperature of 47.5 °C and temperature difference of 9.23 °C across the rack. The inlet temperatures in this case are the highest compared to the default design (Case 3) and other failure scenarios. Hence, the heat exchanger fan PWM control has to be adjusted according to the return air temperature at the inlet as mentioned in the previous case as well.

Overall, it has been noticed that the system is redundant with one of the heat exchanger failed, there is only 4.3 °C increased in the inlet temperatures. If the maximum return air temperature limit is assumed to be 55 °C, then the case 3B with heat exchangers failing on either side is reaching the maximum limit. However, the relatively

worse case is heat exchangers along with their fan systems failing only on one side. The worst case scenario is heat exchangers failing on one side and fans are running at a higher PWM (above 50% in our case).

Case 2A: This case corresponds to the simultaneous heat exchangers and attached fan systems failures. HX1 and HX2 air flow rate is about 3.3 times lower compared to the other two active heat exchangers. The air temperature across HX1 and HX2 is 52.1 °C which is very close to the assumed higher limit i.e. 55 °C. The air temperature across HX3 and HX4 is about 12.6 °C higher than the default case. The return air temperatures have reached their maximum limits. So even with the presence of rack fans to move the air in the heat exchanger failure on one side imposes a huge risk of rising inlet temperatures in the room. The average rack air flow is is 1215.1 CFM. Maximum rack inlet temperature is 43.2 °C. Maximum hot air temperature across the rack is 55 °C.

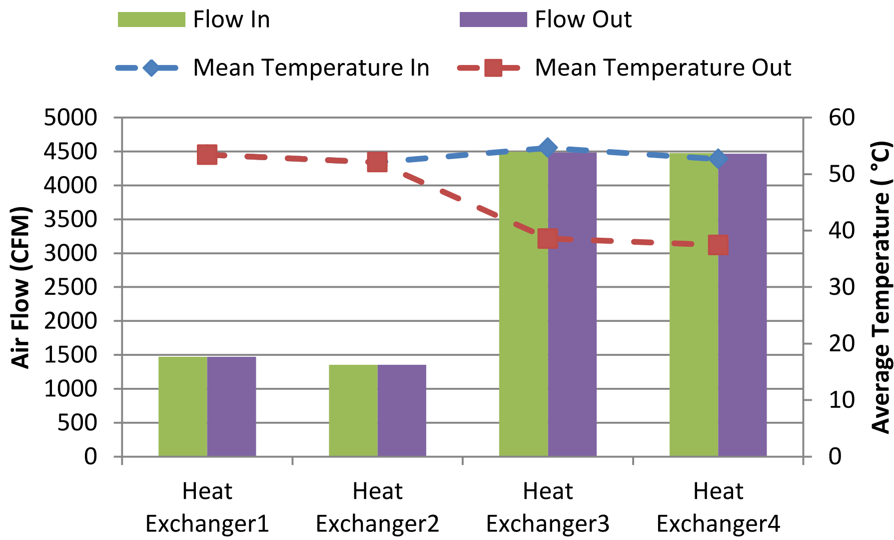

Figure 3-22: Heat Exchanger flow and Temperature Parameters

Case 2B: This case describes the scenario where the top two heat exchangers are turned off and but all the heat exchanger fan systems are running.

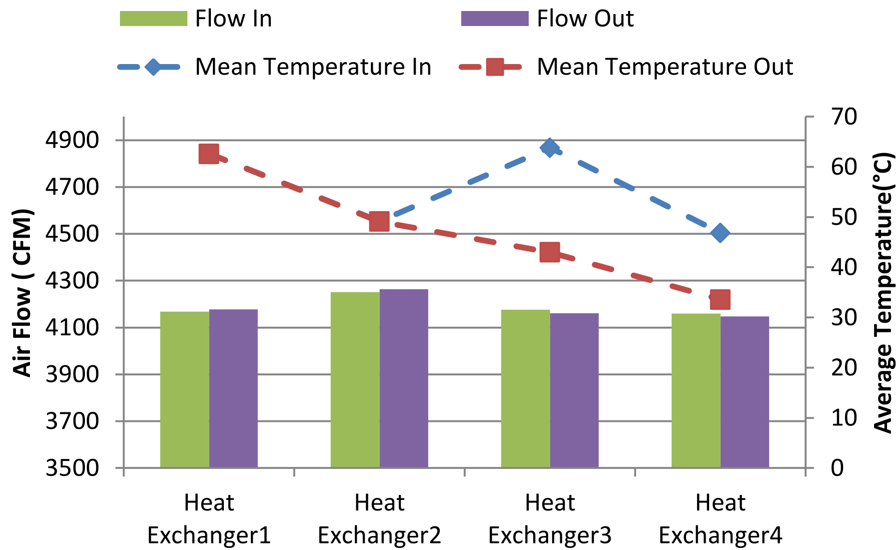

Figure 3-23: Heat Exchanger Flow and Temperature Parameters

The average heat exchanger air flow is 4188.75 CFM. The air temperature across the failed heat exchangers is 1.5 times higher than the active heat exchangers. The HX1 and HX2 show 62.6 °C and 49.1 °C return/supply air temperatures respectively. The heat exchanger failure without fan failure is the worst case scenario to happen. Compared to 3C, this case shows that a return air temperature across the heat exchangers as well as higher inlet air temperatures to the rack (46.7 °C) is not very different. The presence of rack fans (running at the same PWM as the default design-Case 2) neither worsen nor improve the hot air exhaust temperatures in the room. The average rack air flow is 1606.6 CFM. This is also not very different from the case 3C (1565.7 CFM).

Pressure plots in Case 3C and Case 2B are vary significantly. Case 2B has hot aisle more pressurized compared to cold aisle and Case 3C has the room at high pressure compared to the hot aisle.

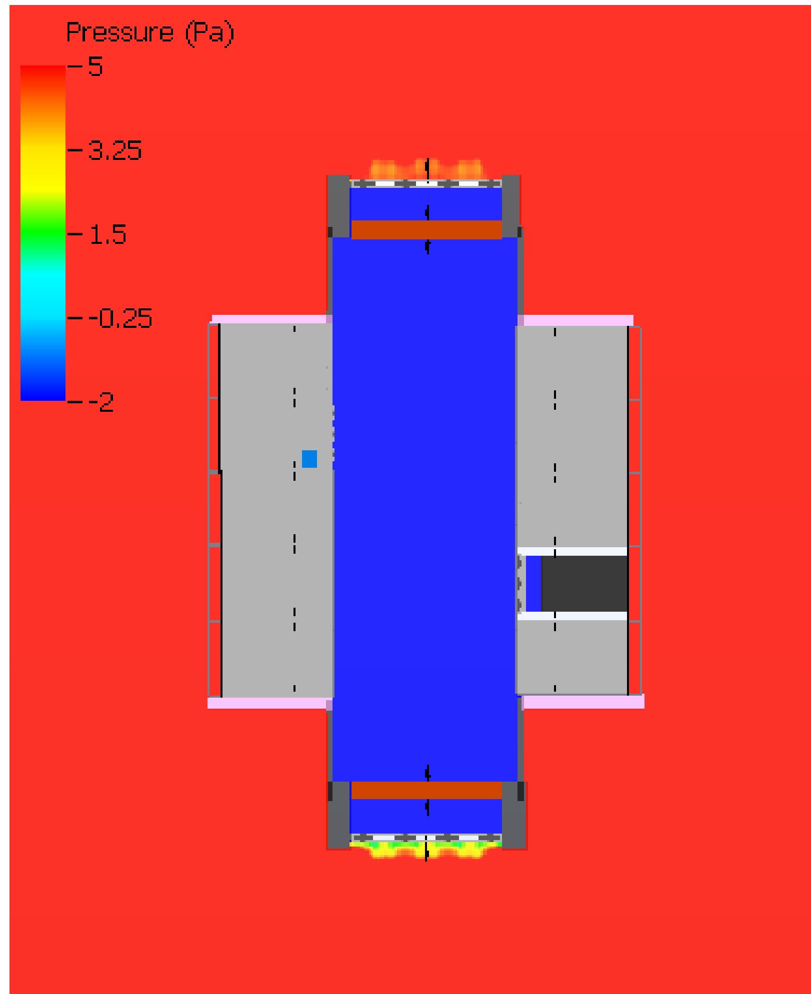

Figure 3-24: Pressure Plot for Case 3C (for same legend)

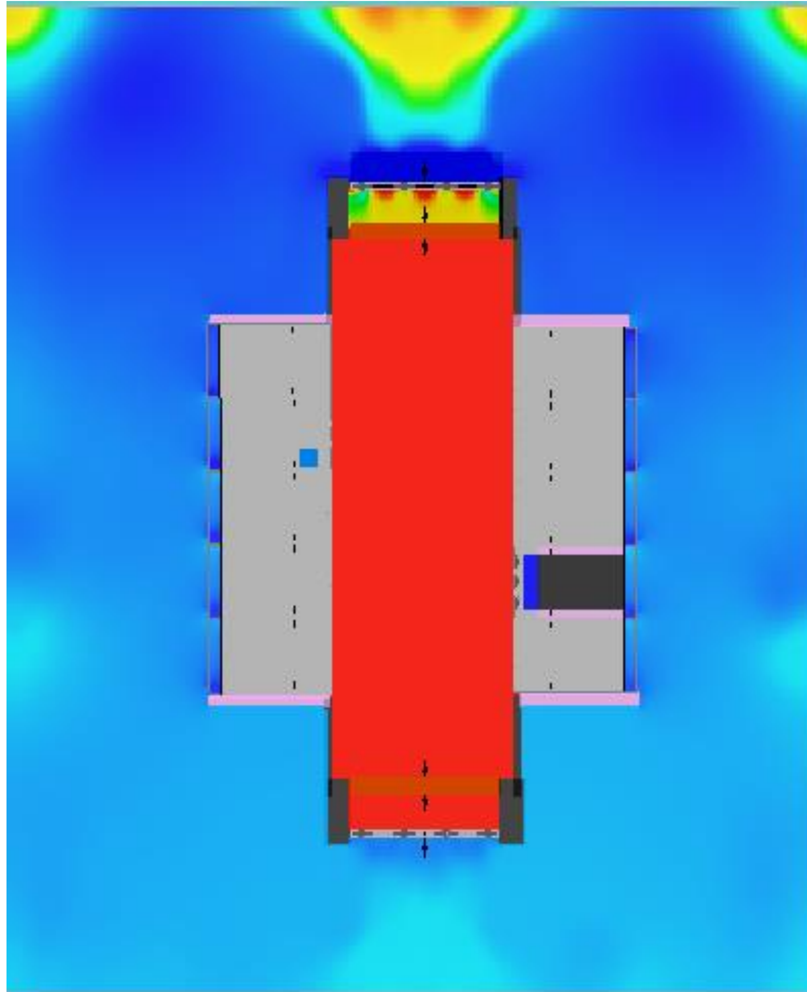

Figure 3-25: Pressure Plot for Case 2B (for same legend as figure 3-24)

The presence of rack fans in Case 2B blowing high pressure air in the hot aisle is driving the flow in this case. That is why the air flow across the heat exchangers is higher than that of Case 3C case.

Case 1A: In this case, the top two heat exchangers HX1 and HX3 are turned off. The rack fans are not turned off. It was seen that the temperatures in the room did not reach a

steady state during simulation. The fan temperatures especially for the fans located at the upper half section of the rack exponentially increased with each iteration. The average inlet temperature into the racks is varying. Since, only top section heat exchangers have been disabled, the top half of the server received inlet temperatures higher than 120 °C and the first half bottom section of the server received temperatures of about 36 °C inlet and second half of the bottom section received about 58.6 °C. The inlet temperature is ranging between 29.7 °C and 170 °C. The location of the heat exchanger failure influences the section of servers being affected by extreme over heating temperatures.

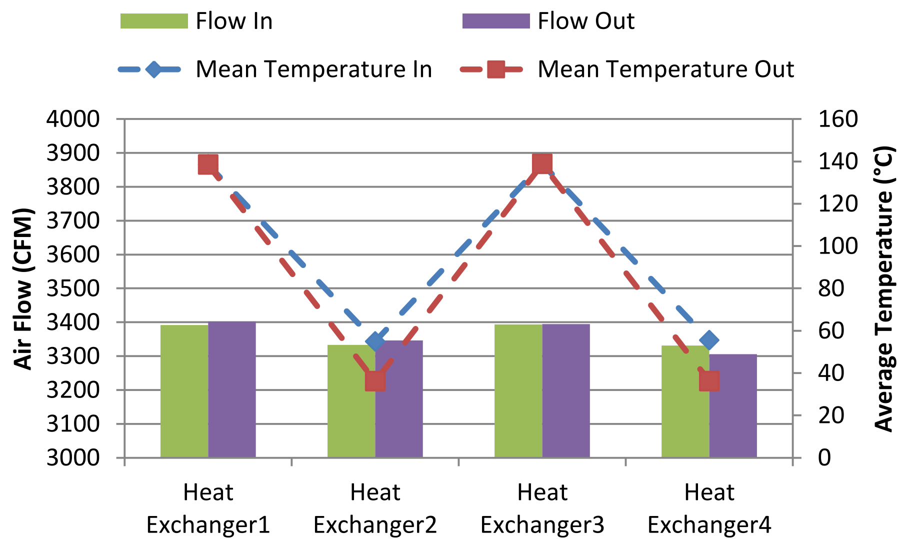

Figure 3-26: Heat Exchanger Flow and Temperature Parameters

The average temperature difference across the heat exchanger for HX2 and HX4 is about 19.2 °C. The average rack air flow rate is 1367.7 CFM. Unlike case 2 and Case 3 failure scenarios, in this case, the rack fans should modulate based on the supply air temperature of the rack (or heat exchanger) not only based on CPU based temperature.

Case 1B: This section considers both the top heat exchangers to be turned off and the rack fans of the middle racks (which typically the racks which receive lower flow rate compared to the exterior racks). It has been noticed again that during the simulation the fan temperatures of the upper section of each rack are increasing with every iteration. The average air flow across the heat exchanger is 2809.5 CFM. The inlet temperature for HX2 and HX4 is 32.7 °C. The inlet temperature from disabled HX is about four times higher. The middle racks J3 and E3 have their fans turned off. Because of lack of pressurization in J3 and E3 racks the hot air exhaust from hot aisle is entering the neighboring racks from them as shown in Figure 3-30.

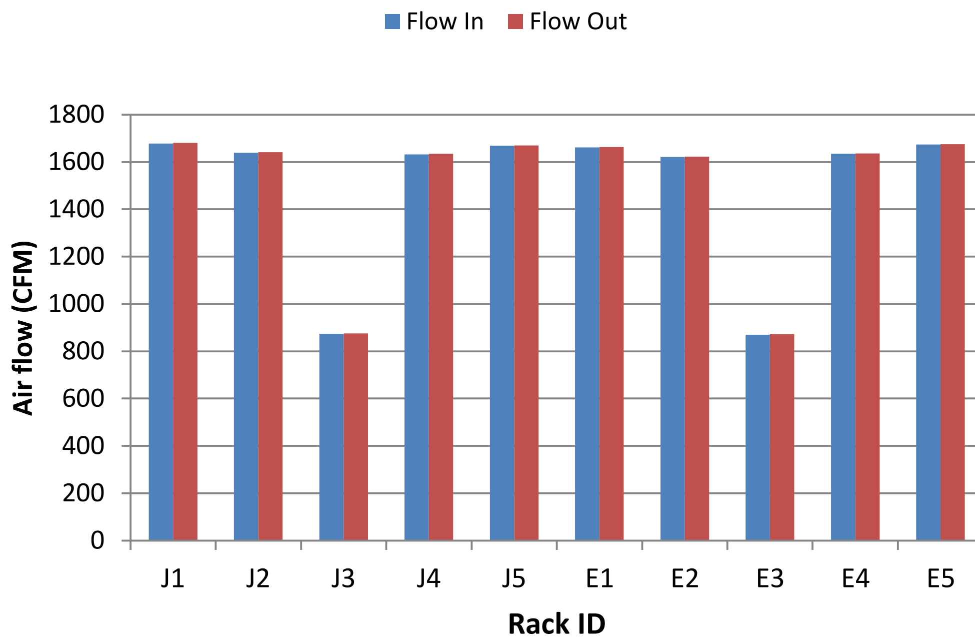

Figure 3-27: Rack Air Flow Rates Showing Lower Flow Rates for J3 and E3

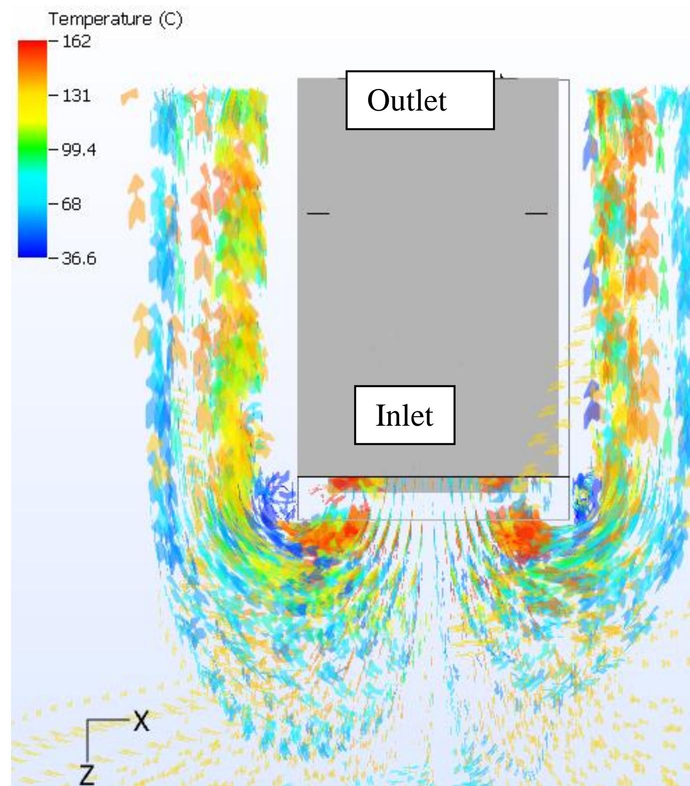

Figure 3-28: Hot Air Exhaust from E3 rack entering neighboring racks

The average rack inlet temperature is 82.9 °C. This scenario can be considered the worst case. The room temperature will quickly escalate to overheating temperatures. The racks J3 and E3 have showing higher temperatures because of the recirculation taking place from the hot air exhaust. The pressure plots shown in figure 3-31 demonstrate the low pressure regions in the hot aisle across servers J3 and E3 that are re-circulating the air into the neighboring cabinets.

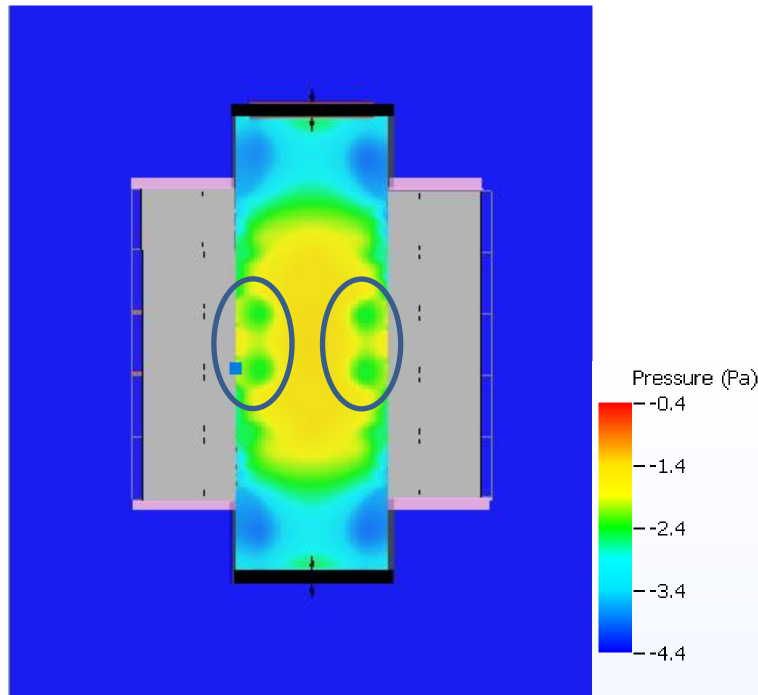

Figure 3-29: Pressure Plot in the room with cut plane across mid height of the racks (circled areas)

Additional case with only one top heat exchanger, HX1, failure has been simulated. It shows that the system is not over heating and the return air temperatures i.e. 47.7 °C are below the maximum limit. The failed heat exchanger would transport air temperature of 46.4 °C. The racks J2, J3 and E2, E3 have received lower CFM compared to other racks. There is non-uniformity in the temperature distribution across the racks. There is about 4 °C variation in the different rack inlet temperatures. But the system is not overheating unlike other failure scenarios Case 1A and Case 1B. Unlike failure scenarios of case 2 and case 3, if the rack fans are running in regular mode, there is no pressure losses in the hot aisle due to heat exchanger failure. Only the temperatures are impacted

not the pressure profiles. The system is redundant for one heat exchanger failure during operation.

Overall, in all three cases of failure scenarios, it has been noticed that if two heat exchangers fail on one side it will be the worst case scenario. The case 1 failure scenarios have so far reported about 40 °C higher temperatures than the assumed upper hot aisle temperature (55 °C). Case 2 and Case 3 shows similar results during worst case failure conditions (both heat exchangers on one side without fan failure). Transient analysis is needed to estimate for each worst failure condition in all three different cases how much time it takes for the return air temperature in hot aisle to reach the maximum limit i.e. 55 °C.

3.7.1 Fan Control considering the failure scenarios

In all the cases, the rack fan control algorithm works in such a way that the rack fan RPM should raise with rise in the CPU temperature. This is one general way of controlling the overheating of CPUs/ major processors in data center racks. However, beyond a certain higher operating limit on the CPU temperature, the server would shut down. Since the servers are do not include any fans within them, the rack fan RPMs should slow down (as a part of secondary fan control scheme) with the increase in rack inlet temperature so that there will be more time for the room to reach unacceptable (i.e. greater than 55 °C) return air temperatures. Considering case 2 and Case 3 i.e. default designs, the second stage heat exchangers can modulate to achieve the desired supply air temperature. Also, the active fan heat exchangers should always maintain a certain minimum PWM such that they would not transfer the fan energy on to rack level fans to

move the air flow in the room. However, when the heat exchangers fail without fan failure, the active fans which would otherwise run at higher RPMs (to reduce the liquid coolant temperature), could distribute the hot air quickly across the room. This would lead to room reaching unacceptable temperature affecting the reliability of the equipment. So, beyond certain coolant inlet temperature (greater than 45 °C) the active HX fans should shut down or run at idle PWM. The overall idea is that the effectiveness of the cooling design is also highly dependent on the effectiveness of fan control algorithm mainly for the heat exchanger fans in case 2 and case 3 and its corresponding failure scenarios.

Both the rack level fans (first stage fans) and the heat exchanger fans (second stage fans) need primary and secondary fan control algorithms. For the first stage fans it is based on the CPU temperature and rack inlet temperature. For the second stage fans, it is based on the supply air temperature and the coolant temperature.

CHAPTER 4

RACK LEVEL STUDY: COMPARISON OF DISTRIBUTED AND CENTRALIZED PUMPING SYSTEMS

© [2017] IEEE. Reprinted, with permission, from [SEMI-THERM 33rd Annual Symposium, and March/2017] [46]

In the wake of ever-growing demand for power and energy across US and worldwide, development of energy efficient solutions has become very important. Considering data center applications, cooling power consumption constitutes significant part of the overall energy usage of the system. In the process of optimizing the energy consumed per performance unit, liquid cooling has become one of the key solutions. In this study, 2OU (OpenU; 1OU = 48mm) web servers are tested in a rack level and the effect of higher inlet temperatures in terms of IT and cooling powers, and internal component temperatures are reported. The study serves as a comparison for two different coolant pumping systems i.e. distributed vs. centralized systems. The cooling set up includes a mini rack capable of housing up to eleven liquid cooled web servers and two heat exchangers that exhaust the heat dissipated from the servers to the environment. Each server is equipped with two cold plates cooling the CPUs while rest of the components are air cooled. The configuration that consists of cold plates with integrated pumps is referred as distributed pumping system. Whereas, the configuration with no integrated pumps at cold plates and only has two pumps placed in series with heat exchanger at the rack is referred as centralized pumping system. To study performance characteristics such as device temperatures and power consumptions of server components, synthetic load has been generated on each server using stress-testing tools. The servers are tested for higher inlet temperatures ranging from 25°C to

45°C which falls within the ASHRAE liquid cooled envelope, W4 [47]. This current work is a follow-up study to the analysis conducted comparing centralized and distributed pumping [48].

4.1 Experimental Setup

4.1.1 Server Configuration

Each server tray consists of mainly an Intel v2.0 motherboard [49], hard disk drive, mid plane board, bus bar clip and two 80mm fans as seen in Figure 1. The cover with ducting is shown in Figure 2. The chassis dimensions are 804x171x88 mm³.

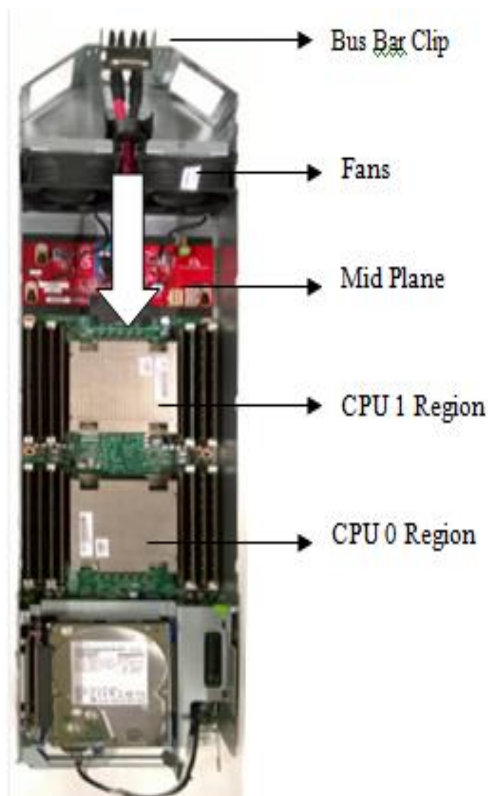

Figure 4-1: Intel based 2OU Air-Cooled Server

Figure 4-2: Cover with ducting for the server

The motherboard has two CPUs and up to 16 DIMMs of installable memory. Each CPU has a thermal design power (TDP) rated up to 115 W. Each server is equipped with active cold plates which indirectly cool the CPUs and a fan-assisted radiator which re-circulates air within the server cooling the rest of the heat dissipating auxiliary components as shown in Figure 4-3. Also, the arrow marks shown in Figure 4-3 indicate the direction of air flow that is circulated within the server and is responsible for cooling the auxiliary components like DIMMS, PCH, VRDs, and HDDs. The fans are 4-wire pulse width modulation (PWM) controlled [50] with 975-10000 rpm range. The baffle shown in Figure 4-2 forced the flow on to the DIMMS present on left hand side (LHS) as the air flow comes from the fans in Figure 4-3. In essence, each server is mainly liquid cooled as the coolant entering the chassis passes through the radiator and two cold plates in series before exiting. Each cold plate has a distributed pump (circled in the figure) integrated to it as shown in Figure 4-4. The flow is driven across the system by means of these pumps. The rated power consumption and speed of the distributed pump is 3.6 W and 6250 rpm. Whereas, in centralized pumping case two pumps are attached in

series to the liquid to liquid heat exchanger as shown in Figure 5. This unit is a 19” rack mount appliance that is sled on top of the servers while running the centralized pump case; this is explained in detail in the later section.

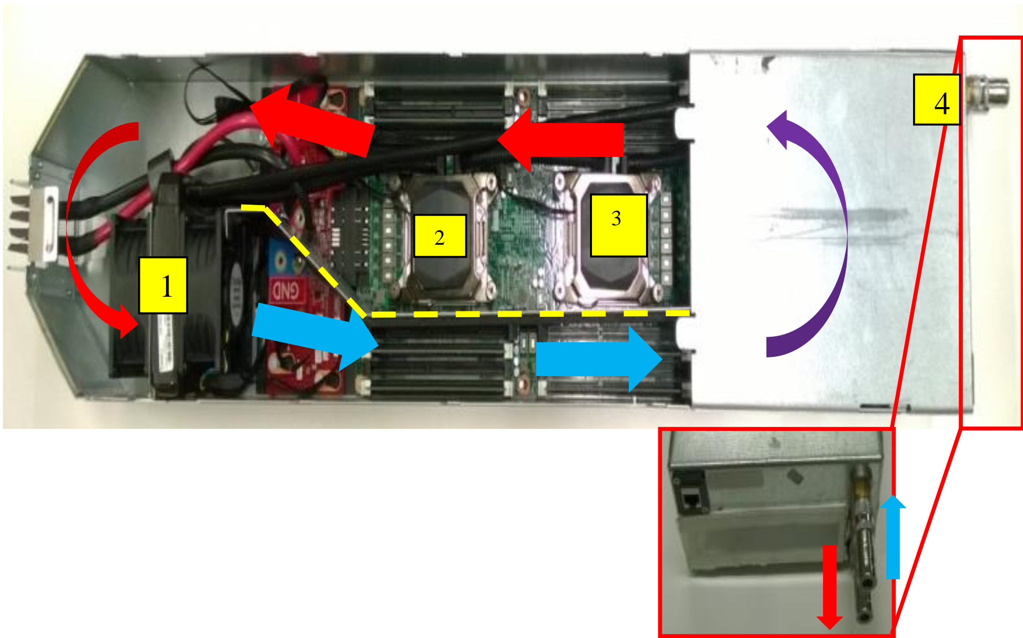

Figure 4-3: Server showing fans and cold plates air circulation 1) fans with radiator 2) cold plate on CPU1 3) Cold plate on CPU0 4)Quick disconnects with arrows showing server inlet and outlet

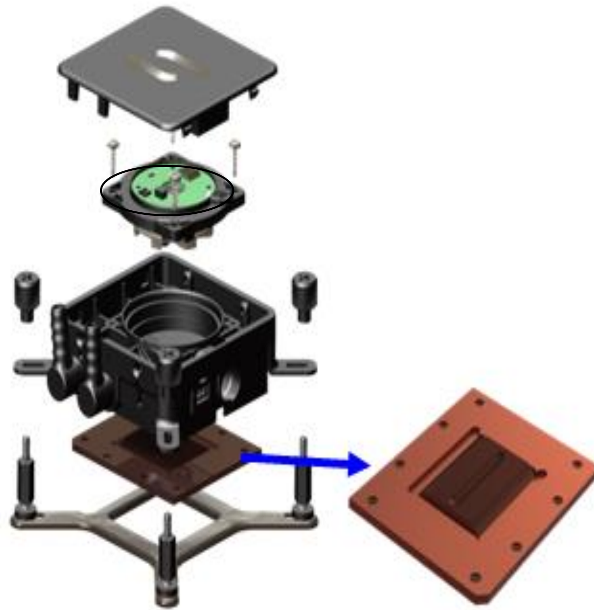

Figure 4-4: Active V-groove cold plate with pump attached to it

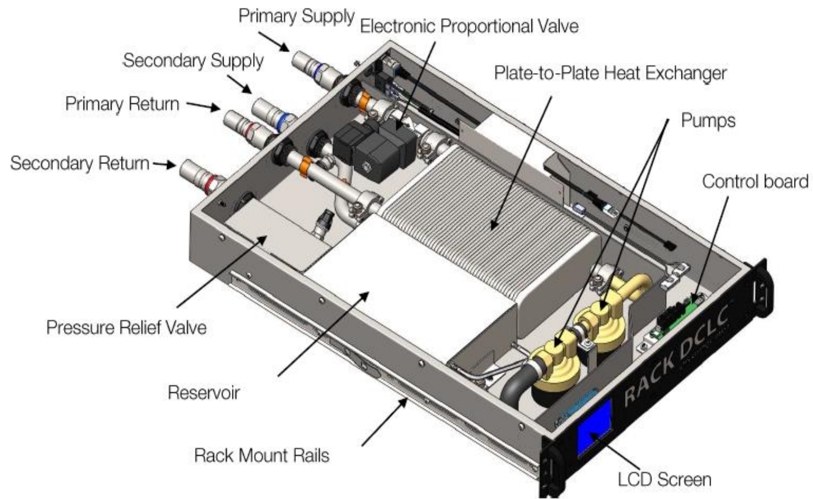

Figure 4-5: 2U Centralized Pumping Module integrated with liquid to liquid heat exchanger (CHX40)

4.1.2 Rack Configuration

The rack is placed in the test bed data center equipped with CRAH Unit and 3 Open compute 45U racks filled with 1U resistive heaters. The experimental setup includes one-third size of an Open Rack V1.0 [51] with a network switch, power shelf and four 2 OU slots as shown in Figure 6. Additionally, the rack is equipped with two heat exchangers, a liquid-to-liquid plate heat exchanger (CHx) in Figure 4-7 and a side car liquid-to-air heat exchanger (AHx) in Figure 8 each incorporated with a corresponding coolant reservoir and a control system. The Ahx consists of twenty 1200 rpm 4-wire fans and two HFD5 pumps. Essentially, there are two cooling liquids which operate the cooling cycle; the liquid that flows through the cold plates into the server is called as primary liquid (coolant) and the liquid with which primary coolant exhausts its heat by means of the plate heat exchanger is called as secondary liquid (facility liquid). The Ahx control system helps in varying the inlet temperature of the facility liquid by controlling the fans and pumps. A shut off valve is in the pipe that carries the facility liquid, as seen in Figure 4-7. The CHx control system reads the temperature of the inlet and outlet primary liquid and is used to control the shut off valve. For the centralized pumping case, the IT hard ware and AHX unit stayed the same while the pumps at server level have been disabled.

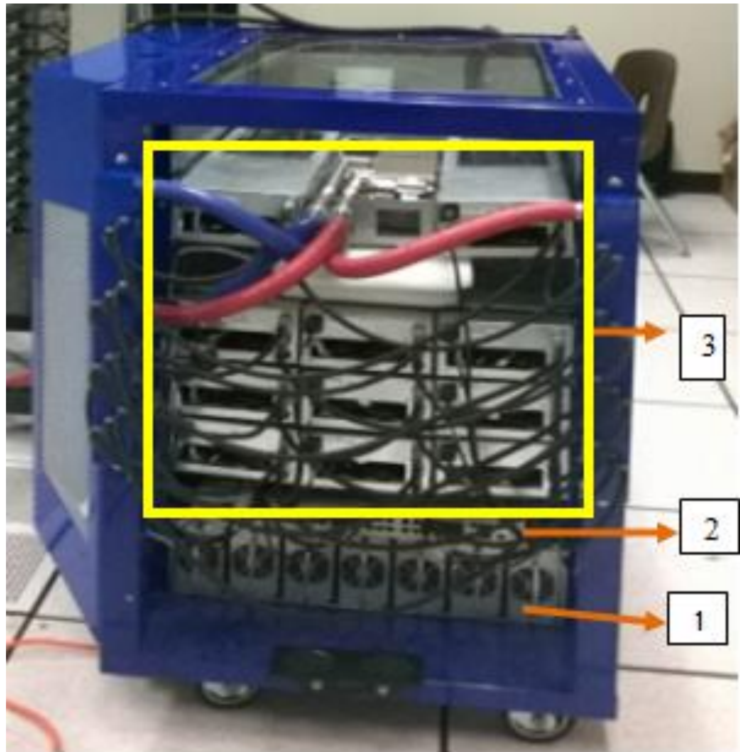

Figure 4-6: Mini-rack showing 1) power shelf 2) network switch 3) four 2OU slots

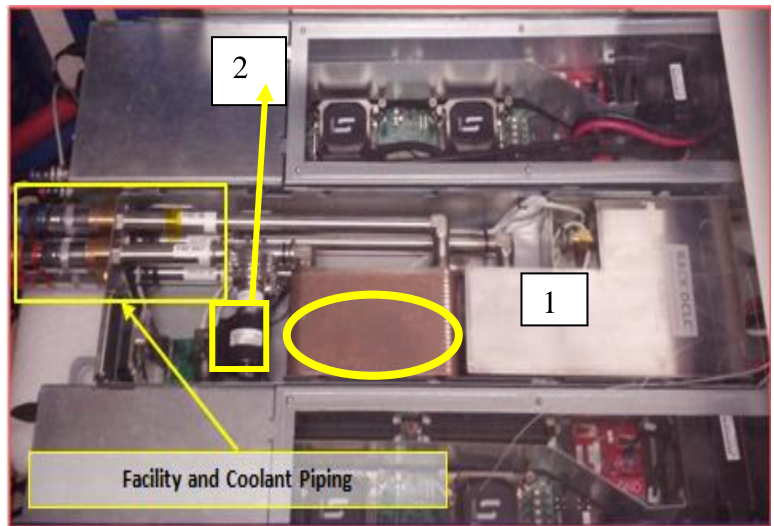

Figure 4-7: Liquid to liquid HX (circled area) 1)CHx coolant reservoir 2)Shut off vale

The CHX unit has been replaced by a 2U centralized pumping unit as shown in figure 4-10 [52]. This unit is a different design compared to the centralized system that is used for the initial set of results [48]. The coolant used in the system is ethylene glycol based water solution. The CHX unit is different for distributed and centralized case. Figure 4-7 shows the unit for distributed case. The CHx40 unit shown in figure 4-5 is the unit used in centralized case i.e. it basically includes the two pumps external to the servers and in series to the liquid-liquid HX. The default flow rate in the CHX 40 is 5.4 lpm being delivered at rack level.

4.2. Cooling Process

The cool primary liquid distributed from the common inlet manifold (Figure 9) enters each server by means of the server inlet (Figure 3). Within the server, it firstly enters the radiator and then into the cold plates in series. The hot coolant from each server is collected into the outlet manifold shown in Figure 9. It then enters into the liquid to liquid plate heat exchangers where it exhausts its heat to the secondary liquid. The cooled primary liquid enters the reservoir and again is distributed into the inlet manifold. On the other hand, the hot secondary liquid then enters the liquid to air heat exchanger where it exhausts its heat to air (Figure 4-8) by means of the 4-wire fans cooling the Ahx coil.

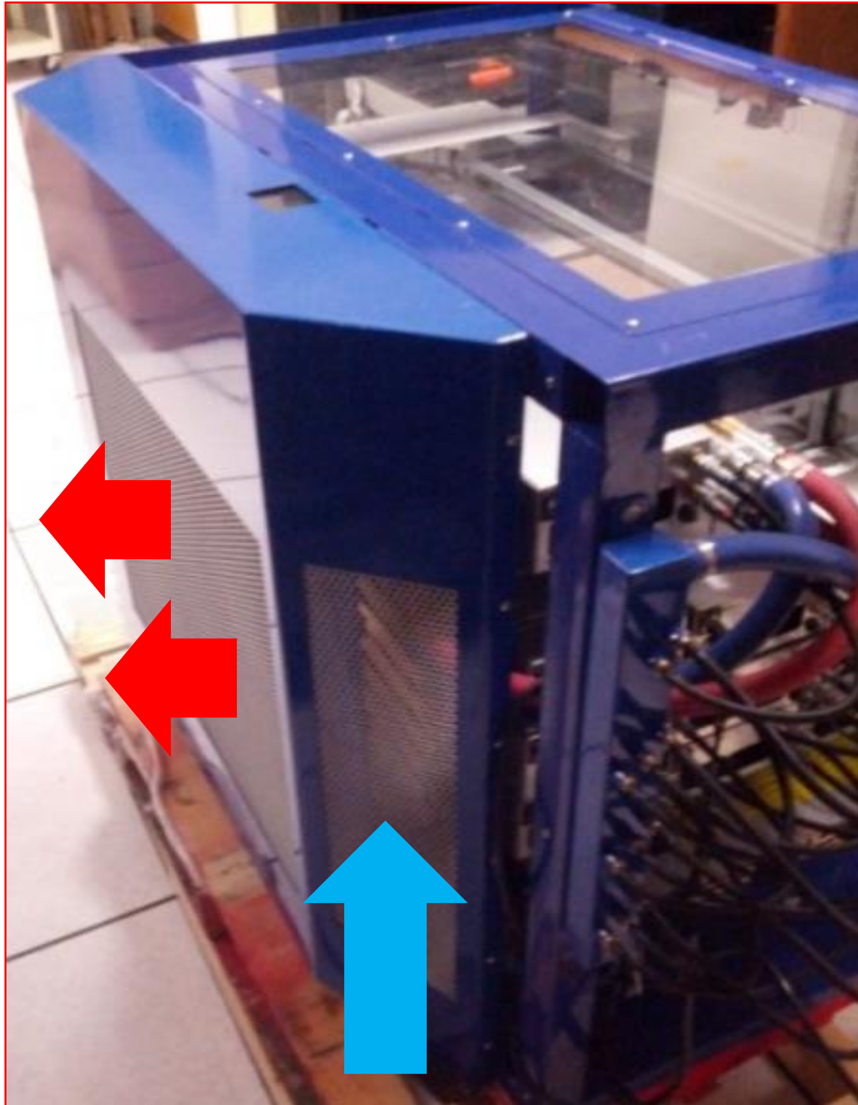

Figure 4-8: Side car liquid to air HX with arrow marks showing the direction of inlet and exhaust air

Figure 4-9: Inlet and Outlet Manifolds (highlighted areas)

4.3 Testing Procedure

Our primary goal is to measure the cooling power consumption and component temperatures associated with each server at different coolant inlet temperature varying from 25°C to 45°C. The power consumption from fans and pumps has been done separately i.e. external prototype PCB boards soldered with shunt resistors, 4-wire connector pins are set up to power fans and pumps using DC power supply units and these values are measured using an Agilent Bench link Datalogger [53]. The pumps are constant flow type and fans are of variable speed control, we can observe the variation in fan power consumption triggered by the component temperatures.

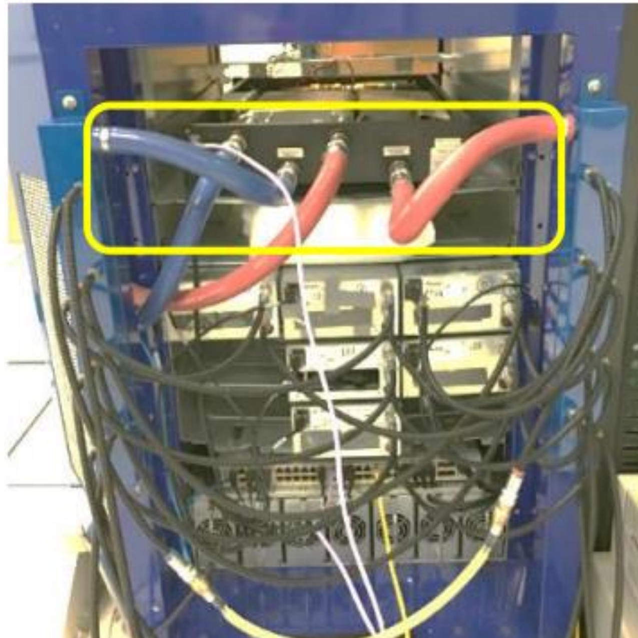

Figure 4-10: a) CHX 40 (left) replaced on the top of the rack with centralized pumps driving the flow in the system b) previous design of centralized system (right) - the location of the pumps are highlighted

4.3.1 Hardware For Power Measurements

Prototype boards, shown in Figure 9, have been used to design the control circuit in such a way that the fans and pumps are powered using external DC power supply but the control signal is sent back to the mid plane control circuit. The power requirements needed for the fan and pump is 12V each. The current consumption is measured using a data acquisition unit.

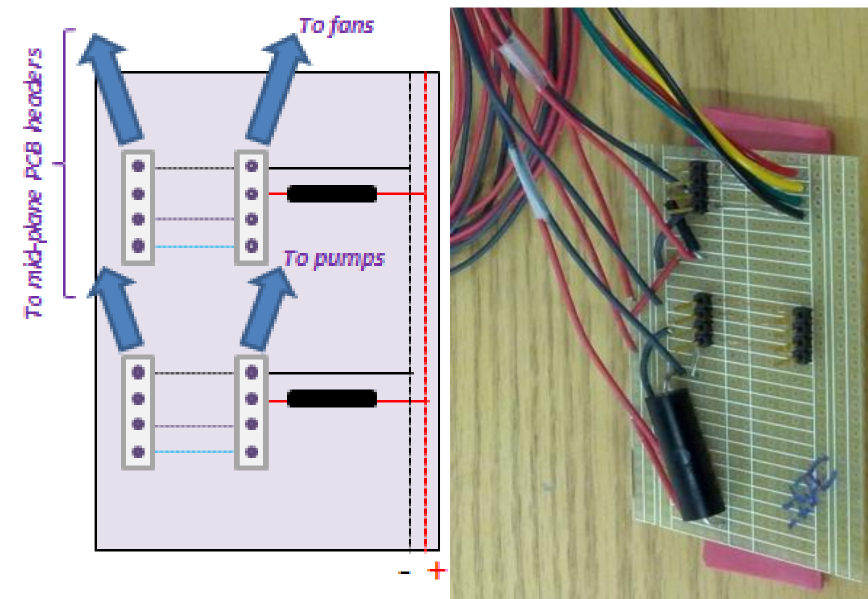

Figure 4-11: Prototype board used to measure the power of fan and pump

4.3.2 Desired Coolant Inlet Temperature

The first part is to achieve the desired inlet temperature of the primary liquid starting from 25°C to 45°C in the increments of 5°C. An allowance of ±1°C in the temperatures is considered in the tests. A control system using *LabVIEW* software [54] is developed to modulate the coolant inlet temperature as shown in Figure 4-11. The

desired set point, say 25°C, is achieved by controlling the shut off valve (ON/OFF) and the Ahx fan speeds.

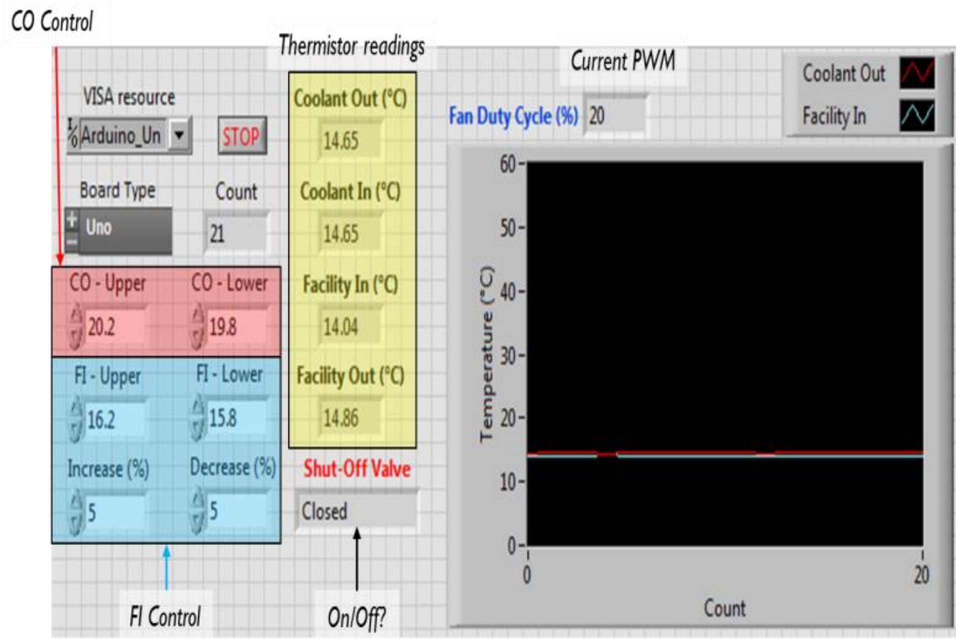

Figure 4-12: LabVIEW interface showing input and control parameters

The software works as an interface between the control parameters and the desired set point temperature. It reads the input from the thermistors that measure the temperature of the coolant liquid in and out and facility liquid in and out (from an Arduino UNO interfaced with CHx control circuit) and adjusts the shut off valve and Ahx fans' speed as shown in figure 10. The offset among the input parameters that are specified in the control system i.e. the coolant out (liquid entering the servers), facility in (liquid entering the Ahx) temperatures and AHX air supply temperature from the CRAC unit is achieved by trial and error.

4.3.3 Synthetic Load Generation and Data Collection

A total of six servers are tested simultaneously in the rack as shown in Figure 12. A communication to each server is made by the static IP address allocated to each server. The servers are referred as shown in Figure 12. The second part of the test is to load each server computationally at different CPU power levels varying from idle to 100% and CPU as well as Memory i.e. CPU at 100% power level while Memory (MEM) runs in read/write mode. For instance, at 40% power level, all the cores are loaded with 40% power usage and at 100% power level all the cores of the CPU are computationally loaded thereby heating the components to the desired level. The operating system used on the servers is Linux. Different parameters like temperatures of CPU, PCH, memory modules and rpm values of the fan and pumps etc. are monitored by the internal thermal sensors and tachometer signals [49] using *Intel PTU tools.* Also, IPMItool [55] is used to monitor the fan-pump speeds, total server power consumption and chipset temperature. Commands like *ptugen, ptumon, ptumem* are run in command prompt to generate load on CPUs, monitor the CPU and DIMM temperatures and stress the memory modules respectively. The data collection is made for the entire test duration. The data is collected into sheets that is further reduced using Microsoft excel.

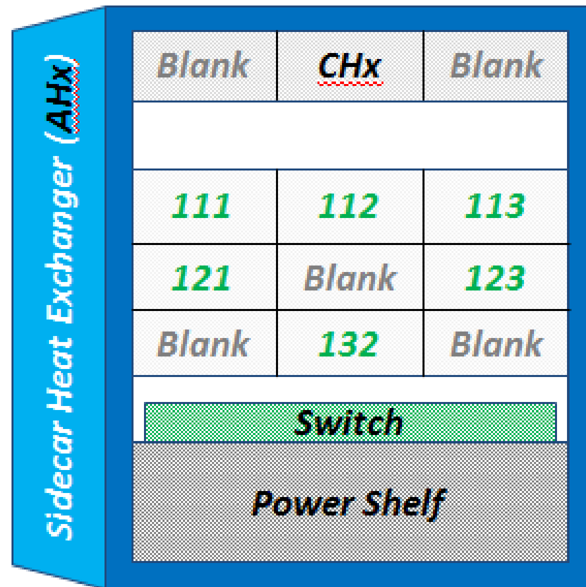

(a)

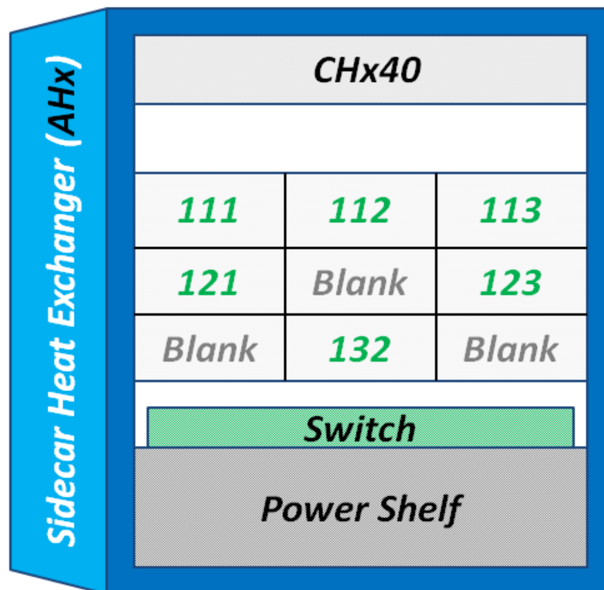

(b)

Figure 4-13: Six servers tested in the rack a) distributed pumping case b) centralized case with CHx 40 replacing CHx

4.3.4 Experiment Process

After setting the coolant inlet temperature to the desired set point using the control interface, the synthetic load test is started on each server simultaneously. The process of load generation on each server from a CPU power level of 0 to 100 and applying a CPU+MEM load in a cyclic fashion is automated using a *bash* script written with relevant commands described in previous section. The bash script runs in a text window executing the commands line by line accessing the stress load and data collection command line packages installed into the system. Each test runs for about six hours and is repeated for three times in order to account for repeatability. The data is averaged for three tests and average temperature and power readings are presented. Data is collected over the last 30 minutes of each test, since steady state is expected to reach during that period. The basic reason for this is to account for the closest steady state value of the different monitored parameters. For instance, the fan speeds may fluctuate within the specific band width (±10% PWM signal). Hence, the average steady state values obtained from all the repeated tests have been used for analysis.

4.4. Results & Discussions

4.4.1 Distributed pumping results

The Intel 2OU server used in our test is mainly CPU dominated in terms of power consumption i.e. more than 80% of the total server power consumption typically is from the CPUs. The rest of the server components like DIMMs, PCH, and HDDs etc. account for the rest of the power consumed. Following this objective, only some of the parameters are considered critical to our study i.e. power consumption of server, server fans and pump speeds and temperatures of the CPUs, DIMMs and PCH. All the critical

temperatures are under the safe operating limits all through the range of 25°C to 45°C. The fan speeds remain at the lower limit of its rpm range i.e. 975 rpm during 25°C and 30°C inlet temperatures and start to ramp up slightly during 35°C test and reaches its higher limit during the 45°C test as anticipated. The power consumption recorded. The fan speeds remain below the upper critical limit i.e. 13897 RPM [49] The increased speeds have impact on the power consumption and the effects are discussed in the later sections.

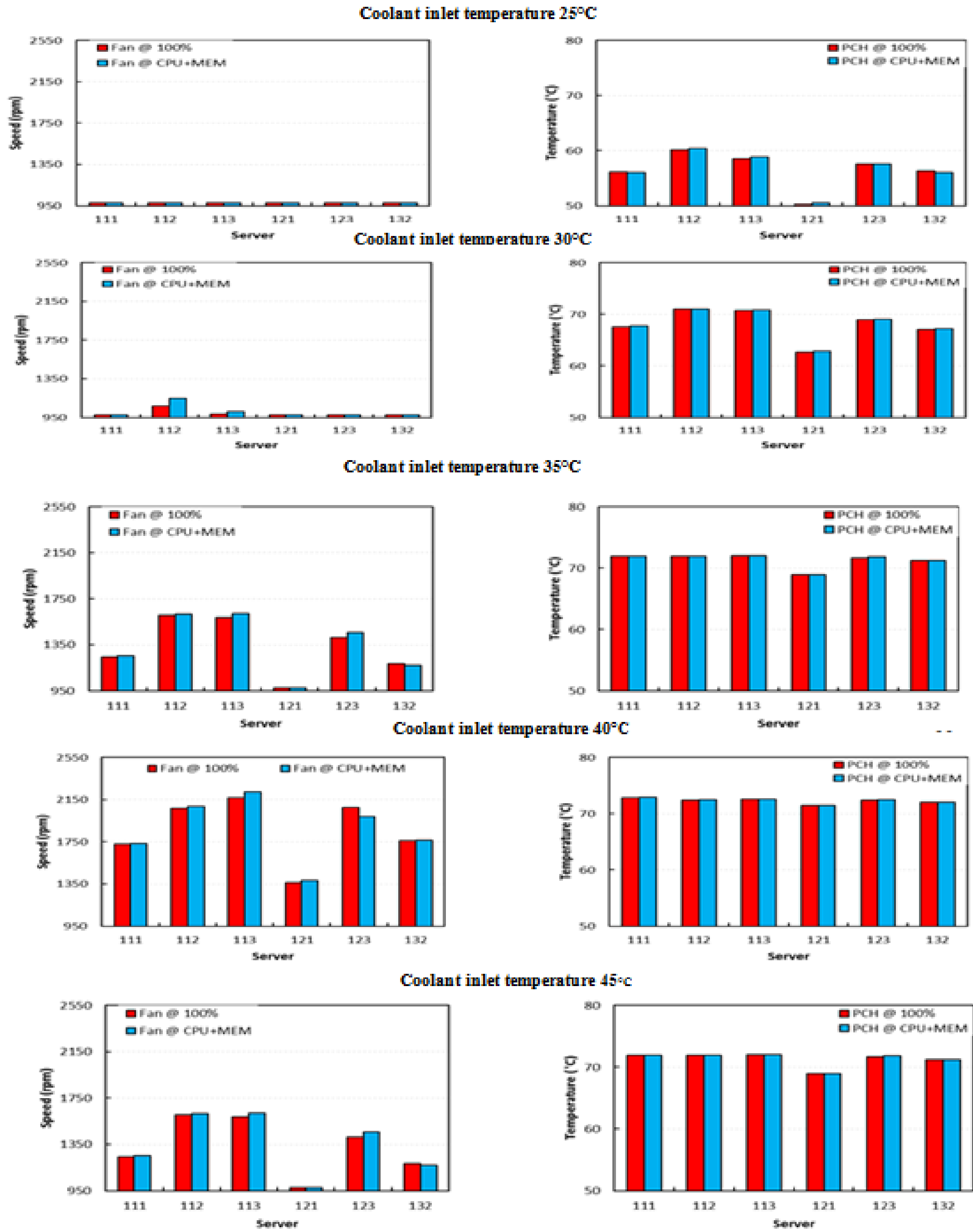

Figure 4-14: Change in fan speeds based on PCH temperatures for various inlet temperatures

The PCH temperatures at different inlet temperatures are reported in Figure 15. The PCH temperatures increase with an increase in inlet temperature but stay below the critical limit of 85°C. As we discussed earlier, the fan speeds ramp up based on the input received from the server component temperatures. Upon observation, it has been noted that fan speeds seem to start rising as soon as the PCH temperatures cross a certain limit, approximately 74°C. Since, PCH temperatures affect the fan speed rpm; it may also have impact on the cooling power consumption of the entire system. So, this observation needs to be taken into consideration in order to further optimize the cooling solution.

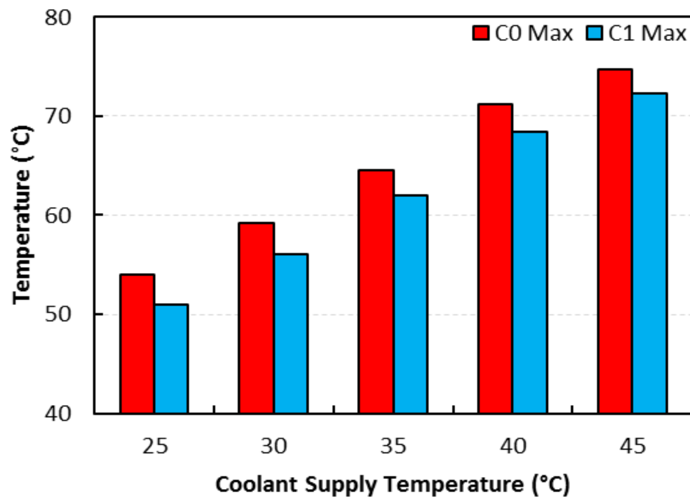

Figure 4-15: Maximum CPU core temperatures at 100% power level for server 123

The results are demonstrated for Server 123 because it has shown the maximum operating temperatures compared to other tested server. For different inlet temperatures, the CPU temperatures running at 100 % power level are reported in Figure 4-16. These can be considered as the maximum die temperature values. All the servers show similar

temperature readings with no major anomaly for a specific coolant IN temperature. Upon observation, we see that temperatures of CPU0 are slightly higher than CPU1 for the same applied load. The coolant flow inside the server is in series fashion and CPU1 receives it before CPU0 and coolant entering CPU0 is slightly higher than CPU1. The die temperatures rise as the coolant temperature increases but it is still below the safe operating point [49].

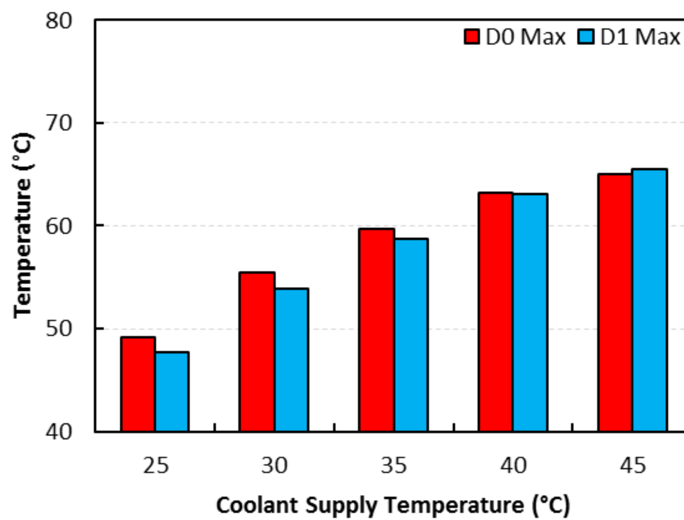

Figure 4-16: Maximum DIMM temperatures at CPU and memory test for server 123

DIMM0 refers to maximum of all DIMM temperatures interfacing with CPU0, and DIMM1 refers to maximum of all DIMM temperatures with CPU1. The DIMM 0 and DIMM 1 temperatures are shown in Figure 17. The DIMM temperatures rise with the increased inlet temperature of the cooling liquid. The maximum temperatures reached during the upper limit of our test range, 45°C is within the operating limit i.e. 82°C. The DIMMs are air cooled and the ones present on the LHS in Figure 1 receive cool air directly from the fans and the DIMMs on the RHS receive slightly hotter air (Figure 3).

The total IT power consumption of the rack at specific inlet temperature varying from 25°C to 45°C is shown in Figure 18. The cooling power consumption (Pcooling) represents the power consumed by server fans and distributed cold plate pumps of all the servers collectively. Cooling is efficient at higher loads i.e. 3% of IT power utilized to cool the components. The increase in coolant inlet temperatures has a noticeable effect on the IT power consumption i.e. the IT power at 40% PTU shows 6.7% increase in IT power at 45°C compared to 25°C.

Table 4-1: The cooling power consumption of the entire rack for different coolant temperatures

		Test					
T_{supply} (°C)	Parameter	Idle	40%	60%	80%	100%	CPU+MEM
25	*IT Power*	307.4	1025.0	1318.9	1574.9	1634.4	1562.1
	Pcooling	49.5	49.3	49.2	48.9	48.8	49.0
	Fraction	*16.1%*	*4.8%*	*3.7%*	*3.1%*	*3.0%*	*3.1%*
30	*IT Power*	293.5	1029.3	1333.1	1576.0	1637.9	1563.3
	Pcooling	48.7	48.3	48.1	48.1	48.1	48.2
	Fraction	*16.6%*	*4.7%*	*3.6%*	*3.1%*	*2.9%*	*3.1%*
35	*IT Power*	297.8	1050.8	1352.1	1587.6	1647.6	1576.5
	Pcooling	48.6	48.2	48.0	47.9	48.2	48.4
	Fraction	*16.3%*	*4.6%*	*3.5%*	*3.0%*	*2.9%*	*3.1%*
40	*IT Power*	301.6	1073.9	1372.6	1599.9	1659.8	1587.3
	Pcooling	48.0	47.6	48.5	49.7	49.4	49.4
	Fraction	*15.9%*	*4.4%*	*3.5%*	*3.1%*	*3.0%*	*3.1%*
45	*IT Power*	305.4	1093.3	1392.4	1606.9	1667.4	1593.5
	Pcooling	47.7	48.5	49.6	49.9	50.9	50.4
	Fraction	*15.6%*	*4.4%*	*3.6%*	*3.1%*	*3.1%*	*3.2%*

4.4.2 Centralized pumping results

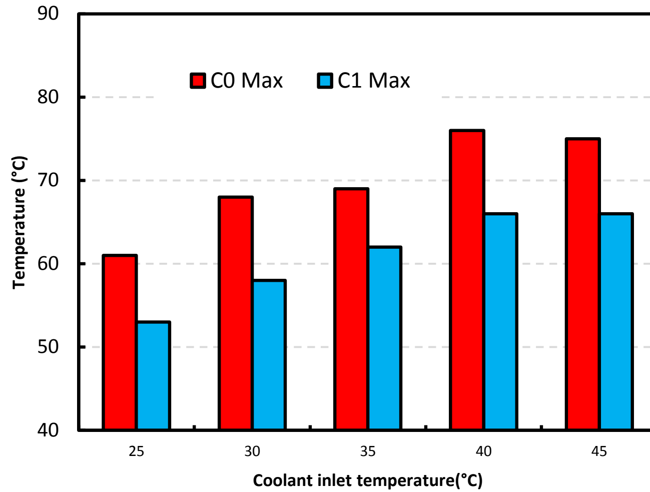

Figure 4-17: CPU core temperature for different inlet temperatures for server 123

In the centralized pumping case, the pump capacity has been downsized such that it would handle the rack heat load because the system is sized to handle about 40kW heat load. The total rack heat load is about 1.6 kW. The pumping power compared to distributed pumping has been set up to be third of the total rack pump power consumption in distributed case. Figure 19 shows the core temperatures of CPU for different inlet temperatures. The temperatures on an average compared to distributed pumping are less as shown in Figure 23.

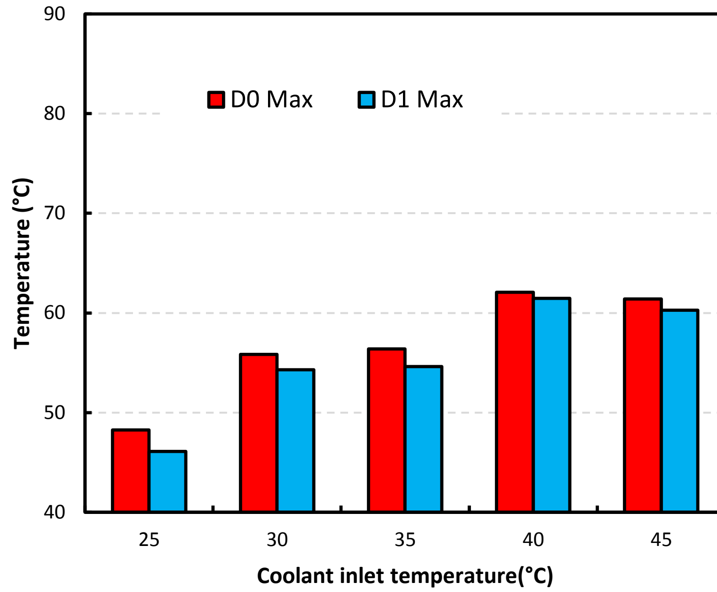

Figure 4-18: DIMM temperatures for different inlet temperatures for server 123

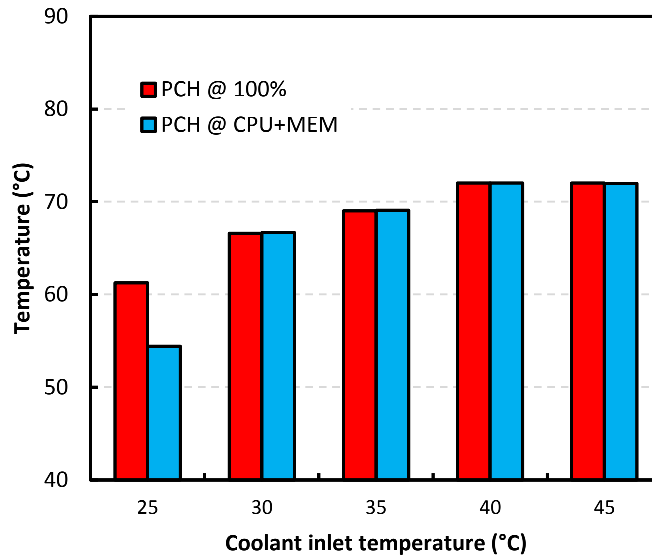

Figure 4-19: PCH temperatures for different coolant inlet temperatures for server 123

Table 4-2: The cooling power consumption of the entire rack for different coolant temperatures

T supply (°C)	Power	Idle	10%	30%	50%	70%	100%
25	IT	300.72	1017.12	1320.54	1572.54	1632.69	1555.62
	Cooling	21.2	21.2	21.2	21.3	21.2	21.1
	Fraction	7.05%	2.08%	1.61%	1.35%	1.30%	1.36%
30	IT	304.98	1051.02	1377.1	1596.31	1656	1579.65
	Cooling	21.3	21.2	21.2	22.12	23.4	19.417
	Fraction	6.98%	2.02%	1.54%	1.39%	1.41%	1.23%
35	IT	307.98	1061.7	1380.03	1598.36	1660.99	1583.47
	Cooling	21.2	22.4	21.8	21.8	22.1	22.3
	Fraction	6.88%	2.11%	1.58%	1.36%	1.33%	1.41%
40	IT	311.28	1075.8	1392.54	1608.15	1668	1593.04
	Cooling	21.5	22.2	22.1	22.2	21.6	22.5
	Fraction	6.91%	2.06%	1.59%	1.38%	1.29%	1.41%
45	IT	309.12	1077.18	1402.78	1608	1670.14	1591.04
	Cooling	21.4	21.4	22.4	22.1	22.1	22.3
	Fraction	6.92%	1.99%	1.60%	1.37%	1.32%	1.40%

The DIMM and PCH temperatures are lower compared to distributed pumping case for the same inlet temperature and stress load as shown in Figure 4-23. As anticipated D1 DIMM temperatures that receive the colder air show lower temperatures compared to D0 DIMM temperatures as shown in Figure 4-3. It has been observed from the tests that the cooling power comprises of around 1.5% of total IT power consumption at 100% stress load. This indicates a more efficient system in terms of cooling power consumption.

Table 4-3: Comparison of average component temperatures and average fan speeds for distributed pumping (DP) and centralized pumping systems (CP)

		T_{CPU0}(°C)		T_{DIMM0}(°C)		T_{PCH}(°C)		N_{Fan}(RPM)	
Tsupply(°C)	*Test*	DP	CP	DP	CP	DP	CP	DP	CP
25	100%	54.1	52.3	40.6	38.7	59.3	57.3	975	975
	CPU+MEM	49.6	45.3	49.6	38.1	59.4	54.5	975	975
30	100%	57.4	57.1	46.2	43.4	64.4	63.9	975	975
	CPU+MEM	53.6	51.9	55.4	44.4	64.6	62.9	975	975
35	100%	62.6	59.1	51.5	47.2	70	67	1053	1025
	CPU+MEM	58.7	56.7	60.3	50.1	70.1	70.1	1076	1040
40	100%	69.2	62.3	56.3	50.1	71.9	68.2	1662	1259
	CPU+MEM	65.7	58.3	64.1	56.9	71.9	71.5	1713	1325
45	100%	72.8	68.1	59.3	52.5	72.4	71.5	2096	1432
	CPU+MEM	68.8	63.6	66.1	53.1	72.5	69.4	2114	1426

The results shown in figure 23 shows the comparison of component temperatures and fan speeds for distributed vs. centralized pumping. It is observed that even at 45°C inlet, the CP system shows a reduction of 6.4% in max CPU temperatures compared to DP system for 100% PTU. The DIMM temperatures for 45°C inlet show 11% reduction for 100% PTU. The fan speeds were reduced by around 31.7% for 45°C comparing the DP vs. CP system.

Compared to the initial set of results for centralized pump testing [48], the current results (using CHx40) show the average operating temperatures of CPU, DIMMs and PCH an increase of around 2-3°C for 25°C-30°C inlet coolant temperatures and stayed the same from 30°C-45°C for 100% CPU power level. The fan operating speeds show

slight increase around 260 RPM for 40°C case using CHx40. However, the rest of the inlet temperature cases show same average fan speeds for 100% fan speeds. It has been observed that CHX40 unit works more effectively at higher inlet coolant temperatures.

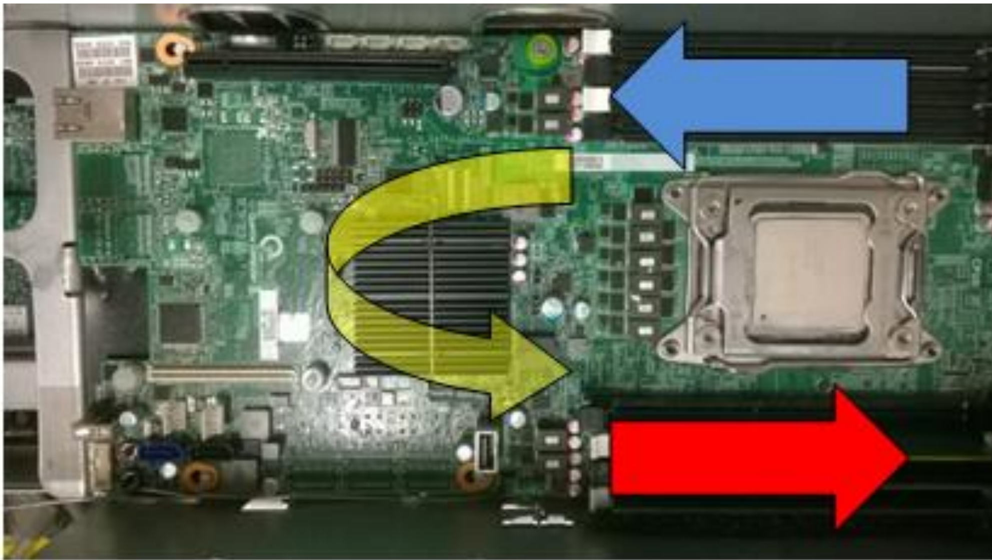

Figure 4-20: PCH extruded heat sink and air flow direction inside the server (arros are colored to represent the cool and hotter air)

Also, the PCH temperatures drive the fan speeds in our case. As the server configuration has been closely observed, one issue has been identified with the placement of the PCH heat sink. The plate heat sink placed on the PCH is not in accordance to the air flow direction in the server as shown in Figure 4-24. Given, the shape of the fin on the heat sink and the air flow direction, the heat transfer may not be effective. These temperatures are critical in fan speed control; hence, optimizing the heat transfer across the PCH is also an important solution. Replacing the plate heat sink with

a pin fin heat sink helps in better movement of cool air across the fins and thereby may help in reducing the PCH temperatures.

Multiple CFD and experimental studies have been conducted to study the selection of optimal PCH heat sink design [56]. Based on the baseline experimental readings a CFD model has been created that accurately represents the physical model of the open compute server using ANSYS Icepak [57]. Heat sinks designs such as cross cut fin, pin fin, elliptical fin, hexagonal pin fin, and compact vapor chamber model have been simulated for different cases. The heat sinks are selected from commercially available catalogue designs [58]. Geometric dimensions, the heat exchanger mechanical attachment (Only Z-clips in our case), thermal resistance are the factors that were considered in selection of the heat sink. These heat sink designs are used in the CFD model and corresponding PCH temperatures are measured in each case. The CFD simulation is run for 8 W power dissipation on the PCH and the corresponding fan PWM cycle as an input. It was found out that the cross-cut fin heat sinks and compact vapor chamber model with air flow restriction set up around the heat sink showed the lowest operating PCH temperatures with a 4 °C decrease.

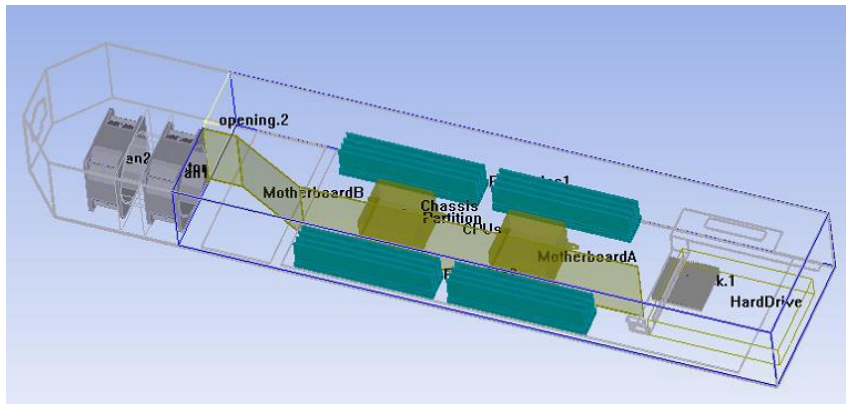

Figure 4-21: ANSYS Icepak model of the open compute server

4.5. Conclusions

Two different types of pumping systems have been tested for a mini rack at different stress loads. The IT design, cooling architecture and experimental test data has been discussed. The rack has been tested for high ambient inlet temperatures ranging between 25°C and 45°C. All the component temperatures remained below reliable operating temperatures. It has been observed that fan speeds are ramping up based on the PCH temperatures. Centralized pumping system has shown relatively lower operating component temperatures compared to distributed pumping system for the specified boundary conditions. For coolant inlet temperatures above 35°C, there is a reduction of about 6-9% in CPU temperatures, 8-11% reduction in DIMM temperatures, the PCH temperatures remained almost the same, and the fan speeds reduced by 24.2% and 31.7% at 40°C and 45°C inlet respectively.

The centralized system performed better at high inlet temperatures i.e. above 35°C. The overall system cooling power consumption has been has been lower for the centralized system compared to the distributed pumping system i.e. the pumping power for CP system has been set to be one third of DP system and the fan powers also showed reduction in power consumption as explained above. Further, the study can be extended to understand the implications when one of the cooling components i.e. fan or pump fail and compare the results for both the pumping systems. The centralized system would reduce the number of mechanical failure points in the system significantly. However, distributed pumping system would render the scalability in the rack because the coolant drives are located within the server. This would permit population of the rack per requirement. Swapping of the servers in and out of the rack is also possible with the

distributed case. During failure scenarios, presence of multiple pumps in system could create back flow in the system for distributed pump case.

The centralized system was also tested for different flow rates varying from 5.4 lpm to 3.4 lpm [59]. It was observed that with the decrease in flow rate to 3.4 lpm at rack level, the CPU0 temperatures increased by 5.7 °C on an average. The DIMM temperatures and PCH temperatures that are essentially air cooled have not been significantly (i.e. less than 1.6% change) impacted by the change in the flow rate. Hence, there are no major fan power consumption at server level as well. At 45 °C inlet with 3.4 lpm flow conditions, the CPU0 has shown a temperature of about 78.5 °C junction temperature at 100% load. This is 22.5 °C below the maximum thermal limit. The results mainly showed that the component temperatures are below the maximum operating limits. There is significant scope for the system to reduce the pumping power i.e. up to 57%. The server IT power consumption has increased for both centralized and distributed pumping system when the coolant inlet temperature has increased from 25 °C to 45 °C. However, the reduction in the pumping power will be a trade-off between potential scalability required for the rack vs. current rack heat load.

4.6. Failure Conditions for Distributed Vs. Centralized Systems

Compared to air cooling in chapter 3, liquid cooled components will have better tolerance when a cooling failure happens. The primary reason for this is about 50% higher thermal margins at server level. More about thermal margins at server level for liquid vs. air cooling will be discussed in chapter 5. However it is important to study an aspect that determines which type of pumping system have better redundancy performance during failure conditions.

The primary objective is to find out if the cooling failure i.e. failure of a fan or pump at server/rack would have catastrophic effect like shutting down, throttling etc. The secondary objective is to identify the critical component temperatures under such scenario. For the distributed pumping case, one of the servers (server 123) is considered and a single fan and pump are turned off. Server 123 has exhibited relatively higher temperatures compared to other servers in the rack. Hence, it is considered as a worst case condition. For the centralized pumping case which has two pumps at rack level driving the flow, one of the pumps is disabled and its effect on the thermal performance of the system is studied.

4.6.1 Distributed Pumping Failure Scenario

In this case, a single fan and pump (downstream) is disabled for server 123 as shown in figure 4-24.

Figure 4-22: Server 123 showing location of fan and pump that are not powered in distributed pumping case

The server has been tested for coolant inlet temperatures of 25 °C, 35 °C and 45 °C inlet. The inlet temperatures have been monitored for +/-1.2 °C accuracy. Different parameters such as critical component temperatures, server power and cooling power are compared for failed vs. regular operation as shown in Figure 4-25.

Table 4-4: Temperature and power parameters for failed vs. regular operation of server

123

T_{supply} (°C)	Test	Operation	C0 T_{max} (°C)	C1 T_{max} (°C)	D0 T_{max} (°C)	D1 T_{max} (°C)	T_{PCH} (°C)	P_{server} (W)	$P_{cooling}$ (W)
25	100%	*Regular*	54.0	51.0	40.4	38.4	61.1	273.8	8.2
		Failure	57.6	53.0	43.7	40.9	67.2	275.5	4.1
		Difference	*6.7%*	*3.9%*	*8.4%*	*6.5%*	*9.9%*	*0.6%*	*-49.9%*
	CPU+MEM	*Regular*	49.5	46.5	49.2	47.7	61.2	261.2	8.2
		Failure	53.8	48.9	53.4	51.1	67.5	261.9	4.1
		Difference	*8.7%*	*5.3%*	*8.6%*	*7.1%*	*10.3%*	*0.3%*	*-49.9%*
35	100%	*Regular*	64.6	62.0	51.3	49.6	71.2	276.0	8.1
		Failure	66.4	63.3	52.6	50.3	72.5	276.1	4.5
		Difference	*2.8%*	*2.2%*	*2.5%*	*1.5%*	*1.8%*	*0.0%*	*-44.6%*
	CPU+MEM	*Regular*	60.4	58.6	59.7	58.7	71.3	263.5	8.2
		Failure	62.3	59.0	60.9	59.6	72.7	263.7	4.5
		Difference	*3.2%*	*0.8%*	*2.0%*	*1.5%*	*2.0%*	*0.1%*	*-44.8%*
45	100%	*Regular*	74.7	72.2	58.7	57.9	72.8	279.8	9.1
		Failure	76.2	72.9	59.3	58.4	74.3	278.1	5.6
		Difference	*1.9%*	*1.0%*	*1.0%*	*1.0%*	*2.2%*	*-0.6%*	*-38.1%*
	CPU+MEM	*Regular*	70.6	68.3	65.0	65.5	72.8	266.2	8.2
		Failure	72.8	68.6	66.4	66.7	74.5	266.2	5.6
		Difference	*3.1%*	*0.5%*	*2.3%*	*1.8%*	*2.2%*	*0.0%*	*-31.7%*

All the parameters are collected as the system reached steady state conditions. As the coolant inlet temperature increased the percentage difference between regular and failure condition for CPU, DIMMs and PCH temperatures have reduced. This emphasizes the concept that if coolant inlet temperatures are increased when employing water-side economization when failure occurs at higher inlet temperatures (in our case above 35 °C inlet) the system temperatures does not deviate much from the regular operation. However, if we consider 45 °C inlet failure condition as a worst case, it shows that compared to default design the processor temperatures have only been deviated by 3.1% for CPU0 and 0.5% for CPU1. For this case, the cooling power deviation has been

only 31.7% compared to 49.9 % for the 25 °C inlet failure condition. This is because of the increase in fan power consumption from 25 °C to 45 °C failure condition. The server power consumption has remained fairly the same with a deviation of less than 1 % between regular and failure condition. This means the increase in operating temperatures due to failure conditions for all inlet temperatures did not have any noticeable impact on degradation of the server performance.

4.6.2 Centralized Pumping Failure Scenario

In the centralized pumping case, one of the two pumps to the downstream of the system has been disabled as shown in figure 4-26. The

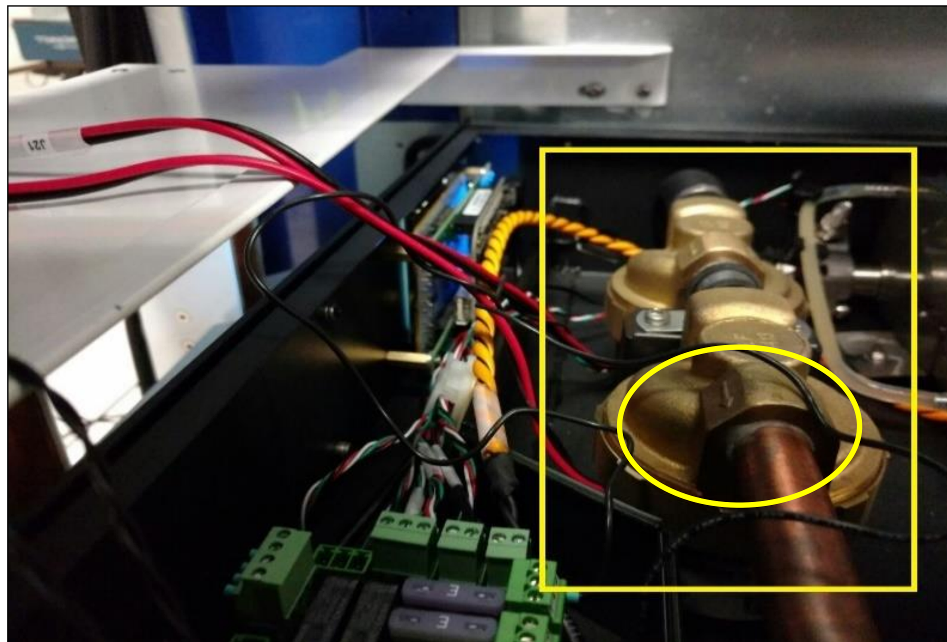

Figure 4-23: Circled Pump is disabled for running the test

The results showed that the failure scenario component temperatures are higher than the regular operation component temperatures. The percentage difference in the CPUs, DIMMs and PCH temperatures has reduced as the inlet temperature of the coolant increased. This behavior is similar to the distributed case. The server power consumption which includes only the power consumption of the IT components is slightly increasing by 2.2% from 25 °C to 45 °C inlet coolant temperature at 100% load condition and it has increased 4.58% for the same coolant temperature range at CPU+MEM load condition.

Table 4-5: Comparison of component temperatures and power for centeralized pumping regular vs. failure design

Tsupply(°C)	Test	Operation	C0 Tmax(°C)	C1 Tmax(°C)	D0 Tmax(°C)	D1 Tmax(°C)	Tpch(°C)	Pserver(W)
25	100%	*Regular*	61	53	48.3	46.1	61.1	272
		Failure	65	54	51	49	66	276
		Difference	***6.56***	***1.89***	***5.59***	***6.29***	***8.02***	***1.47***
	CPU+MEM	*Regular*	59.5	51	43	45.1	61	261.2
		Failure	63.1	54	42	48.2	65	262
		Difference	***6.05***	***5.88***	***-2.33***	***6.87***	***6.56***	***0.31***
35	100%	*Regular*	69	62	55.1	52.7	69	274
		Failure	71	64	57	54.6	71	278
		Difference	***2.90***	***3.23***	***3.45***	***3.61***	***2.90***	***1.46***
	CPU+MEM	*Regular*	64.1	55	56.4	51.1	69.1	263.5
		Failure	67	56.1	60	55	72	268
		Difference	***4.52***	***2.00***	***6.38***	***7.63***	***4.20***	***1.71***
45	100%	*Regular*	75	66	61	60.3	71	276
		Failure	77	69	64	62	73	280
		Difference	***2.67***	***4.55***	***4.92***	***2.82***	***2.82***	***1.45***
	CPU+MEM	*Regular*	71.2	62	61	58	71.2	267
		Failure	73	65	63	62	73	274
		Difference	***2.53***	***4.84***	***3.28***	***6.90***	***2.53***	***2.62***

For the centralized failure case, the CPU1 core frequency has shown 0.8% increase and CPU0 core frequency has increased by 2% due to increase in coolant inlet temperature from 25 °C to 45 °C. This means the server performance has not reduced drastically due to existing high thermal limits on the processor temperatures. These values are not significant because of the lower operating temperatures on the CPUs. The obvious reason for CPU0 showing higher core frequency percentage increase is that the CPU0 has been consistently higher than CPU1 core temperatures. As mentioned in the earlier section, CPU1 is thermally shadowed by CPU0 with the series cooling loop connection. In the centralized pumping case, the penalty in the operating temperatures due to failure is higher compared to the distributed case. Because the loss of one pump at rack level will reduce the cooling significantly compared to the distributed case. However, there will not be a backflow condition and the distribution of liquid will be more uniform compared to the distributed pumping case.

Overall, the failure scenarios in both distributed and centralized case has demonstrated that the system component temperatures were all operating below the allowable thermal limits. The cooling redundancy was working without any catastrophic failure of the system. The operating temperatures were higher compared to regular operation as expect. In both the pumping case, the percentage difference (for regular vs. cooling failure) in the operating temperatures reduced due to increase in the coolant inlet temperatures. The penalties due to failure are higher for centralized pumping than the distributed pumping case. Future extension of this work can be to study the failure scenarios under variable pumping condition for centralized pumping. Because cooling redundancy is an additional factor that needs to considered when thermal design and sizing of the cooling system is studied.

CHAPTER 5

SERVER LEVEL STUDY: EFFECT OF HIGH TEMPERATURE INLET CONDITIONS ON THERMAL PERFORMANCE OF AIR VS. LIQUID COOLED SOLUTIONS

© [2017] IEEE. Reprinted, with permission, from [IEEE ITHERM CONFERENCE, and June/2017 [60]]

The primary objective of the study is to evaluate air vs. liquid cooled enterprise-class server for the effects of high ambient inlet temperatures. The air-cooled server has five hot swappable fans and two CPU heat sinks to dissipate the total heat in the server. The water-cooled counter-part consists of two-cold plates with integrated pumps to cool the CPUs while the dual in-line memory modules transfer the heat using a heat transfer tape attached to the manifold that is carrying the coolant. The existing practice in the industry is to maximize the use of economizer usage by reducing/eliminating the usage of chiller while taking advantage of outside ambient conditions to cool the data centers. However, higher ambient temperatures would lead to higher operating temperatures of the processors. The operating temperature of the CPU has direct influence on the static power which is known to reduce the performance of the processor. In this study, the air as well as liquid cooled servers will be tested at inlet temperatures ranging from 25°C-45°C (ASHRAE T.C 9.9 A4 and W4 classes) and the corresponding thermal and flow parameters will be compared for both cases. The current work primarily focuses on evaluating the critical inlet temperatures (for air cooled vs. liquid cooled server) at which CPU die temperatures have an influence of the static power. Collectively, a case will be presented as to why liquid cooling would provide a viable option to operate the data centers at wider inlet temperatures with reduced risk of leakage current
and sustain the performance and reliability of the IT equipment.

5.1 Experimental Set Up

The IT enterprise class server consists of two Intel Xeon E5 2690 v2 processors, 16 DIMMs, up to eight drives, PCH and other auxiliary components [61]. The air-cooled server has five hot swappable fans and two CPU heat sinks to dissipate the total heat in the server. The water-cooled counter-part consists of two-cold plates with integrated pumps to cool the CPUs while rest of the components are air cooled as shown in figure 5-1. The coolant is being circulated over the loop by means of a set of flexible tubes which are in turn connected to the miniature dry cooler i.e. a finned tube heat exchanger coupled with two 120 mm 4-wire fans as shown in the figure 5-2. Since the CPUs are the main heat dissipating components are now being liquid cooled the overall air flow requirement in the server has been significantly reduced. The liquid coolant is 35% propylene glycol and 65% di-water by volume.

The server has been installed with Linux supported software called Ubuntu 14.04 [62]. The server is stressed using a bash script that automates the application of computational load for certain amount of time period. The stress load is applied at different time intervals with server running at idle in-between stress loading. A command line interface called IPMItool [63] has been used to read various BMC parameters such as component temperatures, fan speeds, power consumption, power status etc. across the motherboard. Ubuntu commands such as stress [64], Prime95 are used to stress the CPUs and DIMMs and monitor the processor utilization during the stress period. For the initial set of testing, the fans are internally controlled i.e. the fan tachometer readings are managed by an internal fan control algorithm set by the manufacturer.

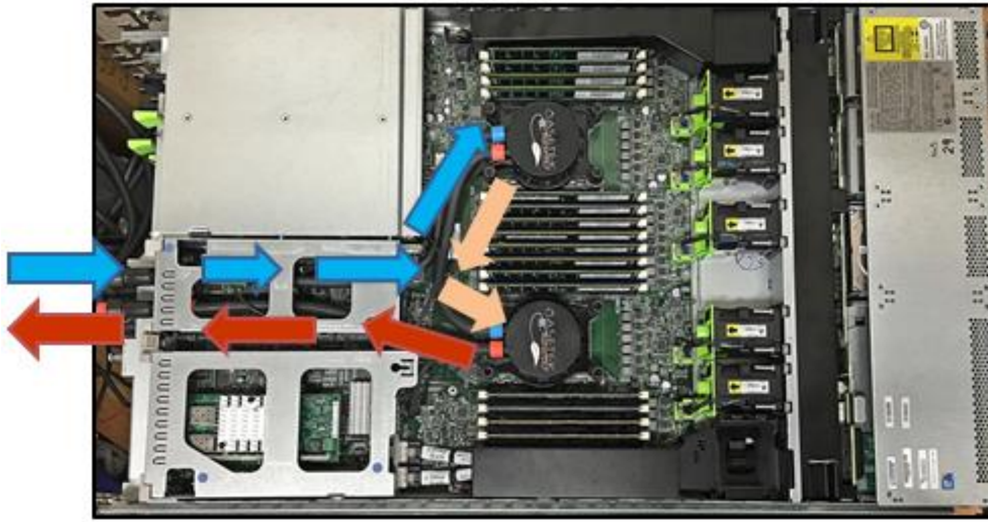

Figure 5-1 : Enterprise Class Liquid Cooled Server (the arrows show direction of liquid coolant in and out of the server)

K-type thermocouples are used to measure inlet and outlet coolant temperatures. The thermocouples are connected to an Agilent Bench link data logger [65]. The varying inlet temperatures for each stress test case are set by controlling the 4-wire 120 mm fans of the miniature dry cooler. The PWM wires of the fans are connected to an Arduino UNO which is interfaced to LabVIEW [66]. To de-couple the cooling power measurement from IT power, the pumps are powered externally by means of an Agilent DC power supply unit [67].. Each server is loaded computationally as explained in the previous section using a bash script that consists of Linux native commands.

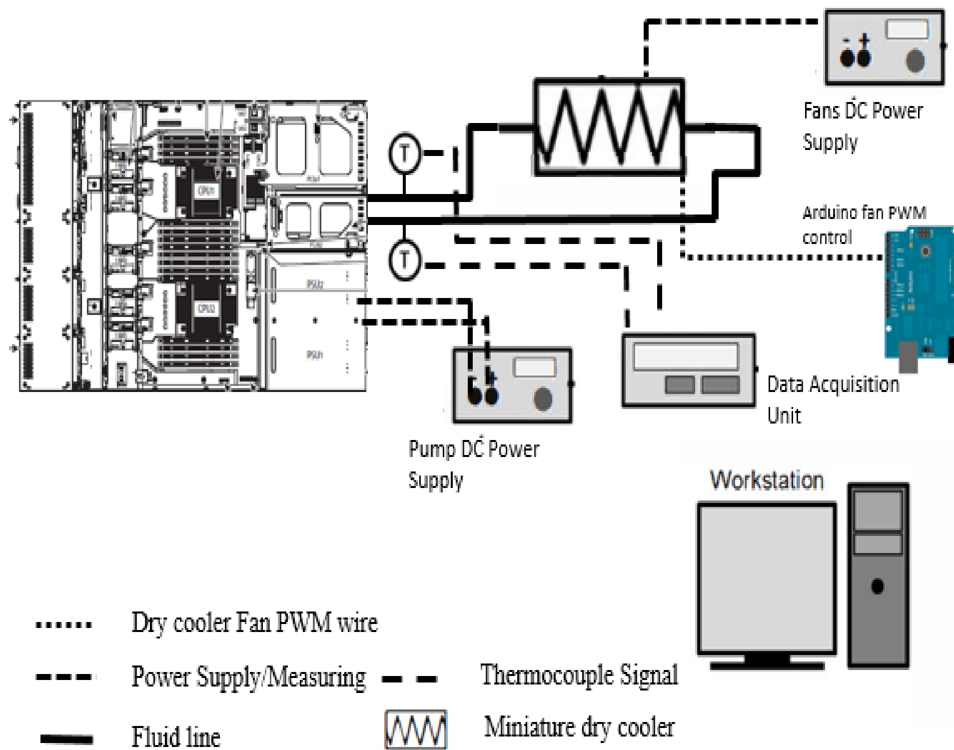

Figure 5-2: Experimental schematic for liquid cooled server testing

The cold plates are replaced by means of heatsinks specific to model C220 M3. The server is now cooled by means of five hot-swappable fans that provide front-to-rear cooling. The fan dimensions are 40x40x56 mm³ with a rated speed of 16000/15400 RPM. Each fan case has two counter rotated fans that operate in push-pull configuration.

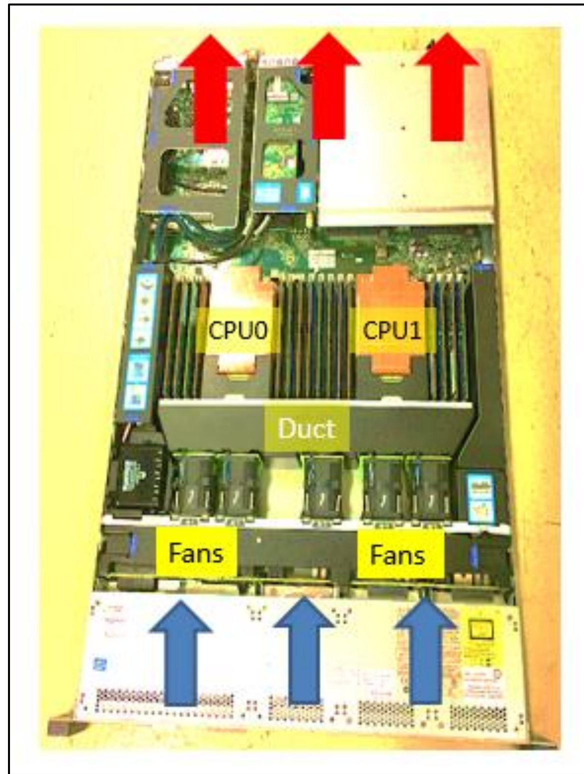

Figure 5-3: 1U enterprise server with front to rear air cooling

In order to characterize the fan and system flow behavior, the fan flow curves have been generated using Air flow Bench testing for 99.99%, 90% and 70% fan PWM as shown in figure 4. The air flow chamber is designed to blow known amount of air flow rate on the object of testing [68]. The fans are externally powered and the PWM control wires have been connected to a function generator unit to fluctuate the PWM cycle in each testing case.

The air-cooled server testing has been conducted in an environmental chamber as shown in figure 5 [69]. The chamber utilizes a refrigeration cycle to maintain the enclosure for specified environmental conditions, in this case, constant inlet temperature

all along the test duration. The inlet temperature deviation is ±0.5°C. The humidity within chamber has varied between 45-60%.

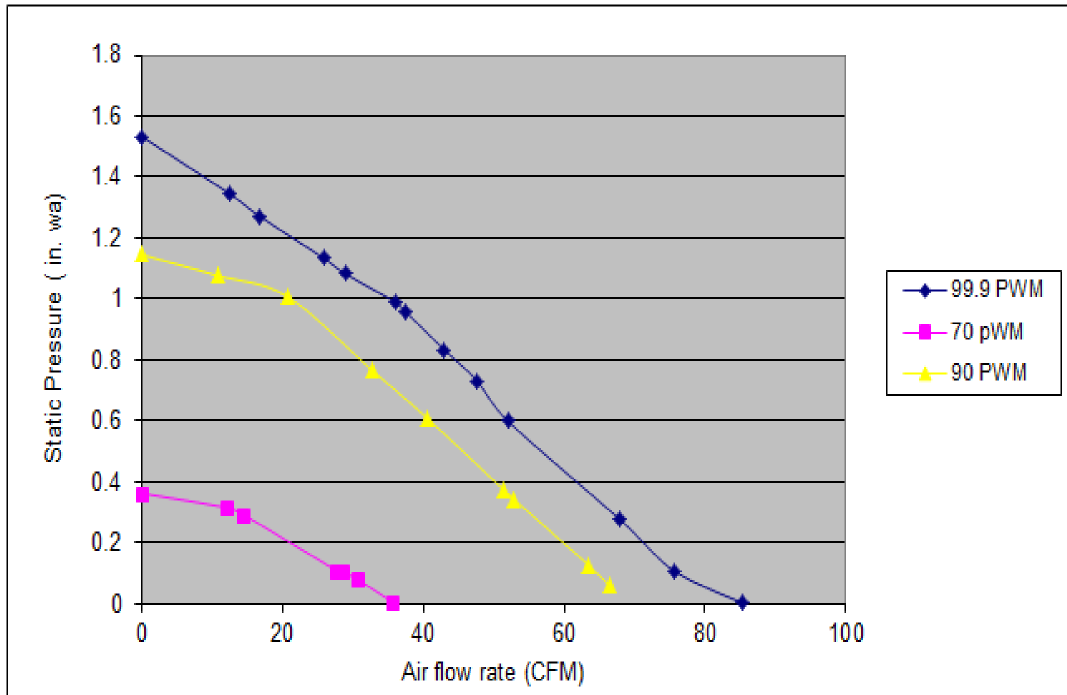

Figure 5-4: Characterization of flow curves for the air-cooled IT server

The temperature difference across the server varied between 10 – 12 °C. For the current study, the fans inside the servers are being controlled by the internal fan control algorithm typically based on the temperature of CPUs. The fan control algorithm is aimed to maintain the CPU operating temperatures below certain temperature limit.

5.2 Test Procedure

The server is installed with packages like *stress* that would stress the processors such that they can generate desired heat output. Based on the input specified in the command line, desired number of cores will be stressed. For data collection, packages such as *ipmitool* and *sensor* have been installed. The main parameters that are collected are the CPU core temperatures, DIMM case temperatures, PCH temperatures, server power consumption. The fan power and pump power are measured separately as they were powered by separate Agilent DC power supply units. The data is collected for the entire test duration. The miniature dry cooler fan RPMs would modulate to set the desired set point of coolant inlet temperature using LabVIEW. The coolant inlet temperature would modulate with an accuracy of +/- 1.4 °C. The server is placed in the lab so only the liquid coolant temperature is being change in each case but not the air temperature. The lab room temperature is calibrated to be 22.6 °C.

For liquid cooled server, the computational load for each testing case is the same, as explained in the previous section. The server is stressed/loaded for different conditions i.e. Idle, 10%, 30%, 50% ,70 % and 98% and an additional test that would stress both CPU and 90% memory using Prime95 [70]. This computational load condition is repeated for different inlet temperatures ranging from 15 °C- 45 °C in air cooling case and 25 °C-50 °C in liquid cooling case. Each stress load is imposed for 30 minutes and the thermal and power measurements are considered for the last 10 minutes to account for steady state condition.

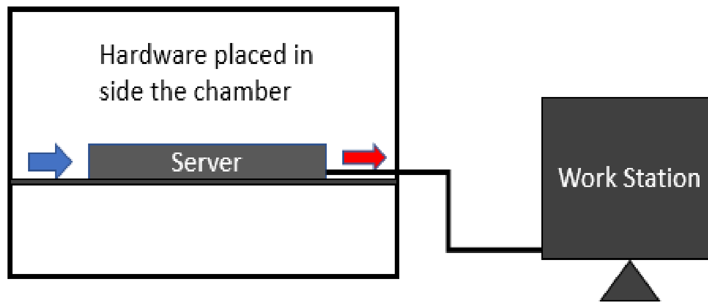

Figure 5-5: Environmental Chamber Thermotron unit (left); Simple schematic of air-cooled IT server testing (right)

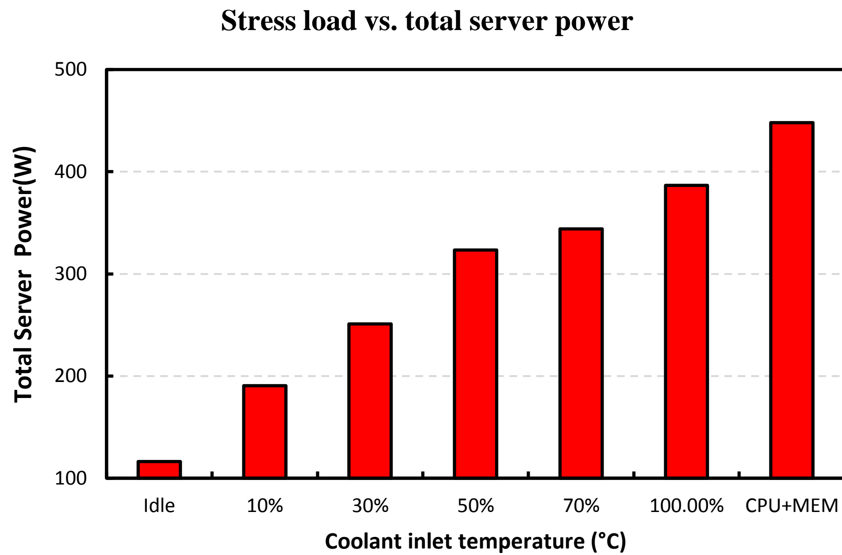

Figure 5-6: Variation of total server power with stress load condition

Power measurements for IT and cooling are made separately. For the liquid cooling case, the pumps are externally powered using DC power supply unit. The readings from the power supply unit have been collected using a software called Benchvue [71]. The server fans speeds are measured from IPMItool. The power vs. fan speed curve has been developed for the fan and the fan power consumption based on this third order polynomial curve as shown in figure 7. Fan power measurements are derived from power vs. RPM of the 40 mm fans. The fan speeds were monitored and curve fit equation from figure 4-7 is used to measure the electrical power input.

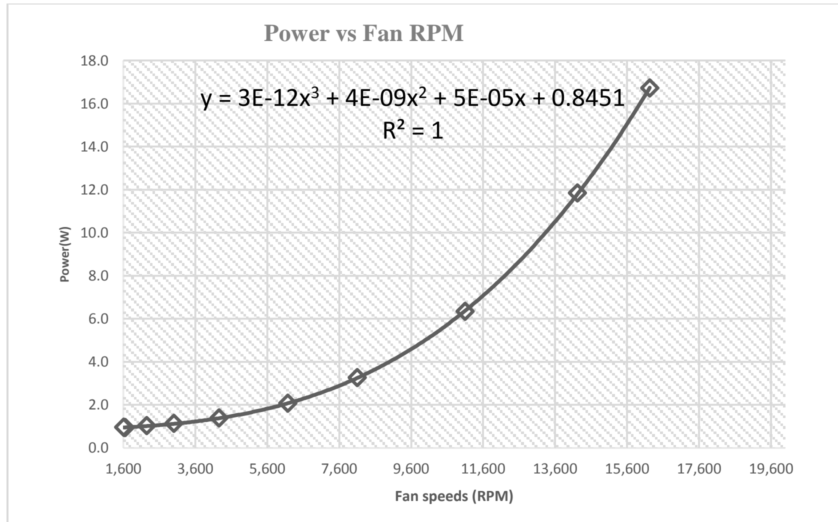

Figure 5-7: Graph for Power vs. RPM for 40 mm Fan

5.3 Results And Discussion

The first set of results reported are for liquid cooling test set up. The graph below shows the maximum core temperatures of the CPUs at different coolant inlet temperatures. At 100% stress load, the CPU temperatures are 63°C and 68°C. The coolant cools the CPUs in a series fashion. CPU1 is where the coolant first enters the cold plate hence, we see that CPU1 temperatures are lower compared to CPU0.

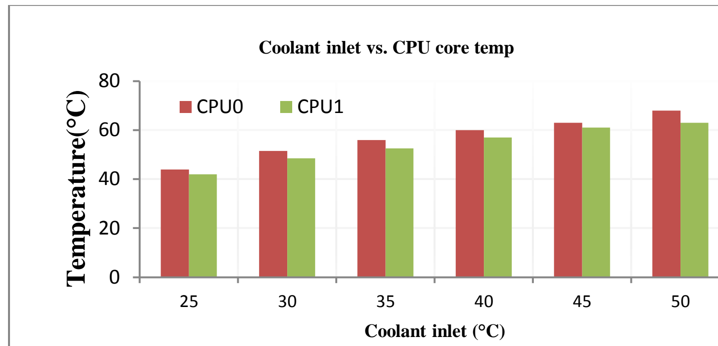

Figure 5-8: Increasing CPU temps with increased coolant temperature at 100% stress load

Even at 50°C inlet, CPU core temperatures remain way below critical operating point i.e. 100°C (this value is obtained using the 'sensors' command line).

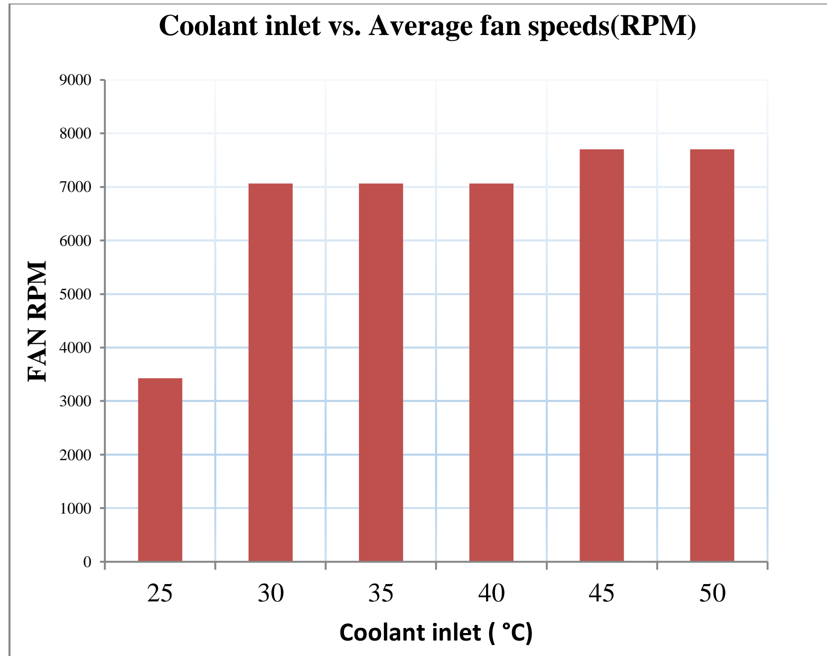

Figure 5-9: Change in fan speeds with increase in coolant inlet temperatures

It has been observed that fan speeds ramp up based on the CPU die temperature. The system has been over provisioned. Hence, the DIMM temperatures are not reported for the liquid cooling test case. This setting is going to be changed in the next set of liquid cooling test results by controlling the fans externally such that the fan speeds vary based on the DIMM/HDD temperatures.

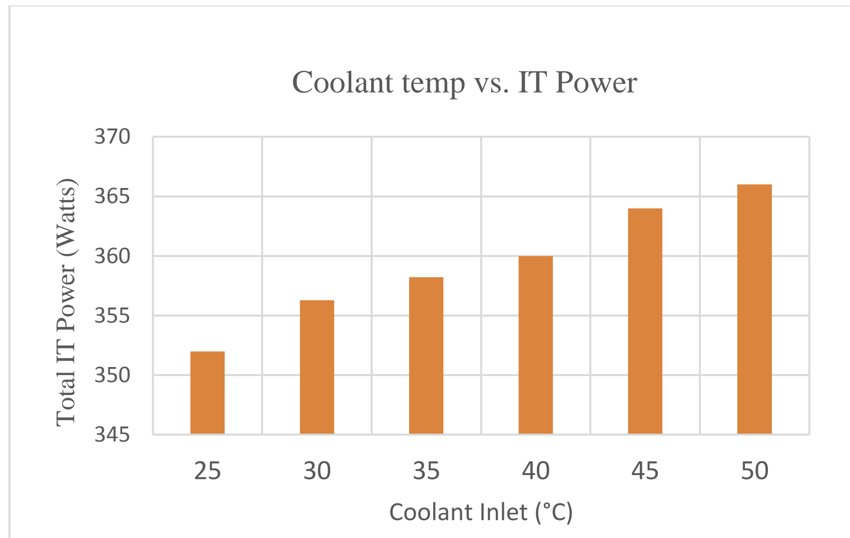

Figure 5-10: IT power dissipation vs. Inlet Coolant Temperature at 100% utilization

Figure 5-10 shows the variation in IT power as the inlet coolant temperature rises. The total server power consumption is considered to be summation of IT power consumption and cooling power consumption i.e. the power consumed by fans and pumps

$$P_{server} = P_{IT} + P_{cooling} \tag{2}$$

The change is not significant however there is noticeable increase in the IT power consumption at 100% stress load. This change is attributed to be the effect of the static power due to increased CPU operating temperatures. Results from internally controlled liquid cooling set up suggest that the components operate at reliable temperatures. Fan speeds ramp up based on CPU temperatures. There is an opportunity for reduction in pumping power because of the lower CPU temperatures and fan power too. At high loads, the cooling accounts for 4.3-6.8% of the IT power.

First set of results with constant the pump power at 12 V input for different inlet temperatures along with the fan power consumption that is controlled based on CPU temperatures exhibited two things. Firstly, CPU temperatures does not approach beyond 68°C at its highest inlet temperature condition with 100% CPU Utilization. Secondly, the resultant total server power consumption could be imprecise due the CPU temperature based fan power consumption.

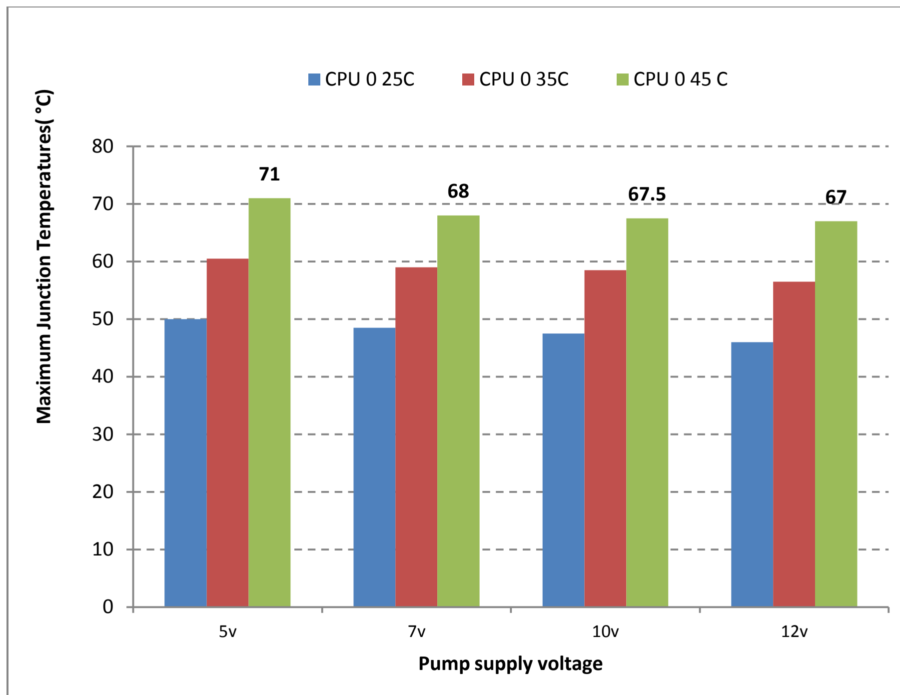

Figure 5-11: CPU0 temperatures for varying pump supply voltage

Based on these conclusions, the second set of testing includes external PWM control of fans and pumps which would give the accurate characterization of the liquid cooled server at high ambient conditions for static power effect.

Pump Impeller speed is rated at 3000 ±300 RPM at full power. The stall power for the pumps is at 4VDC. The pumps integrated in the cold plates are centrifugal velocity type. CPU die temperatures for varying pump operating voltage and different inlet coolant conditions are shown in figure 11. The die temperatures at 5V supply did not exceed 71°C. IT power change is not significant i.e. 4% increase with rise in inlet coolant temperature due to low operating temperatures as shown in figure 13.

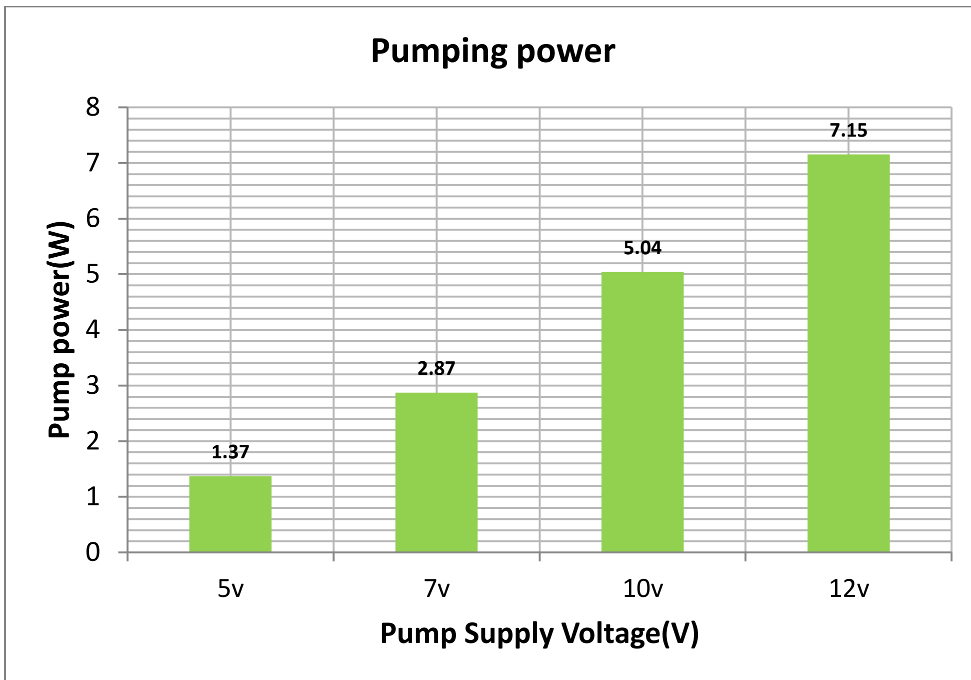

Figure 5-12: Pumping power for different supply volatage conditions

The change in pumping power for same inlet does not drastically effect the IT power. Pump design is overprovisioned. Even with 80% reduction in pump power, shown in figure 12, the CPU temperatures remain below safe operating limits at 45°C coolant inlet condition.

The DIMMs are tested using Prime95 for up to 92% memory while using external function generator supplying fixed PWM signals for the fans ranging from 30% (IDLE fan rpms) and 100% PWM. It is noticed that the maximum DIMM case temperature (@30% PWM and 25°C inlet) has been 51°C way below the critical operating limit i.e. 81° C.

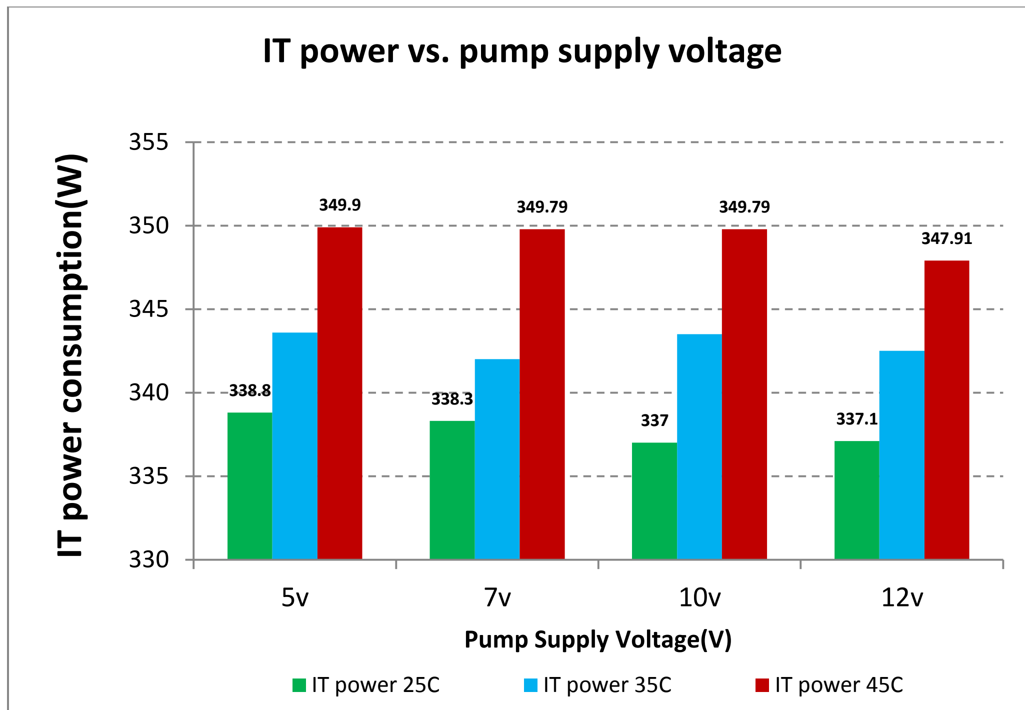

Figure 5-13: IT power vs. pump supply voltage for different coolant inlet temperatures

The temperature difference across the water for different test cases varied. For 25 °C inlet case, the average temperature difference across the inlet and outlet coolant temperature is 5.9 °C. For 35 °C inlet case, the waterside average temperature difference reduced and it is 4.57 °C. For the 45 °C inlet case, the water side average temperature difference further reduced to 3.28 °C.

In the following section, the air-cooled server test results are reported. As mentioned earlier, the environmental test chamber has been used to stress test the server at different air inlet temperatures.

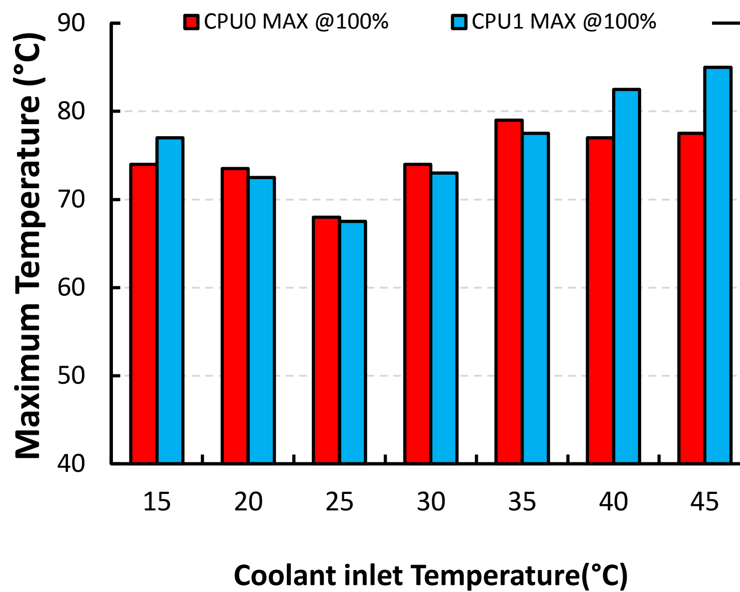

Figure 5-14: CPU maximum core temperatures for different air inlet temperatures at 100% CPU load

The maximum CPU core temperatures for different air inlet temperatures are reported in figure 14. The temperatures are higher at 15°C inlet compared to 25°C inlet for the same stress load boundary condition. This is because at 15°C inlet the fan speeds are lower compared to 25°C as shown in figure 15. The inlet temperature of the air going into the miniature dry cooler is the room temperature in the lab i.e. 22.6 °C. The approach temperature across the dry cooler reduced with the increasing coolant inlet temperature.

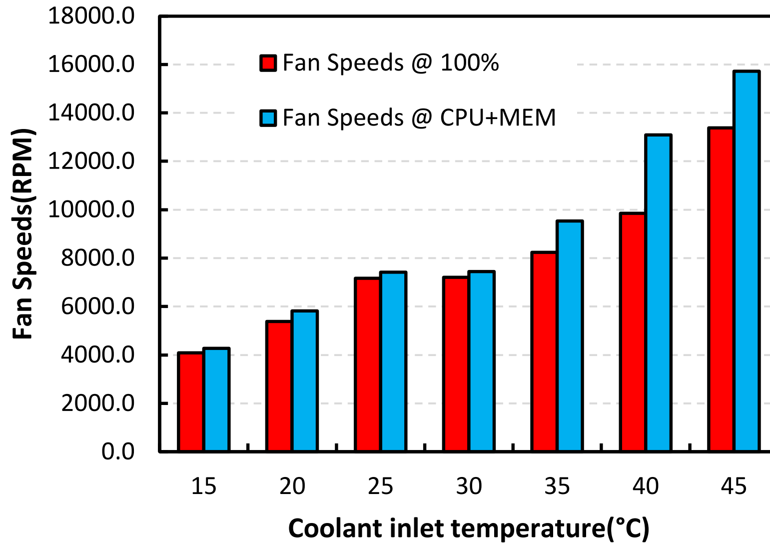

Figure 5-15: Average Fan Speeds varying with respect to inlet air temperature

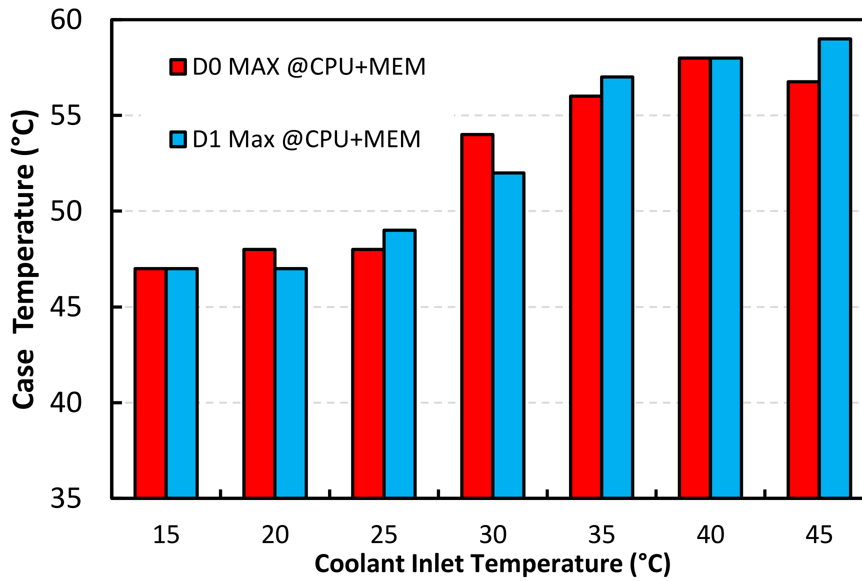

Figure 5-16: Maximum DIMM temperatures for varying air inlet conditions at CPU+MEM load

The fan speeds are observed to be operated based the coolant inlet temperature. The maximum CPU core temperatures remained below high operating limit of 86°C at 100% stress condition and 45°C inlet.

To stress the CPU as well as memory, prime95 has been installed. The torture test is set up such that 90.8% of memory has been stressed with 100% CPU load and the corresponding DIMM temperatures have been reported. The DIMM temperatures remain below the safe operating limit of 85°C [72].

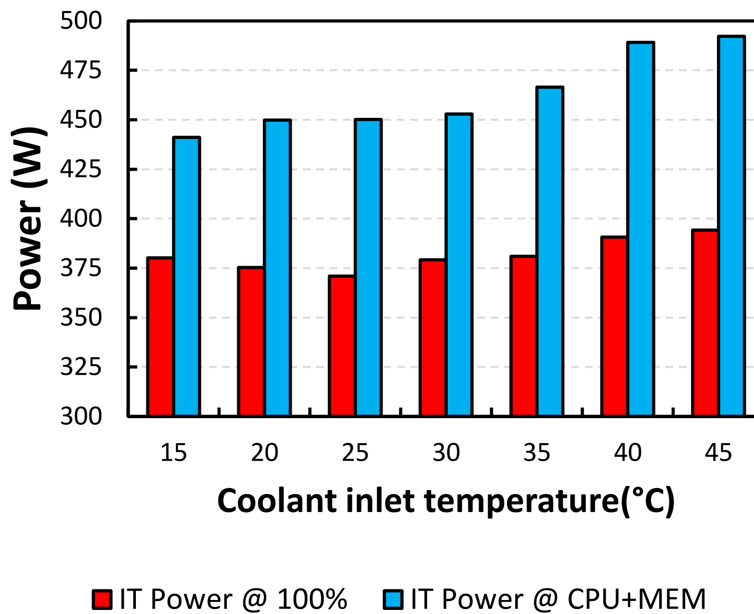

Figure 5-17: Total IT power consumption for different inlet air temperature for 100% CPU stress load and prime95 memory stressing test (CPU+MEM)

The IT power consumption has increased with coolant inlet temperatures for 100% CPU load. The IT power consumption is higher in the CPU+MEM stress test because of the power dissipated from memory modules is also accounted for. The static

power effect has been significant in CPU+MEM test as shown in figure 17. The DIMM temperatures are around 6°C higher in CPU+MEM test compared to 100% CPU stress test for inlet temperatures 15°C-40°C.

Table 5-1: Cooling power consumption vs. IT power consumption

Test	15	20	25	30	35	40	45
Idle	5.30%	4.95%	4.88%	4.61%	3.61%	10.05%	12.92%
10%	3.32%	3.69%	5.01%	6.60%	6.89%	6.54%	11.11%
30%	2.68%	3.42%	5.07%	5.01%	4.91%	6.73%	11.19%
50%	2.08%	2.70%	4.01%	3.90%	3.93%	5.93%	9.33%
70%	1.95%	2.56%	3.82%	3.72%	3.64%	5.88%	9.68%
100.00%	1.74%	2.26%	3.39%	3.35%	4.21%	5.88%	11.95%
CPU+MEM	1.55%	2.07%	3.07%	3.13%	4.60%	9.59%	13.35%

The cooling power consumption is reported as a percentage of IT power consumption in figure 18. It must be noticed that beyond 35°C the server operation becomes inefficient as cooling power consumption rises in terms of both static power effect as well as rise in cooling power consumption. Hence, air cooled IT are restricted to a temperature range narrower compared to the liquid cooling case.

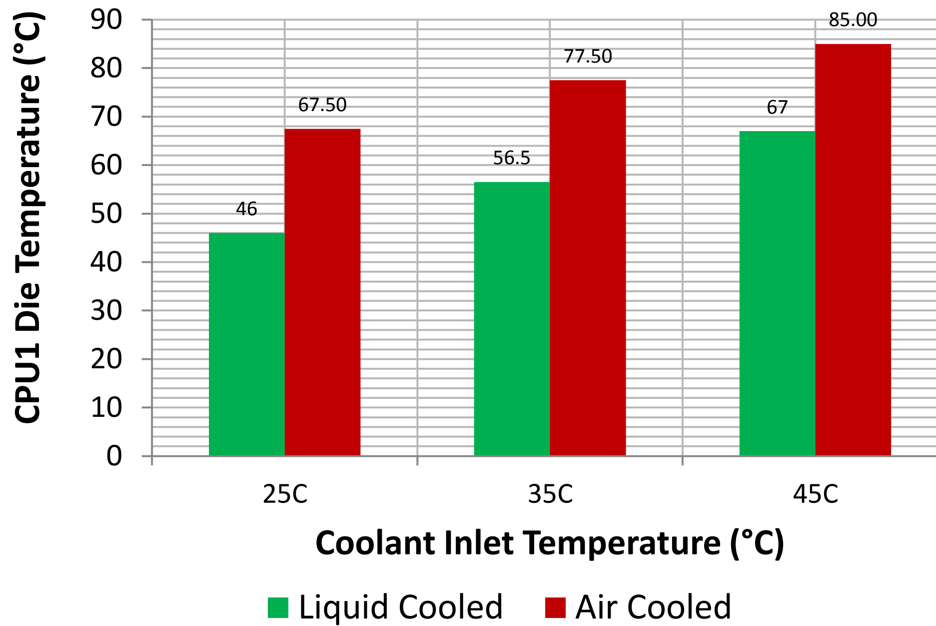

Figure 5-18: Air vs. Liquid Cooled CPU die temperatures for varying inlet temperatures at 100% stress load

5.4 Conclusion

The air-cooled and liquid-cooled IT servers are tested for different computational load at varying coolant inlet temperatures with in ASHRAE (A1-A4) and (W4-W5) thermal guidelines. The liquid cooled component temperatures are lower compared to air cooling counter parts. The CPU temperatures showed a difference of ~20°C for the same stress load for air vs. liquid cooled system as shown in figure 19. The static IT power has not been significant in liquid cooling case, this is due to lower operating temperatures as a resultant of an overprovisioned system even at reduced pump supply voltage. Due to

very low operating temperatures of CPU and memory, there is still scope for improving pumping as well as fan powers.

The air-cooled counter-part has shown that the cooling becomes inefficient after 35°C inlet air temperature and shows an increased static power effect for 100% CPU load and CPU+MEM testing. This means the operating limits of the air cooled IT cannot be widened. This would reduce the scope for maximizing the number of operation hours in economizer mode. While in the liquid cooling case, even at 45°C inlet temperature, the CPU temperatures are lower and the cooling has been seen to operate effectively with increased stress loading and coolant inlet. However, the trade-offs for selecting a specific energy efficient system would also include cost and maintenance factors which will be more in the case of liquid cooling. Overall, the study has demonstrated the testing procedure to conduct experimental test on air vs. liquid cooled IT and measure individual hardware temperature data. Detailed data collection has been employed to compare the two different cooling solutions for same IT hardware. Future work will include external control of cooling components in liquid cooled server and focus on HDD stress and its operating temperatures due to increase in ambient conditions which would contribute to setting up holistic design considerations for high ambient inlet temperatures.

CHAPTER 6

Conclusion

The main objective of this work has been to study the energy efficiency of the data center IT at room, rack and server level. Extensive literature review has been conducted to understand the different approaches that enhance the cooling energy efficiency in data centers. Specific focus is given to two main areas. First one is the usage of close-coupled cooling solutions for small sized data center rooms and the second area is the promotion the concept of free cooling/air-waterside economization.

The new end-of-aisle cooling system has been proposed for three different configurations. Thermal design considerations were discussed for all three configurations based on computational modeling. The volume of the room, the size of the hot aisle, the numbers of racks in each row, numbers of heat exchanger banks have been kept constant with minimum parametric alteration. These factors can be further investigated to study their impact on the performance of the cooling system. The Case 1 where rack fans are the only air movers could not handle denser IT equipment. The multiple turns needed by the air flow volume has because energy losses and when denser systems are placed in the racks, the resultant air flow across the racks is not sufficient to adequately cool the electronics. Case 2 and case 3 has shown to handle denser IT systems. It was clear that the location of the fan movers has also played an important role in affecting the thermal performance of of the IT room. Fan power consumption for case 2 (under steady state operation to achieve same temperature different across the rack) is 2.05 times that of Case1 and 2.1 times that of case 3. Case 3 where active heat exchanger fans are the only air movers has shown lower fan power consumption among all three cases.

However, it also led to an increased pressure profile in the room that could risk the air leakages and loss of air flow energy. Case 2 has been identified to be a tradeoff design that would mitigate the disadvantages associated with the other two cases. To control of the cooling in the data center room, two stage fan control algorithm and variable frequency drive pumps can be employed and this aspect can be further explored through experiments. The heat exchanger and fan failure scenarios have been discussed showing that all three cases are redundant for one HX failure and overheating of the IT has been noticed when two heat exchangers fail and have been considered the worst case failure scenarios.

The concept of free cooling and its impact on the performance of different types of IT equipment has been experimentally studied at rack level and server level. Depending on the location of the data center, the outside temperature and humidity conditions could be favorable to fall in ASHRAE allowable classes A1, A2 thereby operating the data center in economizer mode. To maximize the economizer hours of operation, data center IT should be operated in A3, A4 or W3, W4 classes. The experimental studies quantify the impact on the thermal performance of the IT servers. The liquid cooled rack study focused conducting empirical analysis on two different pumping systems for the first time when the IT is exposed to high ambient inlet conditions (up to 45°C inlet). The centralized pumping cooling system has performed better than distributed pumping system. The pump power consumption is about one-third that of distributed pumping case. The overall component temperatures were maintained lower. The CPU operating temperatures has reduced by 6-9% in centralized pumping case. The fan power consumption was lower by 27%. By further controlling the rack coolant flow rate, energy savings up to 57% have been shown with reliable operating component

temperatures. The server level study has compared the thermal performance between an air cooled vs. liquid cooled server. This data is critical as it shows the differences on thermal margins of the components that impacts the performance of the system. The air cooled server has been tested for 15 °C and 45 °C inlet temperatures. The server performance has reduced beyond 35 °C with a significant increase in fan power power consumption. There is a 12.6% increase in the IT power consumption ($P_{server}=P_{IT}+P_{cooling}$) beyond 35 °C inlet. The CPU temperatures are lower by 22.3 °C compared to the liquid cooled counterpart. The liquid cooled server is an over-provisioned system. The pumps and fans are externally controlled and demonstrated a scope for about 80% reduction in the pump power and about 40% reduction in fan power using an fan control algorithm different to the existing in-built algorithm. There is a 4% increase in the IT power consumption when coolant inlet temperature increases. When exposed to higher ambient inlet temperatures, liquid cooled server has shown thermal margins (double) compared to the air cooled counterpart. Overall, the work aims to provide computational and experimental data to understand energy efficiency at multiple cooling scales in data centers especially when exposed higher ambient inlet temperatures.

REFERENCES

[1] H. Geng, Data Center Handbook, Hoboken,NJ: John Wiley & Sons, 2015.

[2] S. Arman, S. J. Smith, D. Sartor, R. Brown , M. Herrlin, J. Koomey, E. Masanet, N. Horner, I. Azavedo and W. Lintner, "United States Data Center Energy Usage Report," Lawrence Berkley National Laboratory, California, 2013.

[3] International Data Corporation, "Worldwide Datacenter Census and Construction 2014-2018 Forecast:Aging Enterprise Datacenters and the Accelerating Service Provider Build Out," 2015.

[4] National Resources Defense Council , Anthesis , "Data Center Efficiency Assessment," 2014.

[5] N. Horner and I. Azavedo, "Power Usage Effectiveness in data centers: Overloaded and Underachieving," *The electricity journal ,* vol. 29, no. 4, p. 65, 2016.

[6] A. Shebabi, "Data center knowledge," 27 June 2016. [Online]. Available: http://www.datacenterknowledge.com/archives/2016/06/27/heres-how-much-energy-all-us-data-centers-consume/.

[7] V. Avelar, D. Azevedo and A. French, "PUE: A comprehensive examination of the metric," The Green Grid, 2012.

[8] The Global TaskForce, "Harmonizing Global Metrics for Data Center Energy Efficiency," 2014.

[9] ASHRAE, Best Practices for Datacom Facility Energy Efficiency, 2016.

[10] Campos Research & Analysis, "North American Data Center Demand Survey," Digital Realty Trust , San Francisco, 2012 .

[11] ASHRAE TC, "ASHRAE Technical Committee 9.9," 2016. [Online]. Available: https://tc0909.ashraetcs.org/.

[12] "2011 ASHRAE Thermal Guidelines," 2011. [Online]. Available: https://datacenters.lbl.gov/sites/all/files/ASHRAE%20Thermal%20Guidelines_%20SVLG%202015.pdf.

[13] M. K. Patterson, "Liquid cooling Guidelines," 14 November 2011. [Online]. Available: http://delivery.acm.org/10.1145/2160000.

[14] Y. Joshi and P. Kumar, Energy Efficient Thermal Management of Data Centers, New York: Springer, 2012.

[15] J. Bean and K. Dunlap, "Energy-Efficient Data centers," *ASHRAE Journal,* 2008.

[16] 42U Solutions for the Next Generation Data Center, "Close-Coupled Cooling," [Online]. Available: http://www.42u.com/cooling/close-coupled-water-cooled.htm.

[17] Mission Critical, "Close-coupled cooling system is right fit for data center," May 2016. [Online]. Available: http://www.missioncriticalmagazine.com/articles/88414-a-close-coupled-cooling-system-is-right-fit-for-data-center.

[18] L. Silva-Llanca, M. d. Valle and A. Ortega, "THE EFFECTIVENESS OF DATA CENTER OVERHEAD COOLING IN STEADY AND TRANSIENT SCENARIOS: COMPARISON OF DOWNWARD FLOW TO A COLD AISLE VERSUS UPWARD FLOW FROM A HOT AISLE," in *ASME* , 2015.

[19] T. Gao, B. G. Sammakia, J. Geer, B. Murray, R. Tipton and R. Schmidt, "Comparative Analysis of different In Row Cooler Management Configuration in a Hybrid Cooling Data Center," in *ASME International Technical Conference and Exhibition on Packaging and Integration of Electronic and Photonic Microsystems*, San Francisco, 2015.

[20] IBM, "Rear Door Heat Exchanger Planning Guide," 2008. [Online]. Available: ftp://ftp.software.ibm.com/systems/support/system_x_pdf/43w7855.pdf.

[21] M. d. Valle, C. Caceres and A. Ortega, "Transient Modeling and Validation of Chilled Water Based Cross Flow Heat Exchangers for Local On-Demand Cooling in Data Centers," in *IEEE ITHERM Conference*, 2016.

[22] M. Sahini, E. Kumar, T. Gao, C. Ingalz, A. Heydari and S. Xiaogang, " Study of Air Flow Energy within Data Center room and sizing of hot aisle containment for an Active vs. Passive Cooling Design," in *2016 15th IEEE Intersociety Conference on Thermal and Thermomechanical Phenomena in Electronic Systems(Itherm)*, Las Vegas, 2016.

[23] T. Gao, E. Kumar, M. Sahini, C. Ingalz, A. Heydari, W. Lu and X. Sun, "Innovative server rack design with bottom located cooling unit," in *2016 15th IEEE Intersociety Conference on Thermal and Thermomechanical Phenomena in Electronic Systems (ITherm)*, Las Vegas, 2016.

[24] J. Sasser, "A look at data center cooling technologies," 2014. [Online]. Available: https://journal.uptimeinstitute.com/a-look-at-data-center-cooling-technologies/.

[25] M. Mescall, "Close Coupled Cooling and reliability," Uptime Institute, 2014. [Online].

Available: https://journal.uptimeinstitute.com/close-coupled-cooling-reliability/.

[26] Federal Energy Department Program, "Improving Data Center Efficiency with Rack or Row based Cooling devices," US Department of Energy, 2012.

[27] K. Dunlap and N. Rasmussen, "Choosing between Room, Row and Rack-based Cooling for Data Centers," Schneider Electric, 2013.

[28] N. El-Sayed, I. Stefanocivi, G. Amvrosiadis and A. A. Hwang , "Temperature Management in Data Centers: Why some(Might) like it Hot," in *SIGMETRICS*, London, 2012.

[29] S. Zhang, N. Ahuja, Y. Han, H. Ren, Y. Chen and G. Guo, "Key Considerations to Implement High Ambient Data Center," in *31st SEMI-THERM Symposium*, San Jose, 2015.

[30] N. Ahuja, "Datacenter power savings through high ambient datacenter operation: CFD modeling study," in *Semiconductor Thermal Measurement and Management Symposium (SEMI-THERM), 2012 28th Annual IEEE*, 2012.

[31] Y. He, G. Chen, J. Zhang, T. Zhou, T. Liu, P. Zhu, C. Liu and N. Ahuja, "Consideration for Running Data Center at High Temperatures and Using Free Air Cooling," in *ASME 2015 International Technical Conference and Exhibition on Packaging and Integration of Electronic and Photonic Microsystems collocated with the ASME 2015 13th International Conference on Nanochannels, Microchannels, and Minichannels*, San Francisco, 2015.

[32] T. J. Breene, E. J. Walsh, J. Punch, A. J. Shah, C. E. Bash, N. Kumari and T. Caden, "From Chip to Cooling Tower Data Center Modeling: Chip Leakage Power and Its Impact on Cooling Infrastructure Energy Efficiency," *Journal of Electronic Packaging,* vol. 134, no. 4, p. 8, 2012.

[33] S. A. Hall and G. V. Kopcsay, "Energy-Efficient Cooling of Liquid-Cooled Electronics Having Temperature-Dependent Leakage," *Journal of Thermal Science and Engineering Applications,* vol. 6, no. 1, p. 12, 2014.

[34] M. Iyengar, M. David, P. Parida , V. Kamath, B. Kochuparambil, M. S. Graybill, R. Schmidt and T. Chainer, "Server Liquid Cooling with Chiller-less Data Center Design to Enable Significant Savings," in *IEEE SEMI-THERM Symposium*, 2012.

[35] S. M. Kerner, "Department of Energy Using Warm Water to Cool New Data Center," 5 September 2012. [Online]. Available: http://www.enterprisenetworkingplanet.com/datacenter/department-of-energy-using-warm-water-to-cool-data-center.html.

[36] S. Zimmermann, I. Meijer, M. K. Tiwari, . S. Paredes, B. Michael and D. Poulikakos, "Aquasar: A hot water cooled data center with direct energy reuse," *Elsevier,* vol. 43, no. Energy, pp. 237-245, 2012.

[37] H. Coles, M. Ellsworth and D. J. Martinez, "Hot for Warm Water Cooling," Seattle, 2011.

[38] M. Sahini, V. Pandiyan and D. Agonafer, "THERMAL PERFORMANCE EVALUATION OF THREE TYPES OF NOVEL END-OF-AISLE COOLING SYSTEMS," in *ASME InterPACK Conference*, San Fransisco, CA, 2017.

[39] Future Facilites, "Our Solutions," 2016. [Online]. Available: http://www.futurefacilities.com/solutions/data-centers/.

[40] J. Niemann, "Best Practices for Designing Data Centers with Infrastruxure InRow DC," APC, 2006. [Online]. Available: http://www.apc.com/salestools/JNIN-6N7SRZ/JNIN-6N7SRZ_R0_EN.pdf.

[41] CoilMaster, "EZ Coil Suite," Coil Master Corporation, [Online]. Available: http://coilmastercorp.com/resources/coilsuite/.

[42] SanyoDenki , "DC Fan," [Online]. Available: http://www.sanyo-denki.com/sda/data/cooling/catalog/DC_Fan.pdf.

[43] N. Shigrekar, "Quantifying Air flow Rate through a server in an operational data center and assesing the impact of using theoritical fan curve," Univeristy of Texas at Arlington, 2015.

[44] R. Jorgenson, Fan Engineering An Engineer's Handbook Sixth Edition, Buffalo, New York: Buffalo Forge Company, 1961.

[45] P. Lin, S. Zhang and J. VanGilder, "Data Center Temperature Rise During a Cooling System Outage," 2014. [Online]. Available: http://www.apc.com/salestools/DBOY-7CDJNW/DBOY-7CDJNW_R1_EN.pdf.

[46] M. Sahini, J. Fernandes, C. Kshirsagar, M. Kumar, D. Agonafer and V. Mulay, " Rack-level study of hybrid cooled servers using warm water cooling for distributed vs. centralized pumping systems," in *SEEMI-THERM 33rd Annual Symposium*, San Jose, CA, 2017.

[47] M. J. Ellsworth Jr., "New ASHRAE Thermal Guidelines for Air and Liquid Cooling," in *High Performance Computing, Networking, Storage and Analysis (SCC), 2012 SC Companion:*, Salt Lake City , UT, 2012.

[48] J. E. Fernandes, M. Sahini, D. Agonafer, V. Mulay, J. Na, P. McGinn, M. Soares and C. Turner, "Evaluating Liquid Cooling at the Rack: Comparing Distributed and

Centralized Pumping," in *International Microelectronics Assembly and Packaging Society (IMAPS Thermal)*, Los Gatos, 2014.

[49] H. Li and A. Michael, "Intel Motherboard Hardware v2.0," 11 april 2012. [Online]. Available: http://www.opencompute.org/assets/download/Open-Compute-Project-Intel-Motherboard-v2.0.pdf. [Accessed 20 august 2014].

[50] Intel, "4-wire pulse width modulation controlled fans," [Online]. Available: http://www.formfactors.org/developer%5Cspecs%5C4_Wire_PWM_Spec.pdf.

[51] J. Ning, "Intel Server in Open Rack Hardware v0.3," 16 01 2013. [Online]. Available: http://www.opencompute.org/assets/download/Open-Compute-Project-Intel-Server-Open-Rack-v0.3.pdf. [Accessed 20 08 2014].

[52] CoolIT Systems, "Rack DCLC CHx40," CoolIT Systems, [Online]. Available: http://www.coolitsystems.com/index.php/data-center/liquid-cooling-options/rack-dclc-chx40.html.

[53] KeySight Technologies, "Benchlink Data Logger 3," [Online]. Available: http://www.keysight.com/main/software.jspx?cc=US&lc=eng&ckey=778242&nid=-33257.922596.02&id=778242&cmpid=zzfinddatalogger3.

[54] Labview, 2013. [Online]. Available: http://www.ni.com/labview/.

[55] SourceForge, "Open Souce Software," [Online]. Available: http://ipmitool.sourceforge.net/.

[56] R. Hart, A. McAvene, D. Norwood, E. Jacobs and B. Tran, "Improved Design and Implementation of Heat Sink for Platform Controller Hub," 2016.

[57] ANSYS, "ANSYS Icepak," [Online]. Available: http://www.ansys.com/products/electronics/ansys-icepak. [Accessed 2017].

[58] Alpha Novatech, "Catalog Index," 2007. [Online]. Available: https://www.alphanovatech.com/en/cindex5e.html.

[59] C. Kshirsagar, "Rack level Study using warm water cooling with variable pumping for centralized pumping system," University of Texas at Arlington, Arlington, 2017.

[60] M. Sahini, U. Chowdhury, A. Siddarth and D. Agonafer, "Comparative study of high ambient inlet temperature effects on the thermal performance for air vs. liquid cooled IT," in *IEEE ITHERM CONFERENCE*, Orlando,FL, 2017.

[61] Cisco , "Cisco UCS C220 M3 Rack Server," Cisco, [Online]. Available: http://www.cisco.com/c/en/us/products/servers-unified-computing/ucs-c220-m3-

rack-server/index.html.

[62] Linux man Page, "Ubuntu Manuals," [Online]. Available: http://manpages.ubuntu.com/manpages/trusty/man1/mpstat.1.html.

[63] Intel, "Intelligent Platform Management Interface," Intel, [Online]. Available: http://www.intel.com/content/www/us/en/servers/ipmi/ipmi-home.html.

[64] Hectic Geek, "Stress Test Your Ubuntu Computer with ‘Stress," [Online]. Available: http://www.hecticgeek.com/2012/11/stress-test-your-ubuntu-computer-with-stress/.

[65] KeySight Technologies, "Benchlink Data Logger," [Online]. Available: http://www.keysight.com/main/software.jspx?cc=US&lc=eng&ckey=778242&nid=-33257.922596.02&id=778242&cmpid=zzfinddatalogger3.

[66] National Instruments, "Labview System Design Software," [Online]. Available: http://www.ni.com/labview/.

[67] KeySight Technologies, "E3633A 200W Power Supply, 8V, 20A or 20V, 10A," [Online]. Available: http://www.keysight.com/en/pd-836386-pn-E3633A/200w-power-supply-8v-20a-or-20v-10a?cc=US&lc=eng.

[68] AMCA, "AMCA 210 Series Wind Tunnel Introduction," [Online]. Available: http://www.longwin.com/download/presentation/AMCA-210-07-WT-Introduction-OP-App-20131024.pdf.

[69] Thermotron, "Environmental and Vibrational Testing Equipment Manufacturer," [Online]. Available: http://thermotron.com/equipment/temperature-chamber/se-series-temperature-chamber.html. [Accessed 2017 16 Jan].

[70] GIMPS, "Great Internet Mersenne Prime Search," Mersenne Research Inc., [Online]. Available: http://www.mersenne.org/download/.

[71] KeySight Technologies, "Benchvue Software," [Online]. Available: http://www.keysight.com/en/pc-2472896/benchvue-software?cc=US&lc=eng.

[72] Samsung, "240pin Registered DI MM based on 2Gb D-die," [Online]. Available: http://www.samsung.com/semiconductor/global/file/2011/product/2011/9/2/900928ds_ddr3_2gb_d-die_based_rdimm_rev13.pdf.

[73] J. E. Fernades, M. Sahini, D. Agonafer, V. Mulay, J. Na, P. McGinn, M. Soares and C. Turner, "Evaluating Liquid Cooling at the Rack: Comparing Distributed and Centralized Pumping," in *International Microelectronics Assembly and Packaging Society*, Los Gatos, 2014.

[74] CoolIT systems, "Rack DCLC CHx40," [Online]. Available: http://www.coolitsystems.com/index.php/data-center/liquid-cooling-options/rack-dclc-chx40.html.

[75] Innovative Research LLC, "MacroFlow: Overview," [Online]. Available: http://inresllc.com/products/macroflow/overview.html.

[76] National Instruments, "Labview System Design Software," [Online]. Available: http://www.ni.com/labview/.

[77] KeySight Technologies, "E3633A 200W Power Supply," [Online]. Available: http://www.keysight.com/en/pd-836386-pn-E3633A/200w-power-supply-8v-20a-or-20v-10a?nid=-35690.384001.00&cc=US&lc=eng.

[78] APC International Ltd, "PIEZOELECTRIC CONSTANTS," 2016. [Online]. Available: https://www.americanpiezo.com/knowledge-center/piezo-theory/piezoelectric-constants.html.